Midwest State's Regional Pooled Fund Research Program
Fiscal Year 1996-1997 (Year 7)
NDOR Research Project Number SPR-3(017)

DEVELOPMENT OF A 7.62-m LONG SPAN GUARDRAIL SYSTEM

<u>Submitted by</u>

Karla A. Polivka, B.S.M.E., E.I.T.
Graduate Research Assistant

Bob W. Bielenberg, B.S.M.E., E.I.T.
Graduate Research Assistant

Dean L. Sicking, Ph.D., P.E.
Associate Professor and MwRSF Director

Ronald K. Faller, Ph.D., P.E.
Research Assistant Professor

John R. Rohde, Ph.D., P.E.
Associate Professor

MIDWEST ROADSIDE SAFETY FACILITY
University of Nebraska-Lincoln
1901 "Y" Street, Building "C"
Lincoln, Nebraska 68588-0601
(402) 472-6864

<u>Submitted to</u>

MIDWEST STATE'S REGIONAL POOLED FUND PROGRAM
Nebraska Department of Roads
1500 Nebraska Highway 2
Lincoln, Nebraska 68502

MwRSF Research Report No. TRP-03-72-99
April 6, 1999

Technical Report Documentation Page

1. Report No.	2.	3. Recipient's Accession No.
SPR-3(017)		

4. Title and Subtitle	5. Report Date
Development of a 7.62-m Long Span Guardrail System	April 6, 1999
	6.

7. Author(s)	8. Performing Organization Report No.
Polivka, K.A., Bielenberg, B.W., Sicking, D.L., Faller, R.K., and Rohde, J.R.	TRP-03-72-99

9. Performing Organization Name and Address	10. Project/Task/Work Unit No.
Midwest Roadside Safety Facility (MwRSF) University of Nebraska-Lincoln 1901 Y St., Bldg. C Lincoln, NE 68588-0601	11. Contract © or Grant (G) No. SPR-3(017)

12. Sponsoring Organization Name and Address	13. Type of Report and Period Covered
Midwest States Regional Pooled Fund Program Nebraska Department of Roads 1500 Nebraska Highway 2 Lincoln, Nebraska 68502	Final Report 1997 - 1999 14. Sponsoring Agency Code

15. Supplementary Notes

Prepared in cooperation with U.S. Department of Transportation, Federal Highway Administration

16. Abstract (Limit: 200 words)

A 7.62-m long span guardrail system was developed for use over low-fill culverts. The long span design was constructed with two 2.66-mm (12-gauge) thick nested W-beam rails totaling 30.48 m in length. The nested W-beam rail was supported by sixteen W150x13.5 steel posts and six standard CRT posts, each measuring 1,830-mm long. Post spacings were 1,905-mm on center except for the 7.62-m spacing between the two CRT posts surrounding the unsupported span.

The research study included computer simulation modeling with BARRIER VII and full-scale vehicle crash testing, using ¾-ton pickup trucks. The first test, impacting at a speed of 101.3 km/hr and an angle of 25.4 degrees, was unsuccessful because the barrier system failed at the simulated BCT anchorage end. Consequently, the long-span barrier system was modified to include additional guardrail posts and new BCT anchorage hardware. The second test, impacting at a speed of 102.7 km/hr and an angle of 24.5 degrees, was unsuccessful due to vehicle rollover. The safety performance of the long-span barrier system was determined to be unacceptable according to the Test Level 3 (TL-3) evaluation criteria specified in NCHRP Report No. 350, *Recommended Procedures for*

17. Document Analysis/Descriptors		18. Availability Statement
Highway Safety, Guardrail, Longitudinal Barrier, Box Culvert	Roadside Appurtenances, Crash Test, Compliance Test	No restrictions. Document available from: National Technical Information Services, Springfield, Virginia 22161

19. Security Class (this report)	20. Security Class (this page)	21. No. of Pages	22. Price
Unclassified	Unclassified	134	

DISCLAIMER STATEMENT

The contents of this report reflect the views of the authors who are responsible for the facts and the accuracy of the data presented herein. The contents do not necessarily reflect the official views or policies of the State Highway Departments participating in the Midwest State's Regional Pooled Fund Research Program nor the Federal Highway Administration. This report does not constitute a standard, specification, or regulation.

ACKNOWLEDGMENTS

The authors wish to acknowledge several sources that made a contribution to this project: (1) the Midwest States Regional Pooled Fund Program funded by the Iowa Department of Transportation, Kansas Department of Transportation, Minnesota Department of Transportation, Missouri Department of Transportation, Nebraska Department of Roads, Ohio Department of Transportation, South Dakota Department of Transportation, and Wisconsin Department of Transportation for sponsoring this project; (2) MwRSF personnel for constructing the barriers and conducting the crash tests; (3) Center for Infrastructure Research, Engineering Research Center, and the University of Nebraska-Lincoln for matching support, and (4) Daniel Mushett, formerly of Buffalo Specialty Products - Timber Division for donating wood posts and blockouts.

A special thanks is also given to the following individuals who made a contribution to the completion of this research project.

Midwest Roadside Safety Facility

J.D. Reid, Ph.D., Assistant Professor
J.C. Holloway, M.S.C.E., E.I.T., Research Associate Engineer
K.L. Krenk, B.S.M.A., Field Operations Manager
E.A. Keller, E.I.T., Computer Design Technician II
M.L. Hanau, Laboratory Mechanic I
Undergraduate and Graduate Assistants

Iowa Department of Transportation

David Little, P.E., Deputy Director, Engineering Division
Jay Chiglo, P.E., Methods Engineer

Kansas Department of Transportation

Ron Seitz, P.E., Road Design Squad Leader

<u>Ohio Department of Transportation</u>

Monique Evans, P.E., Roadway Standards Engineer

<u>Minnesota Department of Transportation</u>

Ron Cassellius, Research Program Coordinator

<u>Missouri Department of Transportation</u>

Vince Imhoff, P.E., Senior Research and Development Engineer

<u>Nebraska Department of Roads</u>

Leona Kolbet, Research Coordinator
Ken Sieckmeyer, Transportation Planning Manager

<u>South Dakota Department of Transportation</u>

David Huft, Research Engineer

<u>Wisconsin Department of Transportation</u>

Rory Rhinesmith, P.E., Chief Roadway Development Engineer
Fred Wisner, Standards Development Engineer

<u>Federal Highway Administration</u>

Milo Cress, P.E., Nebraska Division Office
Frank Doland, P.E., Nebraska Division Office
John Ballantyne, P.E., Region VII

<u>Dunlap Photography</u>

James Dunlap, President and Owner

TABLE OF CONTENTS

List of Figures

Page

List of Tables

Page

1 INTRODUCTION

1.1 Problem Statement

Guardrails are often placed over box culverts to protect motorists from the hazard presented by cross-drainage culverts installed under highways. Unfortunately, the performance of these guardrails is seriously diminished when the box culvert is installed with less than 1,016 mm of fill material. In a situation where the guardrail extends across a culvert, it is usually necessary to attach the guardrail posts to the culvert surface. When the guardrail is impacted, these posts are severely deformed and often pulled loose, thereby causing significant damage to the culvert. The damage and expensive repair costs could be avoided if an unsupported guardrail segment could span across the culvert.

The Ohio Department of Transportation's (OhDOT's) Office of Structural Engineering issued a special plan sheet which provided details on several options for spanning culverts in low-fill situations which would not require attaching the guardrail posts to the culvert. However, these options for spanning culverts permitted the use of span lengths much longer than those successfully crash tested in previous research studies. It is noted that crash tests, based on passenger cars, have been performed successfully on span lengths of 3,810 mm and 5,715 mm according to the evaluation criteria provided by the National Cooperative Highway Research Program (NCHRP) Report No. 230, *Recommended Procedures for the Safety Performance Evaluation of Highway Appurtenances* (1). Since span lengths in excess of 5,715 mm have not been subjected to full-scale crash testing, these designs can no longer be used on Federal-aid highways unless shown to meet impact safety standards. Therefore, if OhDOT wishes to use longer unsupported span lengths (i.e., 7.62 to 9.14

m) to extend over low-fill culvert installations, then a need exists to develop and crash test a new guardrail system according to current safety guidelines.

1.2 Objective

The objective of the research project was to develop a new guardrail system for box culverts capable of unsupported spans on the order of 7.62 m. The new guardrail system was designed to meet the Test Level 3 (TL-3) safety performance criteria set forth in the NCHRP Report No. 350, *Recommended Procedures for the Safety Performance Evaluation of Highway Features* (2).

1.3 Scope

The research objective was to be achieved by performing several tasks. First, a literature review was performed on existing long-span guardrail systems as well as guardrail systems attached to culverts. Second, a concept development phase was performed to identify several prototype configurations to be further analyzed and evaluated. Third, computer simulation modeling was conducted to aid in the analysis, design, and evaluation of several long-span guardrail configurations. Fourth, full-scale vehicle crash tests were performed using ¾-ton pickup trucks, weighing approximately 2,000 kg, with target impact speeds and angles of 100.0 km/hr and 25 degrees, respectively. Finally, the test results were analyzed, evaluated, and documented. Conclusions and recommendations were then made that pertain to the safety performance of the new long-span guardrail system.

2 LITERATURE REVIEW

When culverts span more than 6.1 m, the American Association of State Highway Transportation Officials (AASHTO) defines them as bridge lengths and thus, normally require the use of a full-strength, rigid bridge rail (3). However, the use of a rigid bridge rail can potentially create a transition problem between the rigid bridge rail and the flexible roadside guardrail commonly used upstream of the bridge rail. Therefore, roadside guardrails are often continued over low-fill culverts to reduce construction costs.

Problems arise when the guardrails must continue across the culverts because of the shallowness of the soil fill. In such cases, full embedment of the guardrail posts is not possible. Crash testing has previously demonstrated that posts with shallow embedment depths can easily be pulled out of the ground, thus resulting in vehicle snagging or vaulting and causing potentially disastrous results (4). Therefore, the guardrail posts need sufficient embedment to: (1) develop the necessary friction to prevent the posts from pulling out of the ground; (2) develop sufficient lateral soil forces to develop the bending strength of the posts; and (3) provide energy dissipation through post rotation in soil.

A design that alleviates the diminished performance of the guardrail with shallow embedded posts has been successfully developed and successfully crash tested. This design involved welding base plates to the short steel posts and bolting them to the top surface of the concrete culvert (4). However, this design required that the front face of the W-beam be placed 914 mm from the head wall of the culvert to provide space for the guardrail and posts to deflect during impact. In some instances, this design required that the culvert be extended outward away from the roadway.

However, this alternative increases the cost of the structure, especially in rehabilitation projects where no other culvert work is needed (4).

In 1992, an alternative design was developed for the Kansas Department of Transportation (KsDOT) that provided a stiffer barrier and reduced the amount of deflection over the culvert (5). The successfully crash tested design consisted of a nested W-beam with half-post spacing. The steel posts were bolted to the top of the concrete culvert and installed adjacent to the concrete culvert head wall. For wood-post guardrail systems, steel posts must be used instead of wood ones for the segment over the low-fill culvert.

Previous designs for wood-post guardrail systems that eliminate the use of the seel posts in the segment over the culvert include unsupported guardrail segments which span across the culverts. Unsupported spans of 3.81 m and 5.72 m have been successfully crash tested according to the NCHRP Report No. 230 criteria using "passenger-size" sedans (6-7). These successful designs consisted of nested W-beam guardrail, which has twice the tensile capacity of a single rail. These designs are simpler and less expensive alternatives to the designs which require attachment of the base of the posts to the top of the culvert. These designs have been recommended for use with both wood-post and steel-post guardrail systems due to the compatible strengths of wood and steel posts (6).

3 TEST REQUIREMENTS AND EVALUATION CRITERIA

3.1 Test Requirements

Longitudinal barriers, such as long-span guardrail systems traversing culverts, must satisfy the requirements provided in NCHRP Report No. 350 to be accepted for use on new construction projects or as a replacement for existing transition designs not meeting current safety standards. According to Test Level 3 (TL-3) of NCHRP Report No. 350, long-span guardrail systems must be subjected to two full-scale vehicle crash tests: (1) a 2,000-kg pickup truck impacting at a speed of 100.0 km/hr and at an angle of 25 degrees; and (2) an 820-kg small car impacting at a speed of 100.0 km/hr and at an angle of 20 degrees. However, W-beam barriers struck by small cars have been shown to meet safety performance standards and to be essentially rigid (8-10), with no significant potential for occupant risk problems arising from vehicle pocketing or severe wheel snagging on the post at the downstream end of the long-span. Therefore, the 820-kg small car crash test was deemed unnecessary for this project.

3.2 Evaluation Criteria

Evaluation criteria for full-scale vehicle crash testing are based on three appraisal areas: (1) structural adequacy; (2) occupant risk; and (3) vehicle trajectory after collision. Criteria for structural adequacy are intended to evaluate the ability of the barrier to contain, redirect, or allow controlled vehicle penetration in a predictable manner. Occupant risk evaluates the degree of hazard to occupants in the impacting vehicle. Vehicle trajectory after collision is a measure of the potential for the post-impact trajectory of the vehicle to cause subsequent multi-vehicle accidents. It is also an indicator for the potential safety hazard for the occupants of the other vehicles or the occupants of the impacting vehicle when subjected to secondary collisions with other fixed objects. These three evaluation criteria are defined in Table 1. The full-scale vehicle crash tests were conducted and reported in accordance with the procedures provided in NCHRP Report No. 350.

Table 1. NCHRP Report 350 Evaluation Criteria for 2000P Pickup Truck Crash Test (2)

Structural Adequacy	A. Test article should contain and redirect the vehicle; the vehicle should not penetrate, underride, or override the installation although controlled lateral deflection of the test article is acceptable.
Occupant Risk	D. Detached elements, fragments or other debris from the test article should not penetrate or show potential for penetrating the occupant compartment, or present an undue hazard to other traffic, pedestrians, or personnel in a work zone. Deformations of, or intrusions into, the occupant compartment that could cause serious injuries should not be permitted.
	F. The vehicle should remain upright during and after collision although moderate roll, pitching, and yawing are acceptable.
Vehicle Trajectory	K. After collision it is preferable that the vehicle's trajectory not intrude into adjacent traffic lanes.
	L. The occupant impact velocity in the longitudinal direction should not exceed 12 m/sec and the occupant ridedown acceleration in the longitudinal direction should not exceed 20 G's.
	M. The exit angle from the test article preferably should be less than 60 percent of test impact angle, measured at time of vehicle loss of contact with test devise.

4 LONG-SPAN GUARDRAIL DESIGN (DESIGN NO. 1)

4.1 Design Considerations

The development of the long-span W-beam guardrail system required the consideration of three key factors: vehicle capture; rail tensile capacity; and the potential for pocketing and wheel snagging. For a long, unsupported length of guardrail extending across a culvert, vehicle capture becomes a significant consideration. Under the guidelines of NCHRP No. 230, previous crash testing of W-beam guardrails demonstrated that unsupported lengths up to 5.72 m were possible. However, the problem of vehicle capture is intensified under the NCHRP No. 350 guidelines due to the increased height of the center of mass for ¾-ton pickup trucks. According to the requirements of NCHRP No. 350, it is unlikely that a single W-beam rail, used in conjunction with a long unsupported length, will be capable of capturing a pickup truck. However, it may be possible to safely contain and redirect a pickup truck with the use of nested W-beam guardrail.

For a long-span guardrail system, the rail tensile capacity also becomes a key consideration in the design. Higher tensile loads and longitudinal strain in the rail would occur since dynamic lateral rail deflections would likely be larger than those observed during an impact into a guardrail system with a standard post spacing. Nested W-beam or single thrie beam, in combination with increased thickness, could be used to provide increased tensile capacity over the single 12-gauge W-beam rail. The final design consideration is the potential for vehicle pocketing and wheel snagging on the posts located on the downstream side of the unsupported length of guardrail. Therefore, the post type, embedment depth, and spacing were selected to minimize vehicle pocketing and wheel snagging. Finally, computer simulation modeling was used to investigate these design considerations to insure that the most cost-effective guardrail system was implemented. The results of the computer analysis are provided in Section 6.

4.2 Long-Span Guardrail Design Details

The total length of the test installation was 48.63-m long, as shown in Figure 1. Photographs of the test installation are shown in Figure 2. The test installation consisted of 30.48 m of nested 12-gauge W-beam rail supported by both CRT and steel posts, standard 12-gauge W-beam guardrail supported by steel posts, a simulated anchorage device on the downstream end, and an anchorage system replicating a Breakaway Cable Terminal (BCT) on the upstream end but installed tangent to the guardrail system and without the buffer head. The computer simulation modeling of the long-span design as well as the selection of the length are described in detail in Section 6.

The entire system was constructed with twenty-four guardrail posts. Post nos. 9A through 4A were part of an existing approach guardrail transition and used to anchor the downstream end. Post nos. 9A and 8A were galvanized, ASTM A36 steel W150x37 sections measuring 2,591-mm long. Post nos. 7A through 4A were galvanized, ASTM A36 steel W150x22 sections measuring 2,134-mm long. Post nos. 3A through 1 and 8 through 13 consisted of galvanized, ASTM A36 steel W150x13.5 sections measuring 1,830-mm long. Post nos. 2 through 7 were CRT timber posts measuring 150-mm wide x 200-mm deep x 1,830-mm long. Post nos. 14 and 15 were timber posts measuring 140-mm wide x 190-mm deep x 1,080-mm long and were placed in steel foundation tubes. The timber posts and foundation tubes were part of an anchor system, similar to a BCT but installed tangent to the system, used to develop the required tensile capacity of the guardrail. Lap-splice connections between the rail sections were configured to reduce vehicle snagging at the splice during the crash tests.

The spacing from the concrete end of the downstream anchor system to post no. 9A was 1,905-mm while the spacing between post nos. 9A through 5A was 952-mm as shown, in Figure 1. Post nos. 5A through 4 and 5 through 15 were spaced on 1,905-mm centers. The unsupported span between post nos. 4 and 5 was 7.62-m long.

The soil embedment lengths for post nos. 9A through 8A, 7A, 6A, and 5A through 4A were 1,838-mm deep, 1,381-mm deep, 1,355-mm deep, and 1,406-mm deep, respectively. For post nos. 3A through 13, the soil embedment depth was 1,102 mm. The posts were placed in a compacted coarse, crushed limestone material that met Grading B of AASHTO M147-65 (1990) as found in NCHRP Report No. 350.

For post nos. 9A through 6A, 150-mm wide x 200-mm deep x 457-mm long wood spacer blocks were used, while 150-mm wide x 200-mm deep x 356-mm long wood spacer blockouts were used at post nos. 5A and 4A. For post nos. 3A through 13, 150-mm wide x 200-mm deep x 360-mm long wood spacer blockouts were used to block the rail away from the posts.

The anchoring system at the downstream end of the barrier system consisted of a concrete buttress and a thrie beam approach guardrail transition system which existed from a previous research study, as shown in Figure 1. A standard 2.66-mm (12-gauge) W-beam rail, measuring 3,810-mm long, was placed between post nos. 5A and 3A, as shown in Figure 1. Subsequently, nested W-beam guardrail, measuring 2.66-mm thick and 31.48-m long, was used to span between post nos. 3A and 11. A standard 2.66-mm thick W-beam rail, measuring 7,620-mm long, was placed between post nos. 11 through 15. The top mounting height of the W-beam rail was 706 mm.

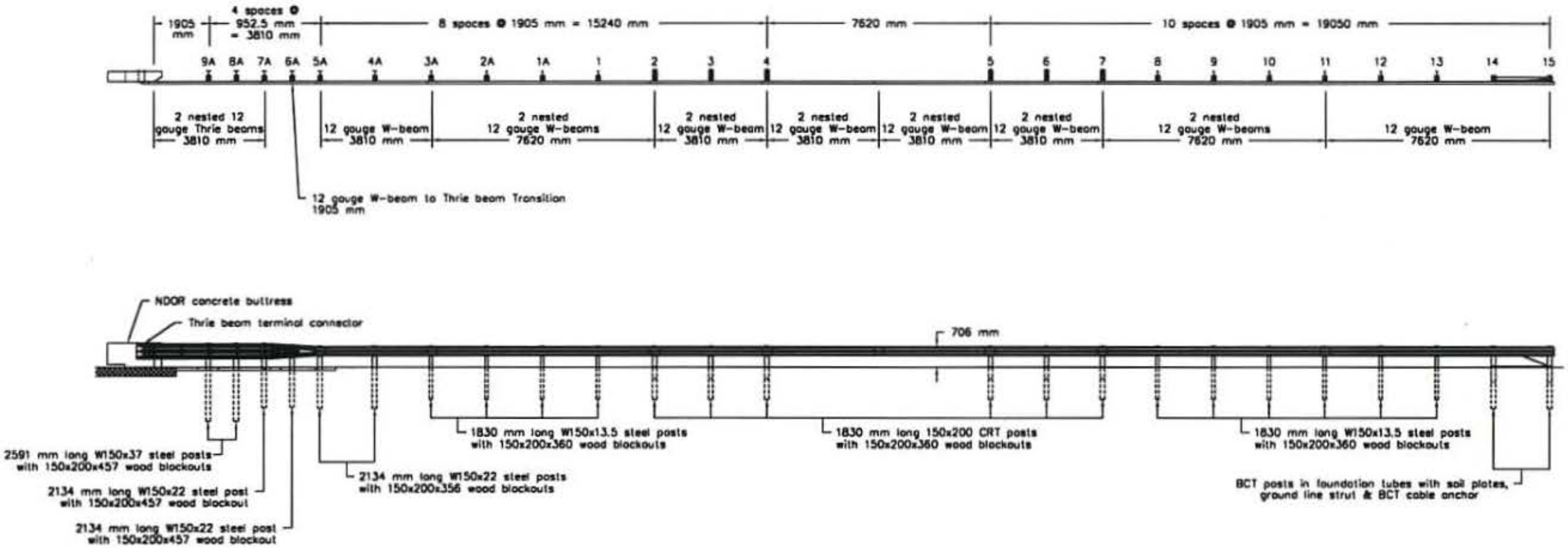

Figure 1. Test Installation Configuration

Figure 2. Long-Span Guardrail Element, Design No. 1

5 TEST CONDITIONS

5.1 Test Facility

The testing facility is located at the Lincoln Air-Park on the NW end of the Lincoln Municipal Airport and is approximately 8.0 km NW of the University of Nebraska-Lincoln. The site is protected by a 2.44-m high chain-link security fence.

5.2 Vehicle Tow and Guidance System

A reverse cable tow system with a 1:2 mechanical advantage was used to propel the test vehicles. The distance traveled and the speed of the tow vehicle were one-half that of the test vehicle. The test vehicle was released from the tow cable before impact with the bridge rail. A digital speedometer in the tow vehicle was utilized to increase the accuracy of the test vehicle impact speed.

A vehicle guidance system developed by Hinch (11) was used to steer the test vehicle. A guide-flag, attached to the front-left wheel and the guide cable, was sheared off before impact. The 9.5-mm diameter guide cable was tensioned to approximately 13.3 kN, and supported laterally and vertically every 30.48 m by hinged stanchions. The hinged stanchions stood upright while holding up the guide cable, but as the vehicle was towed down the line, the guide-flag struck and knocked each stanchion to the ground. The vehicle guidance system was approximately 457.2-m long.

5.3 Test Vehicles

For test OLS-1, a 1991 Chevrolet C-2500 ¾-ton pickup truck was used as the test vehicle. The test inertial and gross static weights were 1,999 kg. The test vehicle is shown in Figure 3, and vehicle dimensions are shown in Figure 4.

Figure 3. Test Vehicle, Test OLS-1

Date: 10/15/97 Test Number: OLS-1 Model: 2500

Make: CHEVROLET Vehicle I.D.#: 1GCFC24K9ME165224

Tire Size: 225/75R16 Year: 1991 Odometer: 153,540

*(All Measurements Refer to Impacting Side)

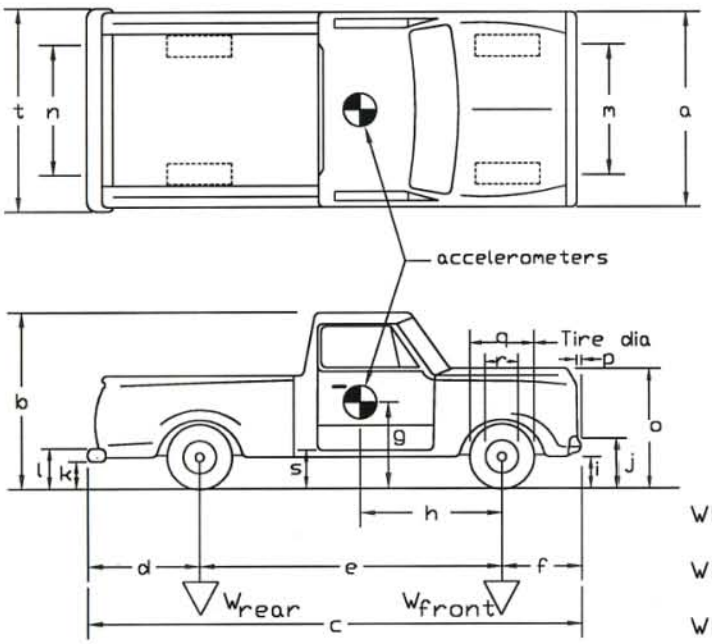

Vehicle Geometry - cm

a	184.15	b	177.8
c	546.1	d	130.81
e	334.01	f	81.28
g	73.66	h	147.32
i	36.83	j	58.42
k	53.34	l	72.39
m	158.75	n	162.56
o	104.14	p	7.62
q	74.93	r	44.45
s	40.005	t	182.88

Wheel Center Height Front 34.925

Wheel Center Height Rear 35.56

Wheel Well Clearance (FR) 83.82

Wheel Well Clearance (RR) 88.9

Engine Type V8

Engine Size 350 ci

Transmission Type:

Automatic or Manual

FWD or RWD or 4WD

Weights - kg	Curb	Test Inertial	Gross Static
W_{front}	1105	1118	1118
W_{rear}	847	881	881
W_{total}	1952	1999	1999

Note any damage prior to test: NONE

Figure 4. Vehicle Dimensions, Test OLS-1

For test OLS-2, a 1991 Chevrolet 2500 ¾-ton pickup truck was used as the test vehicle. The test inertial and gross static weights were 1,997 kg. The test vehicle is shown in Figure 5, and vehicle dimensions are shown in Figure 6.

The Suspension Method (12) was used to determine the vertical component of the center of gravity for the test vehicles. This method is based on the principle that the center of gravity of any freely suspended body is in the vertical plane through the point of suspension. The vehicle was suspended successively in three positions, and the respective planes containing the center of gravity were established. The intersection of these planes pinpointed the location of the center of gravity. The longitudinal component of the center of gravity was determined using the measured axle weights. The location of the final centers of gravity are shown in Figures 7 and 8.

Square, black and white-checkered targets were placed on the vehicle to aid in the analysis of the high-speed film, as shown in Figures 7 and 8. One target was placed on the center of gravity on the driver's side door, the passenger's side door, and on the roof of the vehicle. The remaining targets were located for reference so that they could be viewed from the high-speed cameras for film analysis.

The front wheels of the test vehicle were aligned for camber, caster, and toe-in values of zero so that the vehicle would track properly along the guide cable. Two 5B flash bulbs were mounted on both the hood and roof of the vehicle to pinpoint the time of impact with the bridge railing on the high-speed film. The flash bulbs were fired by a pressure tape switch mounted on the front face of the bumper. A remote controlled brake system was installed in the test vehicle so the vehicle could be brought safely to a stop after the test.

Figure 5. Test Vehicle, Test OLS-2

Date: 4/21/98 Test Number: OLS-2 Model: 2500

Make: CHEVROLET Vehicle I.D.#: 1GTFC24K8MI12042

Tire Size: 225/75R16D Year: 1991 Odometer: 6,511.5

*(All Measurements Refer to Impacting Side)

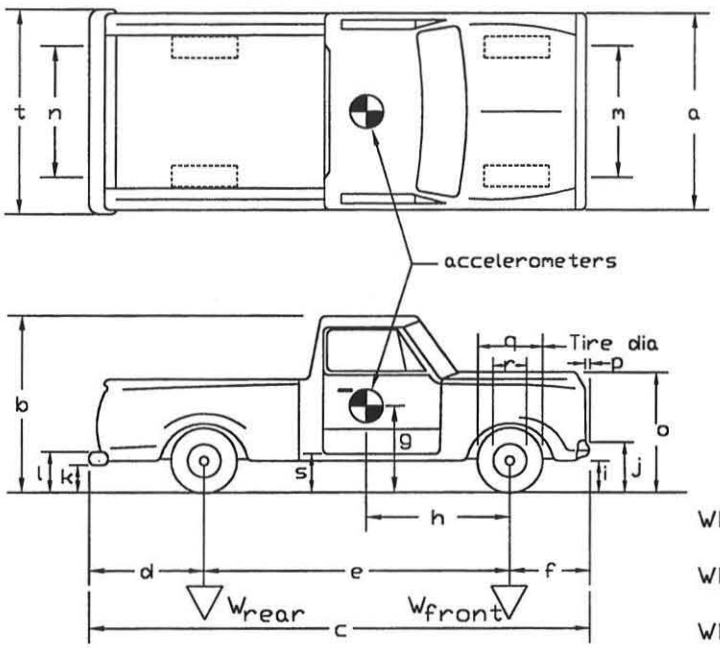

Vehicle Geometry - cm

a	193.68	b	176.53
c	554.99	d	132.08
e	334.01	f	88.9
g	74.93	h	149.86
i	38.1	j	59.69
k	76.2	l	57.15
m	158.75	n	161.93
o	99.06	p	9.53
q	72.39	r	44.45
s	40.64	t	186.69

Wheel Center Height Front 35.24

Wheel Center Height Rear 36.20

Wheel Well Clearance (FR) 82.55

Wheel Well Clearance (RR) 91.44

Engine Type V8

Engine Size 305

Transmission Type:

Automatic or Manual

FWD or RWD or 4WD

Weights - kg	Curb	Test Inertial	Gross Static
W_{front}	964	1081	1081
W_{rear}	767	916	916
W_{total}	1731	1997	1997

Note any damage prior to test: NONE

Figure 6. Vehicle Dimensions, Test OLS-2

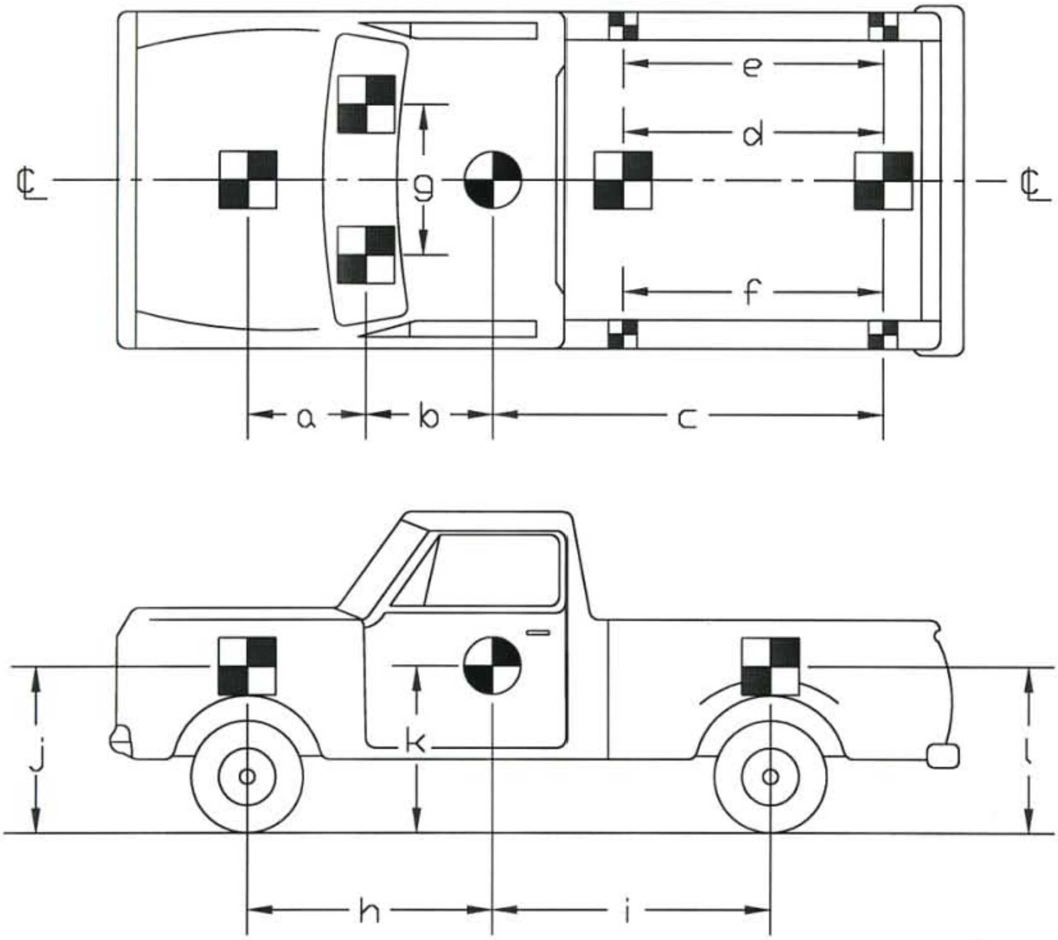

TEST #: OLS-1

TARGET GEOMETRY (cm)

a 101.6	b 63.5	c 266.7	d 175.9
e 175.3	f 175.3	g 73.7	h 147.3
i 187.3	j 96.5	k 73.7	l 104.1

Figure 7. Vehicle Target Locations, Test OLS-1

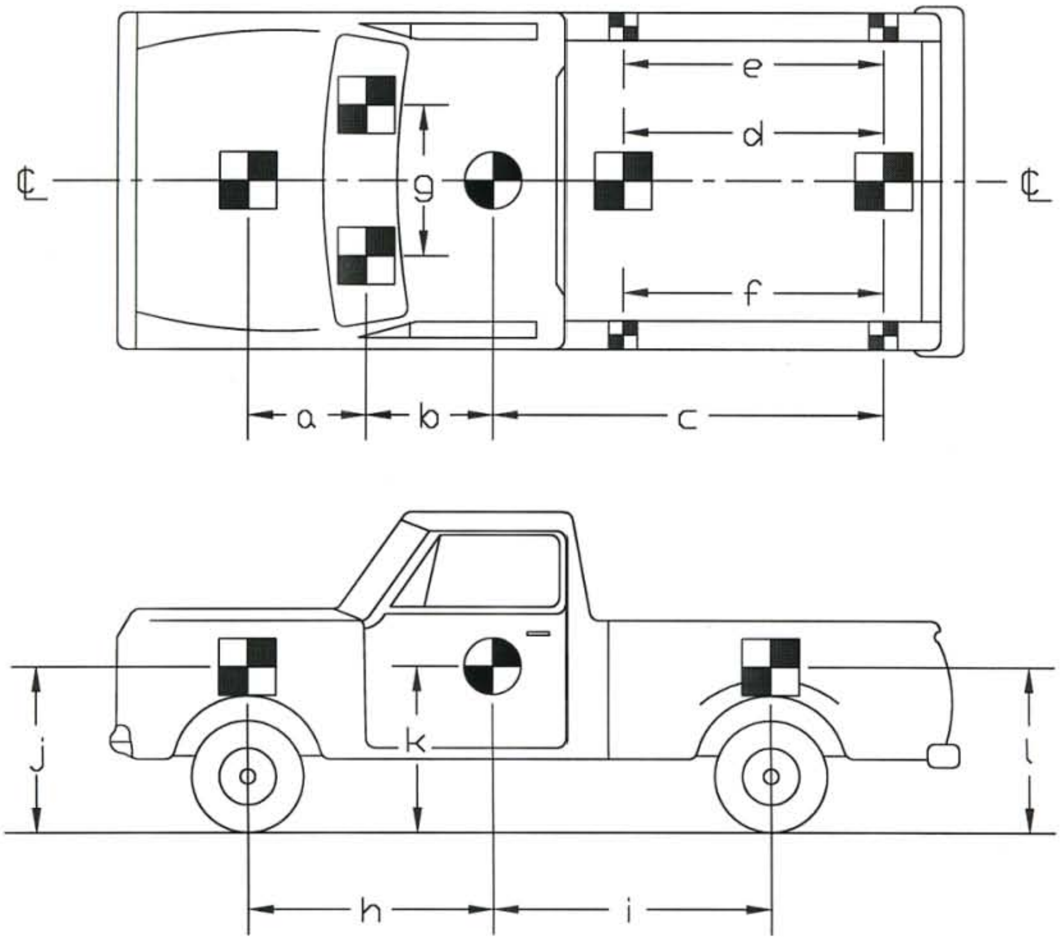

TEST #: OLS-2

TARGET GEOMETRY (cm)

a	130.2	b	68.6	c	275.0	d	154.9
e	215.3	f	215.3	g	101.6	h	149.9
i	184.2	j	92.7	k	74.9	l	101.6

Figure 8. Vehicle Target Locations, Test OLS-2

5.4 Data Acquisition Systems

5.4.1 Accelerometers

One triaxial piezoresistive accelerometer system with a range of ±200 G's was used to measure the acceleration in the longitudinal, lateral, and vertical directions at a sample rate of 10,000 Hz. The environmental shock and vibration sensor/recorder system, Model EDR-4M6, was developed by Instrumented Sensor Technology (IST) of Okemos, Michigan and includes three differential channels as well as three single-ended channels. The EDR-4 was configured with 6 Mb of RAM memory and a 1,500 Hz lowpass filter. Computer software, "DynaMax 1 (DM-1)" and "DADiSP" were used to digitize, analyze, and plot the accelerometer data.

A backup triaxial piezoresistive accelerometer system with a range of ±200 G's was also used to measure the acceleration in the longitudinal, lateral, and vertical directions at a sample rate of 3,200 Hz. The environmental shock and vibration sensor/recorder system, Model EDR-3, was developed by Instrumented Sensor Technology (IST) of Okemos, Michigan. The EDR-3 was configured with 256 Kb of RAM memory and a 1,120 Hz lowpass filter. Computer software, "DynaMax 1 (DM-1)" and "DADiSP" were used to digitize, analyze, and plot the accelerometer data.

5.4.2 Rate Transducer

A Humphrey 3-axis rate transducer with a range of 250 deg/sec in each of the three directions (pitch, roll, and yaw) was used to measure the rates of motion of the test vehicle. The rate transducer was rigidly attached to the vehicle near the center of gravity of the test vehicle. Rate transducer signals, excited by a 28 volt DC power source, were received through the three single-ended channels located externally on the EDR-4M6 and stored in the internal memory. The raw data measurements were then downloaded for analysis and plotted. Computer software, "DynaMax 1 (DM-1)" and "DADiSP" were used to digitize, analyze, and plot the rate transducer data.

5.4.3 High-Speed Photography

For test OLS-1, six high-speed 16-mm Red Lake Locam cameras, with operating speeds of approximately 500 frames/sec, were used to film the crash test. A Locam, with a wide-angle 12.5-mm lens, was placed above the test installation to provide a field of view perpendicular to the ground. A Locam with a 76 mm lens, a SVHS video camera, and a 35-mm still camera were placed downstream from the impact point and had a field of view parallel to the barrier. A Locam, with a 16 to 64-mm zoom lens, and a SVHS video camera were placed on the traffic side of the barrier and had a field of view perpendicular to the barrier. A Locam and a SVHS video camera were placed upstream and behind the barrier. Another Locam was placed two-thirds closer upstream and behind the barrier. A Locam was placed on the back side of the barrier and had a field of view perpendicular to the barrier. A schematic of all ten camera locations for test OLS-1 is shown in Figure 9.

For test OLS-2, five high-speed 16-mm Red Lake Locam cameras, with operating speeds of approximately 500 frames/sec, were used to film the crash test. A Locam, with a wide-angle 12.5-mm lens, was placed above the test installation to provide a field of view perpendicular to the ground. A Locam with a 76 mm lens, a SVHS video camera, and a 35-mm still camera were placed downstream from the impact point and had a field of view parallel to the barrier. A Locam, with a 16 to 64-mm zoom lens, and a SVHS video camera were placed on the traffic side of the barrier and had a field of view perpendicular to the barrier. A Locam and a SVHS video camera were placed downstream and behind the barrier. Another Locam was placed two-thirds closer downstream and behind the barrier. A schematic of all ten camera locations for test OLS-2 is shown in Figure 10. The film was analyzed using the Vanguard Motion Analyzer. Actual camera speed and camera divergence factors were considered in the analysis of the high-speed film.

5.4.4 Pressure Tape Switches

For tests OLS-1 and OLS-2, five pressure-activated tape switches, spaced at 2-m intervals, were used to determine the speed of the vehicle before impact. Each tape switch fired a strobe light which sent an electronic timing signal to the data acquisition system as the left-front tire of the test vehicle passed over it. Test vehicle speed was determined from electronic timing mark data recorded on "EGAA" software. Strobe lights and high-speed film analysis are used only as a backup in the event that vehicle speed cannot be determined from the electronic data.

5.4.5 Long-Span Guardrail Instrumentation

For test OLS-2, electronic sensors were placed on selected regions and components of the long-span guardrail system. Two types of sensors, strain gauges and string potentiometers, were used for the crash test and are described below.

5.4.5.1 Strain Gauges

For test OLS-2, ten strain gauges were installed on the W-beam guardrail, consisting of six gauges located on the back side of the W-beam guardrail and four gauges located on the front side of the W-beam guardrail. The strain gauge positions are shown in Figure 11.

For the test, weldable strain gauges, type LWK-06-W250B-350, were used. The nominal resistance of the gauges was 350.0 ± 1.4 ohms with a gauge factor equal to 2.02. The operating temperature limits of the gauges was -195 to +260 degrees Celsius. The strain limits of the gauges were 0.5% ($5000\mu\epsilon$) in tension or compression. The strain gauges were manufactured by Micro-

Measurements Division of Measurements Group, Inc. of Raleigh, North Carolina. The installation procedure required that the metal surface be clean and free from debris and oxidation. Once the surface had been prepared, the gauges were spot welded to the test surface.

A Measurements Group Vishay Model 2310 signal conditioning amplifier was used to condition and amplify the low-level signals to high-level outputs for multichannel, simultaneous dynamic recording on "Test Point" software. After each signal was amplified, it was sent to a Keithly Metrabyte DAS-1802HC data acquisition board, and then stored permanently on the portable computer. The sample rate for all gauges was 10,000 samples per second (10,000 Hz), and the duration of sampling was 6 seconds.

5.4.5.2 String Potentiometers

For test OLS-2, three string potentiometers (linear position transducers) were installed on the top of the W-beam surrounding the splice at post no. 22 and on the upper and lower bolts of post no. 26. The string potentiometer positions are shown in Figure 12. A schematic of the guardrail system and new post numbering for test OLS-2 is provided in Section 8.

Three UniMeasure PA-20 string potentiometers were used, each having a range of 20 in. During the test, the output voltage signals from the string potentiometers were sent to a Keithly Metrabyte DAS-1802HC data acquisition board, acquired by the "Test Point" software, and then stored permanently on the portable computer. The sample rate for the string potentiometers was 10,000 samples per second (10,000 Hz), and the duration of sampling was 6 seconds.

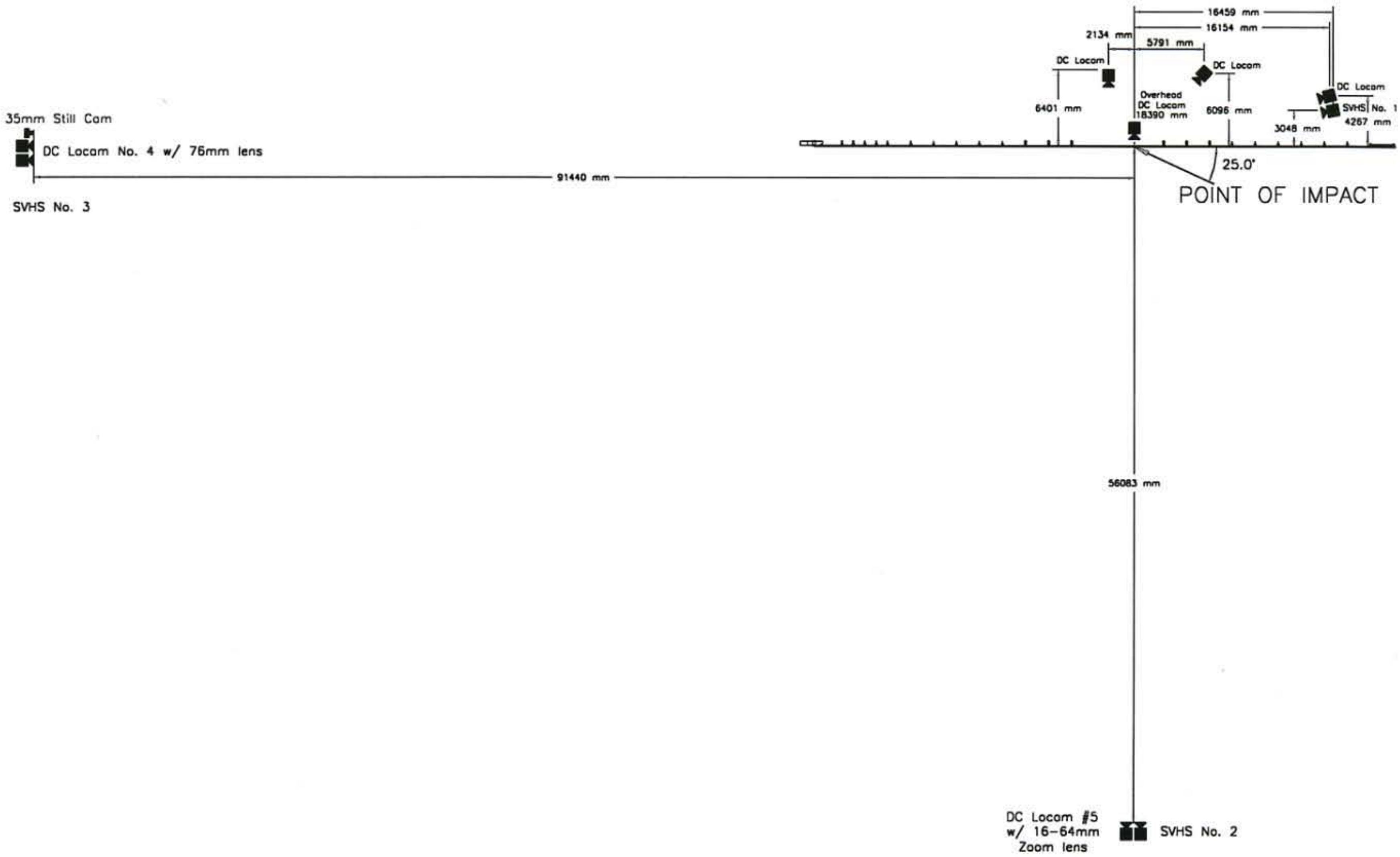

Figure 9. Location of High-Speed Cameras, Test OLS-1

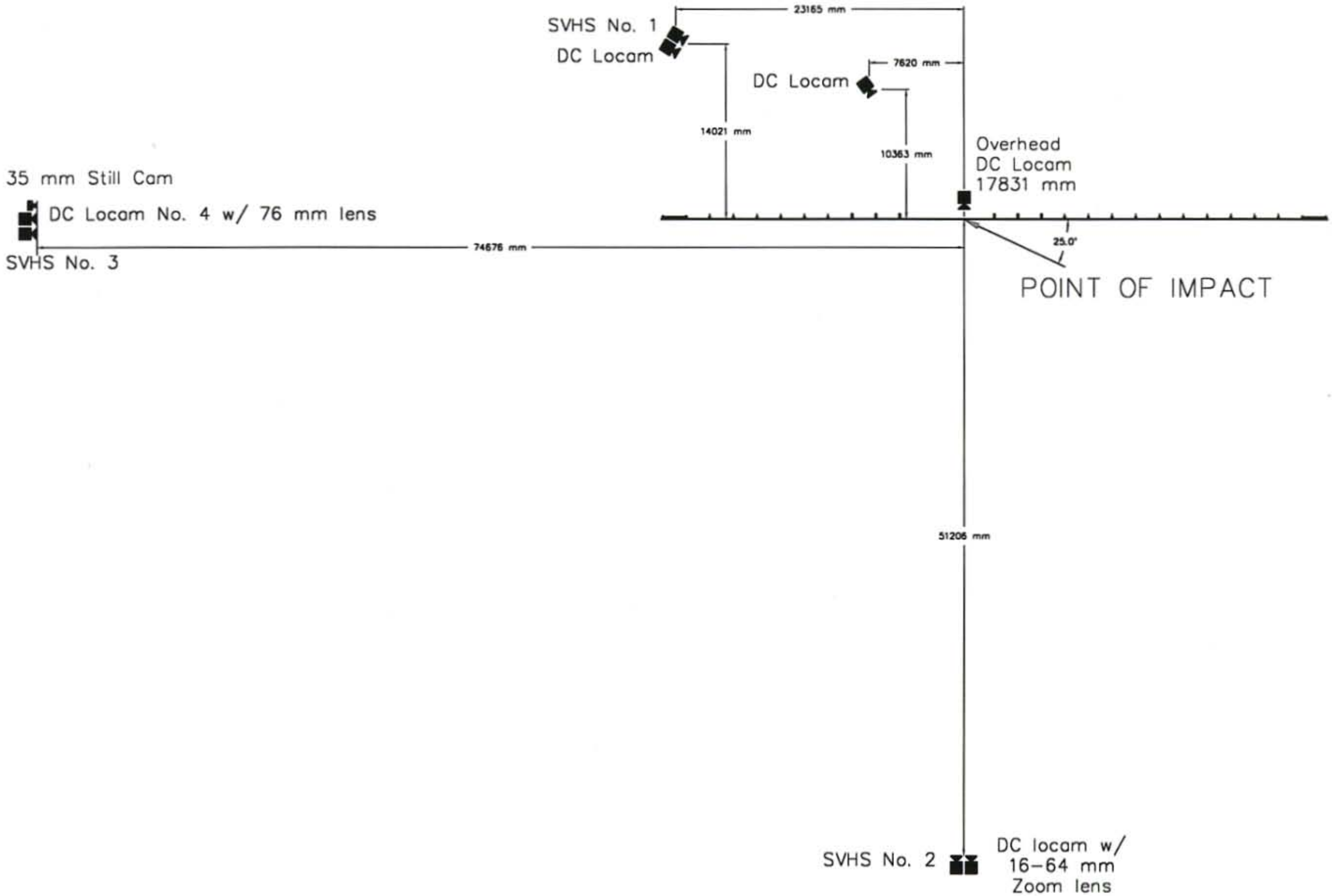

Figure 10. Location of High-Speed Cameras, Test OLS-2

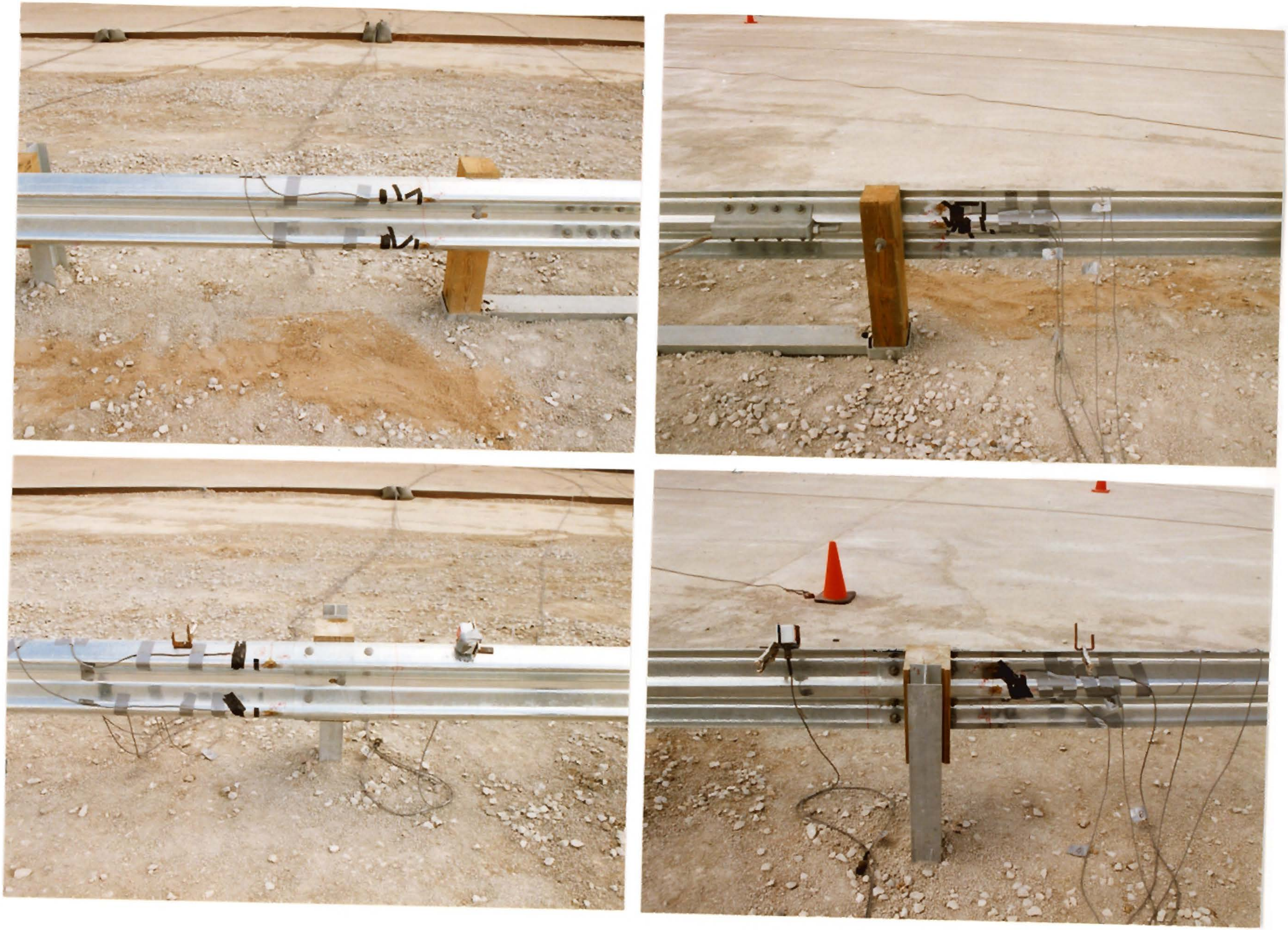

Figure 11. Strain Gauge Locations, Test OLS-2

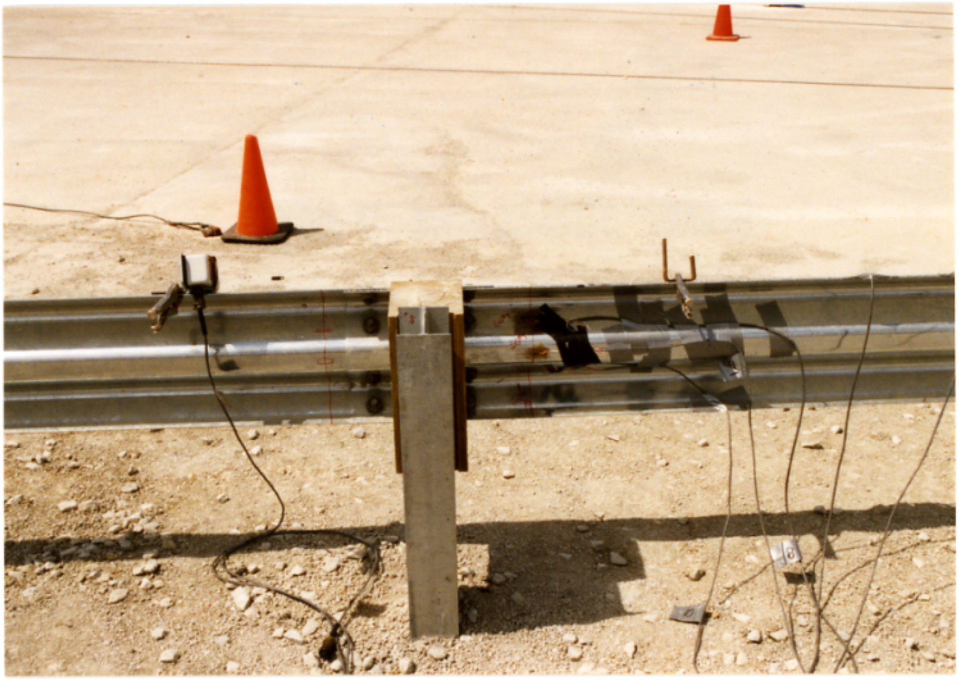

Figure 12. String Potentiometer Locations, Test OLS-2

6 COMPUTER SIMULATION (DESIGN NO. 1)

Computer simulation modeling with BARRIER VII (13) was performed to analyze and predict the dynamic performance of various long-span guardrail alternatives prior to full-scale vehicle crash testing. The simulations were conducted modeling a 2,041-kg sedan and an 1,996-kg pickup truck impacting at a speed of 96.6 km/hr and at an angle of 25 degrees. The BARRIER VII finite element models of the long-span guardrail systems and the idealized finite element, 2-dimensional vehicle models for both the 2,041-kg sedan and the 1,996-kg pickup truck are shown in Appendix B. A typical computer simulation input data file is shown in Appendix C.

Computer simulation was also used to determine the critical impact point (CIP) for the long-span guardrail system. The CIP was based upon the impact condition which produced the greatest potential for wheel-assembly snagging or vehicle pocketing on the first post at the downstream end of the long-span section (i.e., post no. 4 of Figure 1) or the greatest potential of rail rupture. Rupture of the W-beam rail was predicted by evaluating the maximum strain in the rail and comparing the value to the rated ductility.

Computer simulations were conducted on four long-span W-beam guardrail alternatives: (1) a 19.05-m nested section; (2) a 22.86-m nested section; (3) a 26.67-m nested section; and (4) a 30.48-m nested section. The finite element models for these design options are provided in Appendix B. A total of eight simulation runs were performed on the four alternatives using both the sedan and pickup truck models. The results of the computer simulations are shown in Table 2. The long-span guardrail alternative that produced the best results incorporated a 30.48-m long nested section of guardrail, as shown in Table 2. For the 30.48-m nested W-beam alternative, the results of the computer simulations indicated that the greatest potential for wheel snagging on CRT post no.

4 would occur with an impact between post nos. 4 and 5. The critical impact points were 2,134 mm and 2,438 mm downstream from post no. 5 for the sedan and the truck, respectively. Additionally, the predicted maximum lateral dynamic rail deflections for the sedan and the pickup truck were 908 mm and 839 mm, respectively, as measured to the center height of the rail.

Table 2. Barrier VII Computer Simulation Results

	19.05-m NESTED		22.86-m NESTED		26.67-m NESTED		30.48-m NESTED	
	SEDAN[1]	TRUCK[2]	SEDAN[1]	TRUCK[2]	SEDAN[1]	TRUCK[2]	SEDAN[1]	TRUCK[2]
Impact Point (mm)	2133.6	2438.4	2133.6	2438.4	2133.6	2438.4	2133.6	2438.4
Max. Dynamic Rail Deflection (mm)	942.09	861.31	932.69	855.98	925.07	837.69	907.54	839.47
Time of Contact (sec)	0.4302	0.3902	0.4302	0.3852	0.4277	0.3902	0.4250	0.3902
Length of Contact (m)	6.83	6.12	6.83	6.04	6.79	6.13	6.79	6.13
Speed @ Parallel (km/hr)	64.34	66.69	64.47	66.77	64.58	67.08	65.37	67.17
Time @ Parallel (sec)	0.2777	0.2572	0.2767	0.2562	0.2752	0.2550	0.2720	0.2540
Exit Speed (km/hr)	62.10	63.34	62.35	63.49	62.51	63.60	63.60	63.75
Exit Angle (degrees)	11.6	6.2	11.5	6.3	11.5	5.8	11.9	5.7
Velocity Change (km/hr)	-34.46	-33.22	-34.21	-32.91	-34.05	-32.96	-32.96	-32.81
Post Damage (failure at post #)	5	5	5	5	5	5	5	5
Max. Strain (splice)	0.000195	0.004088	0.002217	0.001631	0.002826	0.001545	0.001360	0.001192
Max. Strain (non-splice)	0.021383	0.005450	0.028377	0.001777	0.013439	0.001547	0.001527	0.001440
Max. Force (splice) (kN)	519.15	504.65	536.41	512.03	553.80	518.48	576.71	534.01
Max. Force (non-splice) (kN)	421.02	421.11	420.80	420.94	420.58	408.21	419.60	395.40

[1] The sedan weighed 2,041-kg and impacted the barrier at a speed of 96.56 km/hr and at an angle of 25.0 degrees.
[2] The pickup truck weighed 1,996-kg and impacted the barrier at a speed of 96.56 km/hr and at an angle of 25.0 degrees.

7 CRASH TEST NO. 1 (DESIGN NO. 1)

7.1 Test OLS-1

The 1,999-kg pickup truck impacted the long-span guardrail system (Design No. 1) at a speed of 101.3 km/hr and an angle of 25.4 degrees. A summary of the test results and the sequential photographs are shown in Figure 13. Additional sequential photographs are shown in Figure 14. Documentary photographs of the crash test are shown in Figure 15.

7.2 Test Description

Initial impact occurred between post nos. 4 and 5 or 2.44-m downstream from the center of post no. 5, as shown in Figure 16. At 0.062 sec after impact, the right-front corner of the vehicle was at the middle splice between post nos. 4 and 5. At 0.150 sec, the guardrail crushed the right-front side of the vehicle, while the right-front tire was deformed and protruded under the guardrail at 0.159 sec. The upstream portion of the guardrail began to move longitudinally at 0.164 sec after impact. At 0.170 sec, the BCT cable anchor failed. Subsequently, post nos. 4 through 6 fractured or split at 0.172 sec. At 0.197 sec after impact, the front end of the vehicle was at post no. 3. The vehicle impacted post no. 3 at 0.235 sec, resulting in post fracture. At 0.285 sec, the front end of the vehicle was at post no. 2, and the guardrail was positioned under the front of the vehicle. The vehicle became parallel to the guardrail at 0.316 sec after impact with a velocity of 57.5 km/hr. At 0.334 sec, the vehicle continued to be redirected when it yawed counter-clockwise (CCW) with the back corner of the vehicle contacting the guardrail. At 0.396 sec after impact, the vehicle's forward motion ceased, but the vehicle continued to rotate in a CCW motion. At 0.458 sec after impact, the rear end of the vehicle reached its maximum position above the ground. At 0.495 sec, the guardrail wrapped around the right-rear tire and moved up into the wheel well. At 0.878 sec, the vehicle was back on the ground and positioned approximately perpendicular to the system. The vehicle's post-impact trajectory is shown in Figure 13. The vehicle came to rest behind post nos. 1 and 2, approximately 6.55-m downstream from impact and 1.27-m laterally behind a line projected parallel to the traffic-side face of the rail, as shown in Figure 13.

7.3 Barrier Damage

Damage to the barrier was extensive, as shown in Figures 17 through 19. Barrier damage consisted mostly of deformed W-beam, contact marks on a guardrail section, deformed and fractured guardrail posts, and rupture of the cable anchor system on the upstream end. The BCT's cable anchor system failed during the test due to structural inadequacies in manufacturing of the swaged fitting, as shown in Figure 19. The lower bolt that anchors the cable between the two BCT posts of the cable anchor pulled out of the swaged fitting. The inside fitting threads became smooth as the bolt was pulled out. The end of the bolt was bent and the bolt threads were deformed, as shown in Figure 19. As shown in Figures 17 through 18, the failure of the BCT cable anchor system caused significant damage to the posts and guardrail.

Four steel posts, post nos. 8 through 11, were twisted and deformed. Both BCT posts were damaged with complete fracture of post no. 14 and partial splitting of post no. 15. Four CRT posts, nos. 3 through 5 were completely fractured, while post nos. 6 and 7 were partially split and remained standing. No significant post or guardrail damage occurred downstream of post no. 2.

The W-beam pulled off of post nos. 5 through 15. Contact marks were found on the guardrail between post nos. 3 and 4. Major guardrail buckling occurred upstream of post no. 2 and at post no. 3, with the buckling point at 3,810-mm downstream from post no. 5, as shown in Figure 18.

7.4 Vehicle Damage

Exterior vehicle damage was moderate, as shown in Figure 20. Occupant compartment damage was negligible. The vehicle experienced extensive frontal crush, as shown in Figure 20. The radiator was crushed inward toward the engine, and the engine was displaced into the firewall. Deformation occurred to both the left-front and right-front quarter panels. Damage to the left-side door occurred on the lower-rear corner. The front bumper was ripped off of the bumper mounts, flattened, and pushed inward toward the engine compartment. Frame damage was evident by the closing of the gap between the vehicle box and cab as well as the damage to the undercarriage, as shown in Figure 20.

7.5 Occupant Risk Values

The normalized longitudinal and lateral occupant impact velocities were not determined due to the failure of the barrier system as the vehicle penetrated through the system. The maximum 0.010-sec average occupant ridedown decelerations in the longitudinal and lateral directions also were not calculated due to the failure of the system. However, these results are shown graphically in Appendix D for use in further analysis and system redesign.

7.6 Discussion

The analysis of the test results for test OLS-1 showed that the long-span guardrail did not contain nor redirect the vehicle with controlled lateral displacements of the guardrail. Detached elements and debris from the test article did not penetrate or show potential for penetrating the occupant compartment. Deformations of, or intrusion into, the occupant compartment that could have caused serious injury did not occur. The vehicle remained upright during and after collision. The vehicle's trajectory did not intrude into adjacent traffic lanes, but the penetration of the vehicle through the system was unacceptable. Therefore, test OLS-1 conducted on Design No. 1 was determined to be unacceptable according to the NCHRP Report No. 350 criteria.

0.000 sec | 0.078 sec | 0.197 sec | 0.285 sec | 0.396 sec

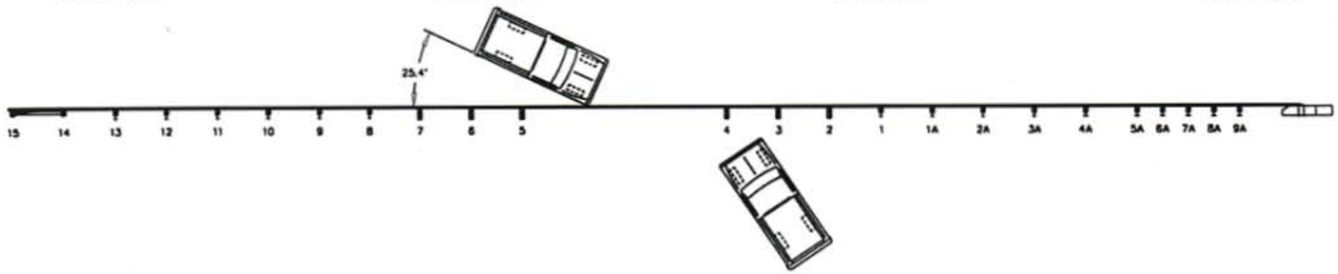

- Test Number OLS-1
- Date 10/15/97
- Appurtenance .... Nested W-beam long-span guardrail system
- Total Length .... 48.63 m
- Steel W-Beam (Nested)
  - Thickness .... 2.66 mm
  - Top Mounting Height ...... 706 mm
- Steel Posts
  - Post Nos. 9A - 8A .... W150x37 by 2,591-mm long
  - Post Nos. 7A - 4A .... W150x22 by 2,134-mm long
  - Post Nos. 3A - 1, 8 - 13 ..... W150x13.5 by 1,830-mm long
- Wood Posts
  - Post Nos. 2 - 7 (CRT) ...... 150 mm x 200 mm by 1,830-mm long
  - Post Nos. 14 - 15 (BCT) .... 140 mm x 190 mm by 1,080-mm long
- Wood Spacer Blocks
  - Post Nos. 9A - 6A .... 150 mm x 200 mm by 457-mm long
  - Post Nos. 5A - 4A .... 150 mm x 200 mm by 356-mm long
  - Post Nos. 3A - 13 .... 150 mm x 200 mm by 360-mm long
- Soil Type .... Grading B - AASHTO M 147-65 (1990)
- Vehicle Model .... 1991 Chevrolet 2500 2WD
  - Curb .... 1,952 kg
  - Test Inertial .... 1,999 kg
  - Gross Static .... 1,999 kg
- Vehicle Speed
  - Impact .... 101.3 km/hr
  - Exit .... NA
- Vehicle Angle
  - Impact .... 25.4 deg
  - Exit .... NA
- Vehicle Snagging .... NA
- Vehicle Pocketing .... NA
- Vehicle Stability .... Satisfactory
- Occupant Ridedown Deceleration (10 msec avg.)
  - Longitudinal .... NA
  - Lateral (not required) .... NA
- Occupant Impact Velocity (Normalized)
  - Longitudinal .... NA
  - Lateral (not required) .... NA
- Vehicle Damage .... Moderate
  - TAD[14] 1-RFQ-4/1-FR-4
  - SAE[15] 1-RFEE3
- Vehicle Stopping Distance .... Behind post nos. 1 and 2
  - Right Front Tire .... 6.55 m downstream, 1.27 m behind
- Barrier Damage .... BCT cable anchor system failure
- Maximum Deflections
  - Permanent Set .... NA
  - Dynamic .... NA

Figure 13. Summary of Test Results and Sequential Photographs, Test OLS-1 (Design No. 1)

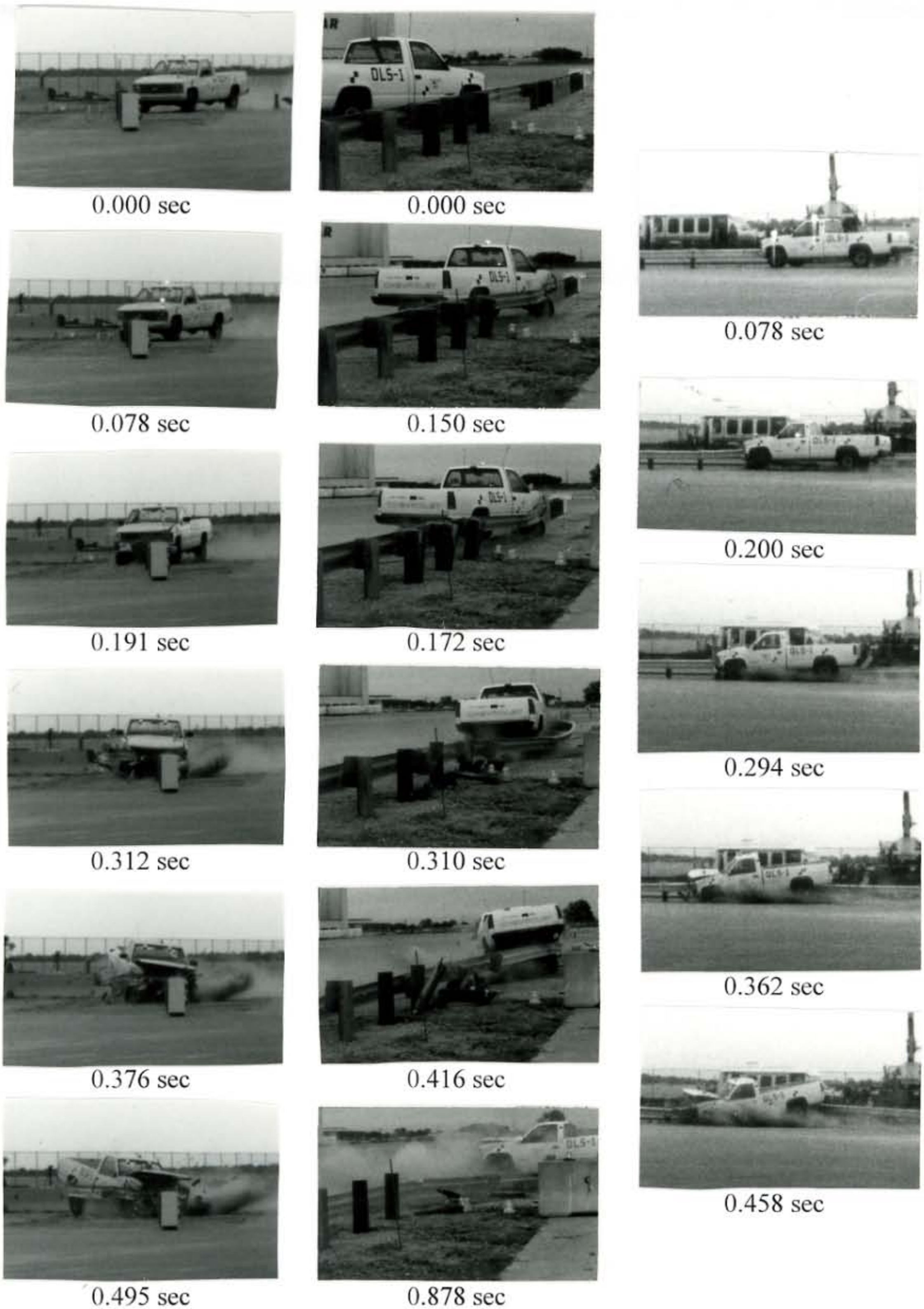

Figure 14. Additional Sequential Photographs, Test OLS-1 (Design No. 1)

Figure 15. Documentary Photographs, Test OLS-1 (Design No. 1)

Figure 16. Impact Location, Test OLS-1 (Design No. 1)

Figure 17. Long-Span Guardrail System Damage, Test OLS-1 (Design No. 1)

Figure 18. Long-Span Guardrail System Damage, Test OLS-1 (Design No. 1)

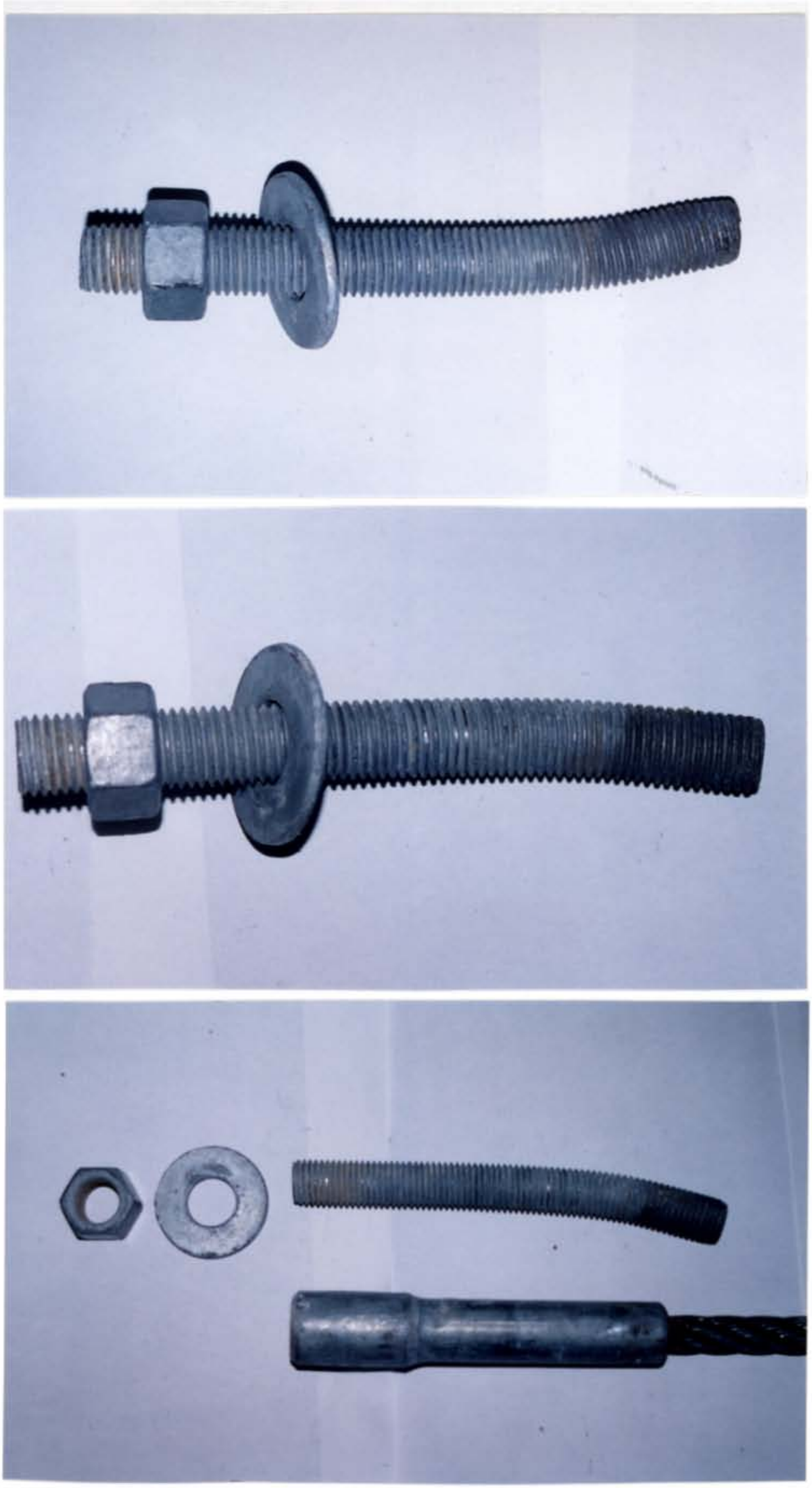

Figure 19. BCT Cable Anchor Damage, Test OLS-1 (Design No. 1)

Figure 20. Vehicle Damage, Test OLS-1 (Design No. 1)

8 DISCUSSION AND MODIFICATIONS (DESIGN NO. 2)

Following test OLS-1, a safety performance evaluation was conducted, and Design No. 1 was determined to be unacceptable according to the NCHRP Report No. 350 criteria. Due to the unsuccessful crash test of Design No. 1, it was necessary to determine the cause of the poor barrier performance so that design modifications could be made to the barrier system in order to improve its overall safety performance.

An analysis of the test results revealed that the vehicle did not override the long-span guardrail during the impact prior to the cable anchor failure. The lower cable anchor stud pulled out of the swaged fitting due to structural inadequacies in manufacturing. The release of the swaged fitting caused the guardrail to loose its tensile capacity. In addition, the loss of tensile capacity led to significant vehicle penetration into the guardrail system.

Following this investigation, MwRSF researchers determined that the safety performance of the long-span guardrail system (Design No. 1) could be significantly improved if the cable anchor system remains intact and develops the guardrail's tensile capacity. In order to overcome the loss of guardrail tensile capacity during test OLS-1, several modifications were made to the long-span guardrail system. The cable in the simulated BCT cable anchor system was replaced with a new cable that was more consistent with the required specifications. In addition, three other modifications were made to the guardrail system configuration prior to the retest. First, the downstream simulated anchorage device was replaced with an anchorage system more closely resembling a BCT but installed tangent to the guardrail system. Secondly, the total length of the test installation was increased to 53.34 m, while the final modification was to incorporate additional posts into the system. These modifications, included in Design No. 2, are shown in Figures 21 through 23.

The total length of the test installation was increased to 53.34-m long, as shown in Figure 21. The test installation consisted of 30.48 m of nested 12-gauge W-beam rail supported by both CRT and steel posts, standard 12-gauge W-beam guardrail supported by steel posts, and an anchorage system replicating a BCT on both the upstream and downstream ends but installed tangent to the guardrail system.

The entire system was constructed with twenty-six guardrail posts. Post nos. 3 through 8 and 15 through 24 were galvanized ASTM A36 steel W150x13.5 sections measuring 1,830-mm long. Post nos. 9 through 14 were CRT timber posts measuring 150-mm wide x 200-mm deep x 1,830-mm long. Post no. 1 through 2 and 25 through 26 were timber posts measuring 140-mm wide x 190-mm deep x 1,080-mm long and were placed in steel foundation tubes. The timber posts and foundation tubes were part of an anchor system, similar to a BCT but installed tangent to the system, used to develop the required tensile capacity of the guardrail.

Post nos. 1 through 11 and 12 through 26 were spaced 1,905-mm on center. The unsupported span between post nos. 11 and 12 was 7.62-m long, as shown in Figure 21. For post nos. 3 through 24, the soil embedment depth was 1,102 mm. In addition, 150-mm wide x 200-mm deep x 360-mm long wood spacer blockouts were used to block the rail away from post no. 3 through 24..

A standard 2.66-mm thick W-beam rail, measuring 7,620-mm long, was placed between post nos. 1 and 5. Subsequently, nested W-beam guardrail, measuring 2.66-mm thick and 30.48-m long, was used to span between post nos. 5 and 18. A standard 2.66-mm thick W-beam rail, measuring

7,620-mm long, was placed between post nos. 18 through 22 and another between post nos. 22 and 26, as shown in Figure 21. The top mounting height of the W-beam rail was 706 mm.

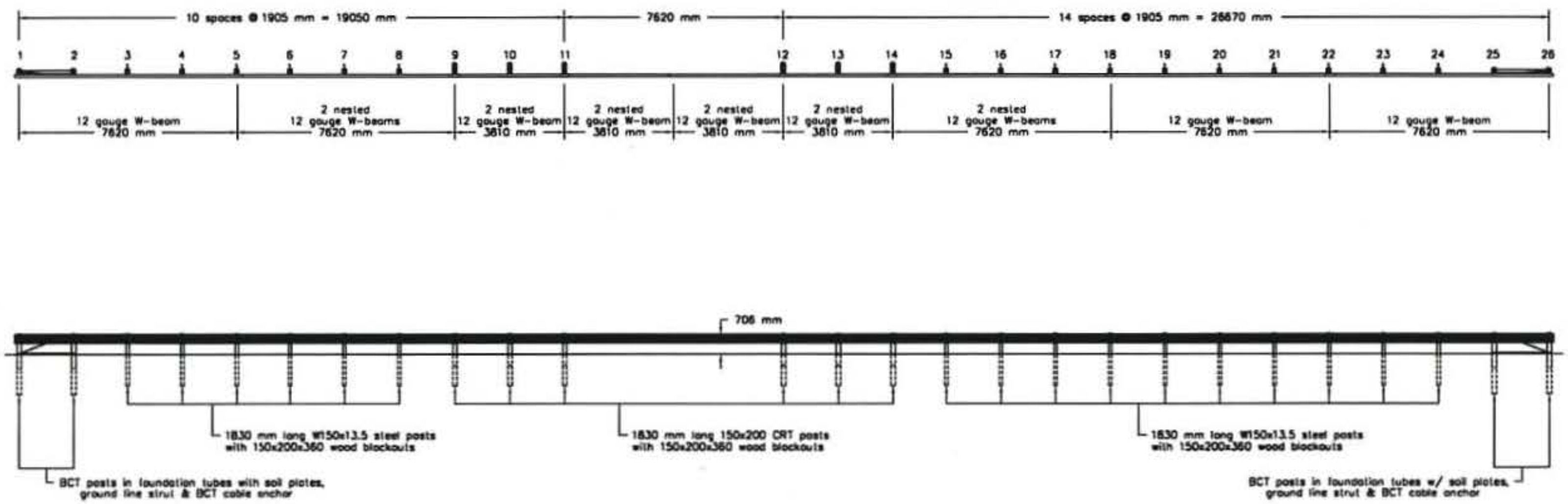

Figure 21. Modified Long-Span Guardrail System, Design No. 2

Figure 22. Long-Span Guardrail System, Design No. 2

Figure 23. Long-Span Guardrail System, Design No. 2

9 CRASH TEST NO. 2 (DESIGN NO. 2)

9.1 Test OLS-2

The 1,997-kg pickup truck impacted the modified long-span guardrail system (Design No. 2) at a speed of 102.7 km/hr and an angle of 24.5 degrees. A summary of the test results and the sequential photographs are shown in Figure 24. Additional sequential photographs are shown in Figures 25 and 26. Documentary photographs of the crash test are shown in Figures 27 through 29.

9.2 Test Description

Initial impact occurred between post nos. 11 and 12 or 2.44-m downstream from the center of post no. 12, as shown in Figure 30. At 0.024 sec after impact, the right-front corner of the bumper deformed. At 0.043 sec, the right-front corner of the vehicle was at the midpoint between post nos. 11 and 12. At 0.111 sec, the right-front corner of the vehicle crushed inward while post no. 11 fractured. At 0.126 sec after impact, the right-front tire protruded under the guardrail. At 0.182 sec, post nos. 10, 12, and 13 deflected, while the right-front corner of the vehicle was at the initial position of post no. 11. At 0.255 sec after impact, the right-front corner of the vehicle was at post no. 10 as the right-rear corner of the bumper contacted the guardrail. The vehicle became parallel to the guardrail at 0.263 sec after impact with a velocity of 73.2 km/hr. At 0.292 sec, the vehicle rolled counter-clockwise (CCW), allowing the left-front and left-rear tires to become airborne and the rear bumper to mount the top of the rail. At 0.302 sec, post no. 10 fractured. At 0.340 sec after impact, the right-front corner of the vehicle was at post no. 9, while the guardrail was positioned under the right-rear corner of the vehicle. At this time, the vehicle exited the guardrail at an angle of 16.7 degrees and a speed of 66.2 km/hr. At 0.428 sec, only the right-front corner of the vehicle was contacting the ground. At 0.450 sec, the right-front corner of the vehicle was at post no. 8, while the rear end of the vehicle yawed CCW into the guardrail. At 0.570 sec, the rear end of the vehicle yawed clockwise (CW) away from the guardrail. At 0.946 sec, the vehicle pitched and rolled across the front end and the right-front corner was airborne. The left-front corner of the vehicle was on the ground and the rear end rotated CW at 1.116 sec. At 1.260 sec, the entire vehicle rolled CW while airborne. At 1.444 sec after impact, the rear end of the vehicle contacted the ground on the left side as the vehicle continued its CW rotation. The vehicle's post-impact trajectory is shown in Figure 24. The vehicle came to rest 34.90 m downstream from impact and 10.73 m away from the traffic-side face of the rail, as shown in Figure 24.

9.3 Barrier Damage

Damage to the barrier was moderate, as shown in Figures 31 through 34. Figures 35 and 36 show the damage to the entire length of the CRT posts, nos. 9 through 14. Barrier damage consisted mostly of deformed W-beam, contact marks on a guardrail section, and deformed and fractured guardrail posts. The W-beam damage consisted of moderate deformation and flattening of the lower portion of the impacted section between post nos. 9 and 12. The W-beam was released from post nos. 2 and 25. Contact marks were found on the guardrail between post nos. 9 and 12.

Two CRT posts, post nos. 10 and 11 completely fractured while CRT post nos. 12 through 14 split longitudinally and remained standing, as shown in Figures 32, 33, 35, and 36. CRT post no. 9 fractured between the breakaway holes but remained upright, as shown in Figure 32. Steel post no. 8 slightly twisted as shown in Figure 34. No significant post or guardrail damage occurred upstream of post no. 15 nor downstream of post no. 7.

The permanent set of the guardrail and posts is shown in Figures 31 through 34. The cable anchor ends encountered slight permanent deformation, as shown in Figure 34. The maximum lateral permanent set rail and post deflections were approximately 956 mm at 5,715 mm downstream from the centerline of post no. 12 and 286 mm at post no. 12, respectively, as measured in the field. The maximum lateral dynamic rail and post defections were 1,342 mm at 6,668 mm downstream from the centerline of post no. 12 and 802 mm at post no. 10, respectively, as determined from the high-speed film analysis.

9.4 Vehicle Damage

Exterior vehicle damage was extensive, as shown in Figure 37. Minimal occupant compartment deformations occurred with only slight deformation of the firewall. The right-front quarter panel was crushed inward, and the right side of the front bumper was also bent back toward the engine compartment. The right-front wheel assembly was deformed slightly. The right-front and right-rear wheels sustained tire holes and rim damage. Longitudinal deformations, due to vehicle-rail interlock, were observed along the entire right side of the vehicle. The front, rear, and left-side window glass as well as the roof's sheet metal were severely crushed during vehicle rollover. The right-side window glass remained undamaged. The engine hood popped open after vehicle rollover.

9.5 Occupant Risk Values

The normalized longitudinal and lateral occupant impact velocities were determined to be 6.74 m/sec and 4.96 m/sec, respectively. The maximum 0.010-sec average occupant ridedown decelerations in the longitudinal and lateral directions were 6.35 g's and 8.27 g's, respectively. It is noted that the occupant impact velocities (OIV) and occupant ridedown decelerations (ORD) were within the suggested limits provided in NCHRP Report No. 350. The results of the occupant risk, determined from the accelerometer data, are summarized in Figure 24. Results are shown graphically in Appendix E. The results from the rate transducer are shown graphically in Appendix F.

9.6 Discussion

The analysis of the test results for test OLS-2 showed that the long-span guardrail satisfactorily contained the vehicle but inadequately redirected the vehicle since the vehicle did not remain upright after collision with the long-span guardrail. Detached elements and debris from the test article did not penetrate or show potential for penetrating the occupant compartment. Deformations of, or intrusion into, the occupant compartment that could have caused serious injury did not occur. After collision, the vehicle's trajectory intruded into adjacent traffic lanes. Therefore, test OLS-2 conducted on Design No. 2 was determined to be unacceptable according to the NCHRP Report No. 350 criteria.

9.7 Barrier Instrumentation Results

For test OLS-2, strain gauges were located on the front side and back side of the W-beam guardrail. The results of the strain gauge analysis are provided in Table 3. Results are shown graphically in Appendix G. For test OLS-2, string potentiometers were located on the top of the W-beam splice at post no. 22 and on the bolts of post no. 26. The results of the string potentiometer analysis are provided in Table 4. Results are shown graphically in Appendix H.

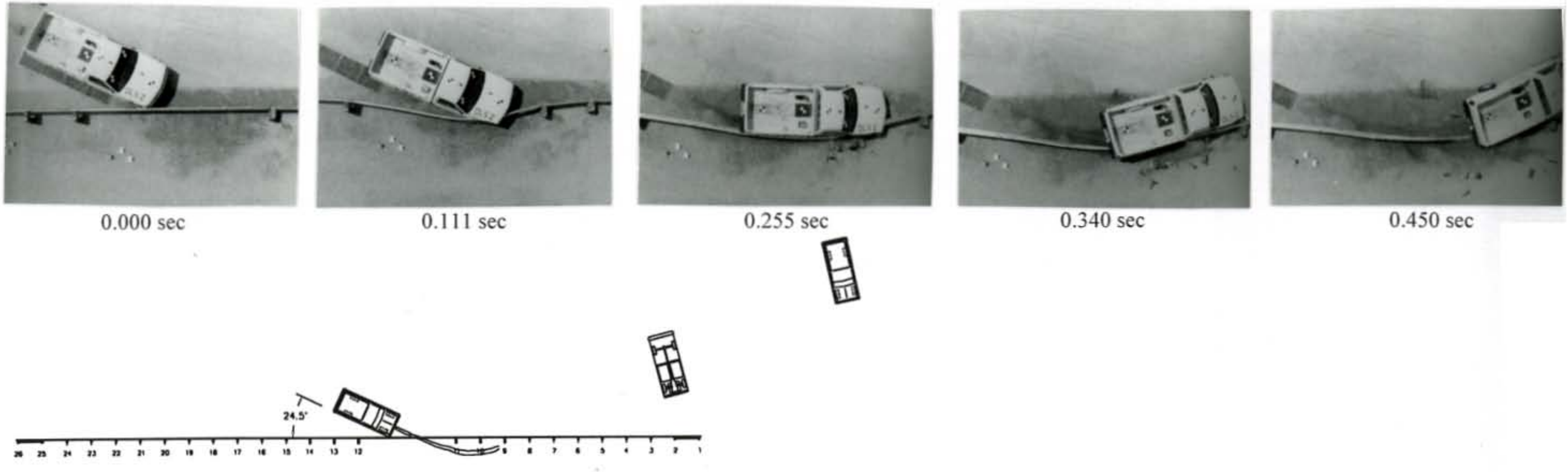

- Test Number OLS-2
- Date 4/21/98
- Appurtenance .... Nested W-beam long-span guardrail system
- Total Length .... 53.34 m
- Steel W-Beam (Nested)
  - Thickness .... 2.66 mm
  - Top Mounting Height ...... 706 mm
- Steel Posts
  - Post Nos. 3 - 8, 15 - 24 ..... W150x13.5 by 1,830-mm long
- Wood Posts
  - Post Nos. 9 - 14 (CRT) ..... 150 mm x 200 mm by 1,830-mm long
  - Post Nos. 1 - 2, 25 - 26 (BCT) 140 mm x 190 mm by 1,080-mm long
- Wood Spacer Blocks
  - Post Nos. 3 - 24 .... 150 mm x 200 mm by 360-mm long
- Soil Type .... Grading B - AASHTO M 147-65 (1990)
- Vehicle Model .... 1991 Chevrolet 2500 2WD
  - Curb .... 1,731 kg
  - Test Inertial .... 1,997 kg
  - Gross Static .... 1,997 kg
- Vehicle Speed
  - Impact .... 102.7 km/hr
  - Exit .... 66.2 km/hr
- Vehicle Angle
  - Impact .... 24.5 degrees
  - Exit .... 16.7 degrees
- Vehicle Snagging .... Minor contact on spacer blocks; Snagging on post no. 11
- Vehicle Pocketing .... Minor
- Vehicle Stability .... Vehicle rollover
- Occupant Ridedown Deceleration (10 msec avg.)
  - Longitudinal .... 6.35 < 20 G's
  - Lateral (not required) 8.27
- Occupant Impact Velocity (Normalized)
  - Longitudinal .... 6.74 < 12 m/s
  - Lateral (not required) 4.96
- Vehicle Damage .... Extensive
  - TAD[14] .... NA
  - SAE[15] .... NA
- Vehicle Stopping Distance .... 34.90 m downstream; 10.73 m traffic-side face
- Barrier Damage .... Moderate
- Maximum Deflections
  - Permanent Set .... 956 mm
  - Dynamic .... 1,342 mm

Figure 24. Summary of Test Results and Sequential Photographs, Test OLS-2 (Design No. 2)

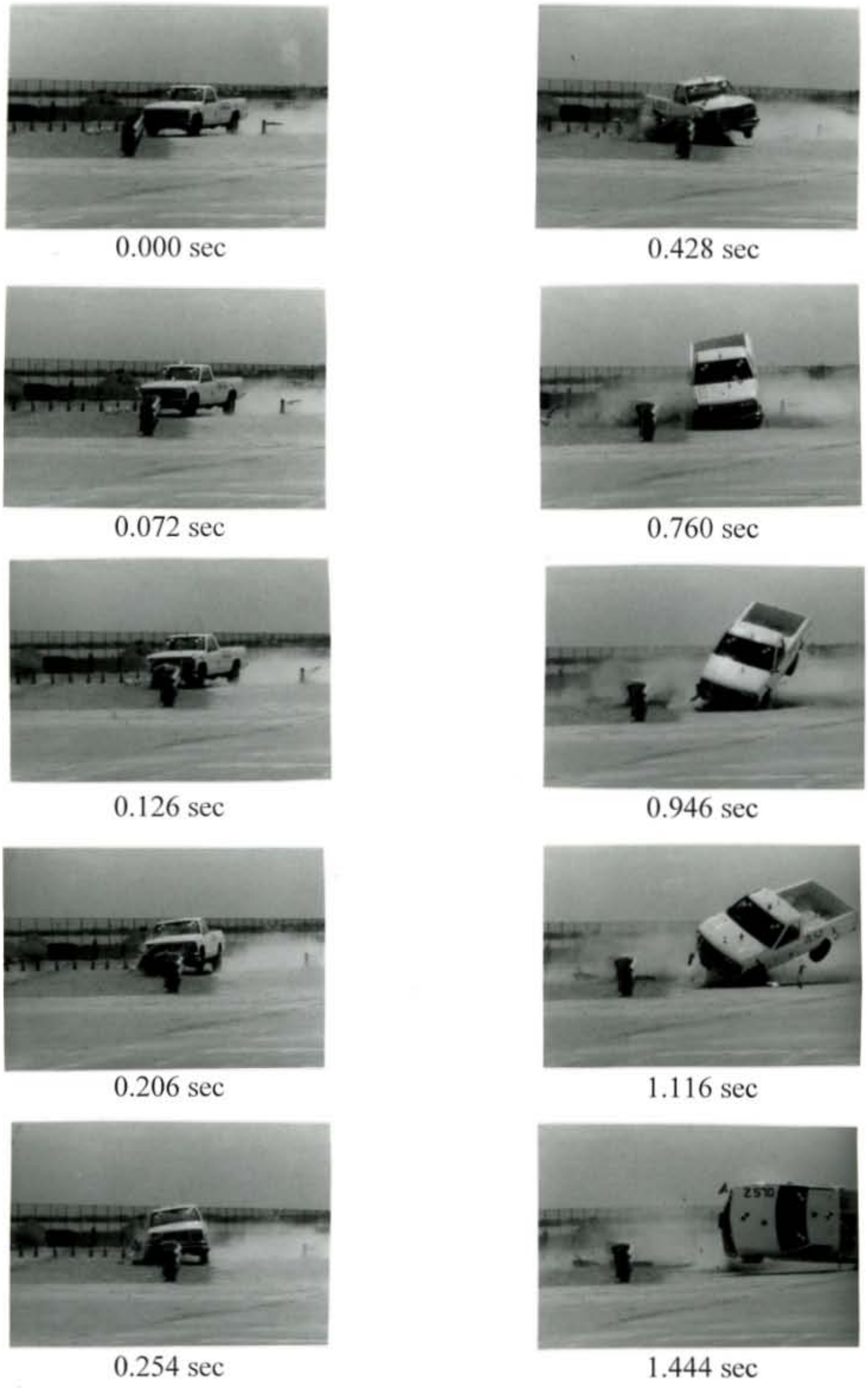

Figure 25. Additional Sequential Photographs, Test OLS-2 (Design No. 2)


0.000 sec


0.124 sec


0.275 sec

0.343 sec

0.547 sec


0.000 sec


0.024 sec

0.132 sec

0.202 sec

0.242 sec

Figure 26. Additional Sequential Photographs, Test OLS-2 (Design No. 2)

Figure 27. Documentary Photographs, Test OLS-2 (Design No. 2)

Figure 28. Documentary Photographs, Test OLS-2 (Design No. 2)

Figure 29. Documentary Photographs, Test OLS-2 (Design No. 2)

Figure 30. Impact Location, Test OLS-2 (Design No. 2)

Figure 31. Long-Span Guardrail System Damage, Test OLS-2 (Design No. 2)

Figure 32. Final CRT Post Positions, Test OLS-2 (Design No. 2)

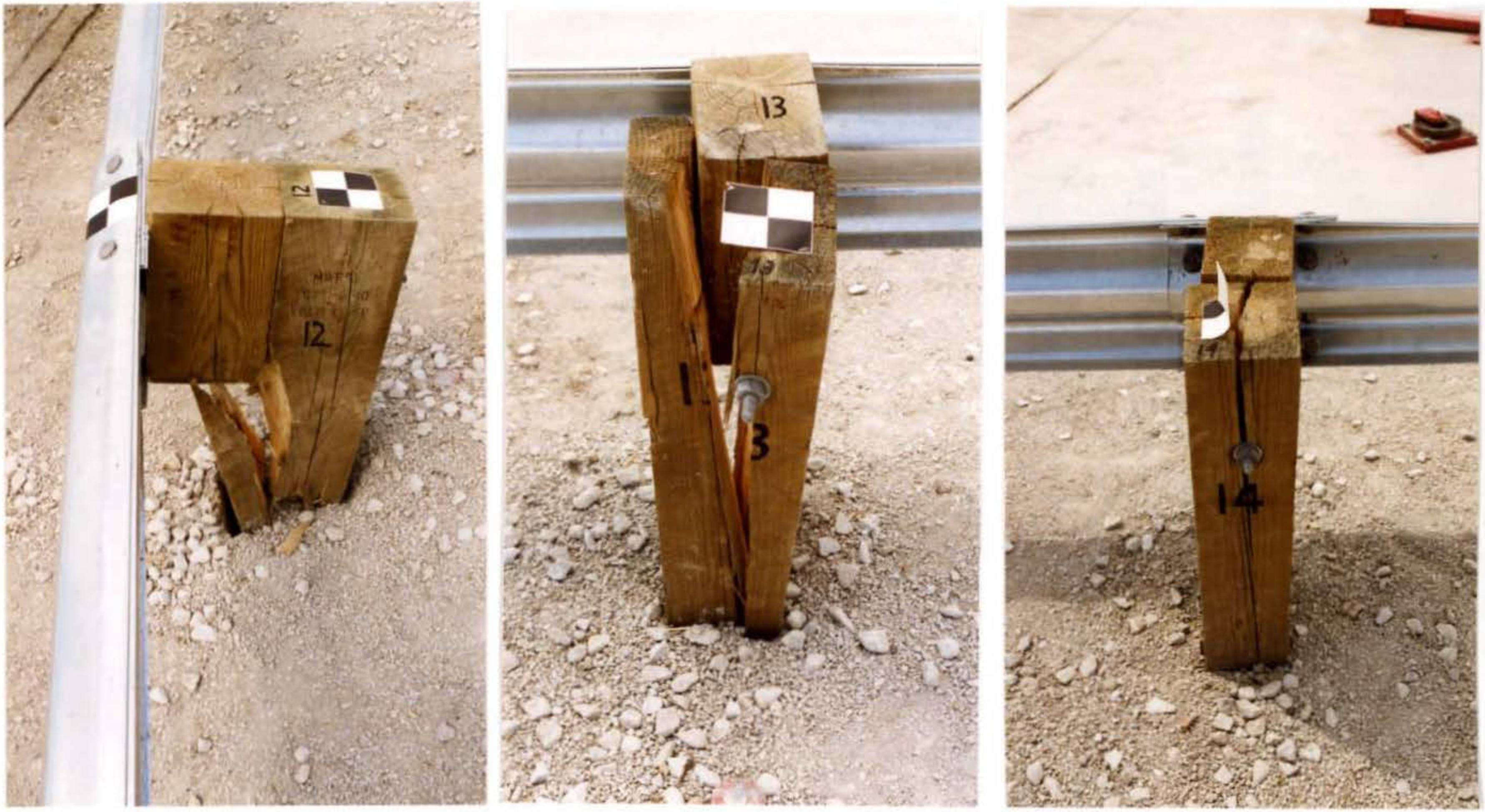

Figure 33. Final CRT Post Positions, Test OLS-2 (Design No. 2)

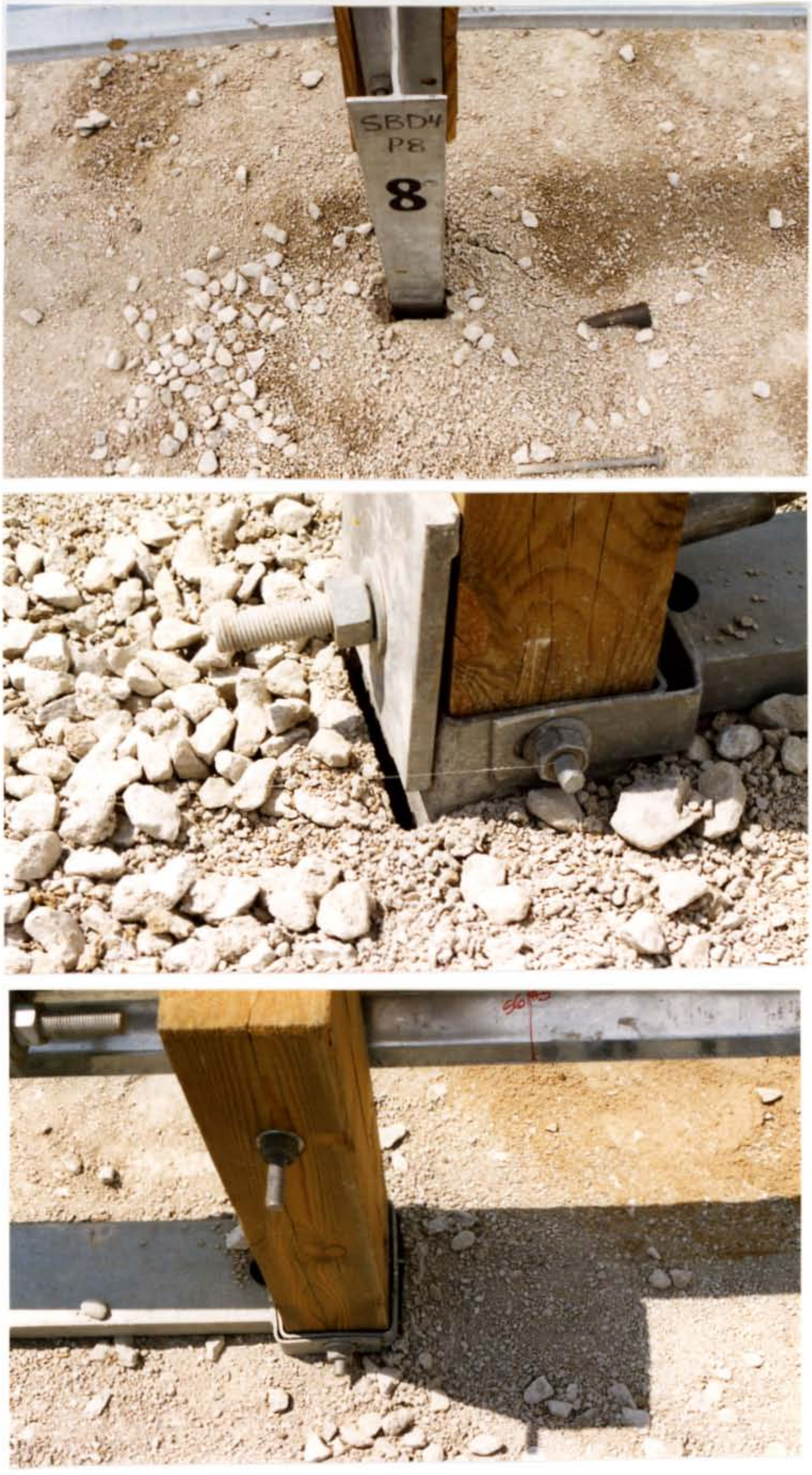

Figure 34. Permanent Set Deflections, Test OLS-2 (Design No. 2)

Post No. 9 | Post No. 10 | Post No. 11

Figure 35. CRT Post Damage, Test OLS-2 (Design No. 2)

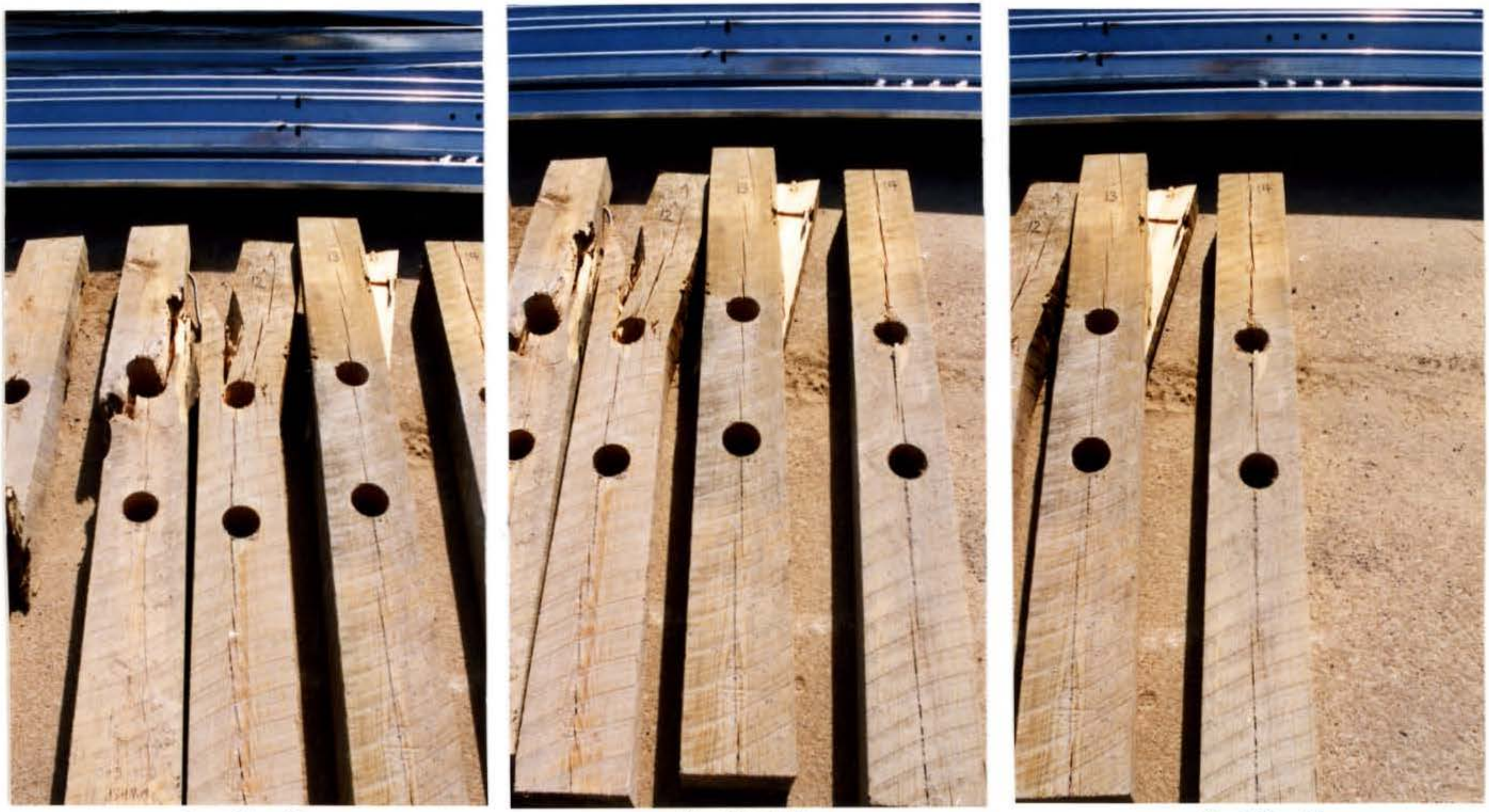

Post No. 12 Post No. 13 Post No. 14

Figure 36. CRT Post Damage, Test OLS-2 (Design No. 2)

Figure 37. Vehicle Damage, Test OLS-2 (Design No. 2)

Table 3. Strain Gauge Results, Test OLS-2 (Design No. 2)

Hardware Type	Strain Gauge No.	Strain Gauge Location	Maximum μ Strain[1] (mm/mm)	Maximum Stress[2] (MPa)	Comments
W-Beam	1	Note[3]	393	81.3	Top peak on front of rail
	2	Note[3]	228	47.3	Bottom peak on front of rail
	3	Note[3]	541	112.0	Neutral axis upper middle region on back of rail[4]
	4	Note[3]	870	180.0	Flat region on back of rail
	5	Note[3]	656	135.7	Neutral axis lower middle region on back of rail[4]
	6	Note[5]	558	115.4	Top peak on front of rail
	7	Note[5]	520	107.6	Bottom peak on front of rail
	8	Note[5]	623	128.9	Neutral axis upper middle region on back of rail[4]
	9	Note[5]	638	131.9	Flat region on back of rail
	10	Note[5]	620	128.2	Neutral axis lower middle region on back of rail[4]

[1] - All strain values are shown as the absolute value only.

[2] - All elastic stress values are shown as the absolute value only and calculated by multiplying the strain by the modulus elasticity equal to 207,000 MPa. Minimum yield stress for the W-beam is 345 MPa.

[3] - Strain gauge location is 229 mm downstream from the center of post no. 25.

[4] - Neutral axis location is 43 mm from the flat surface on the back of the rail.

[5] - Strain gauge location is 229 mm downstream from the center of post no. 22.

NA - Not available.

Table 4. String Potentiometer Results, Test OLS-2 (Design No. 2)

Hardware Type	String Pot. No.	String Pot. Location	Displacement (mm)	Comments
W-Beam	1	Note[1]	5.3	Top of rail surrounding the splice at post no. 22
Bolt	2	Post 26	34.8	Lower bolt at post no. 26
	3	Post 26	70.3	Upper bolt at post no. 26

[1] - String potentiometer location is the splice at post no. 22.

10 SUMMARY AND CONCLUSIONS

A long-span guardrail design for use over low-fill culverts was developed and full-scale vehicle crash tested. The long-span guardrail system was configured with a nested W-beam rail and incorporated an unsupported length of guardrail equal to 7.62 m. Two full-scale vehicle crash tests were performed according to the TL-3 criteria found in NCHRP Report No. 350. The first crash test, OLS-1 (Design No. 1), failed due to severe vehicle penetration into the guardrail system. This vehicle penetration occurred as a result of a loss of rail tensile capacity during vehicle redirection. The loss of rail capacity was determined to have occurred when the cable released from the swaged fitting in the BCT cable anchor assembly.

Based on knowledge gained from test OLS-1, the long-span guardrail system was redesigned. The primary changes included: replacing the downstream concrete anchor with a simulated BCT anchorage system, increasing the total system length, and adding extra guardrail posts. A second test, test OLS-2 (Design No. 2) was performed on the modified long-span guardrail system. During vehicle redirection, the pickup truck rolled over, and the test was determined to be unacceptable according to the safety performance criteria presented in NCHRP Report No. 350. The vehicle's instability was attributed to the interaction of the vehicle's front tire and suspension with the CRT posts immediately beyond the long-span section. A summary of the safety performance evaluation is provided in Table 5.

Table 5. Summary of Safety Performance Evaluation Results - Long-Span Guardrail System

Evaluation Factors	Evaluation Criteria	Test OLS-1 (Design No. 1)	Test OLS-2 (Design No. 2)
Structural Adequacy	A. Test article should contain and redirect the vehicle; the vehicle should not penetrate, underride, or override the installation although controlled lateral deflection of the test article is acceptable.	U	U
Occupant Risk	D. Detached elements, fragments or other debris from the test article should not penetrate or show potential for penetrating the occupant compartment, or present an undue hazard to other traffic, pedestrians, or personnel in a work zone. Deformations of, or intrusions into, the occupant compartment that could cause serious injuries should not be permitted.	S	S
	F. The vehicle should remain upright during and after collision although moderate roll, pitching and yawing are acceptable.	S	U
Vehicle Trajectory	K. After collision it is preferable that the vehicle's trajectory not intrude into adjacent traffic lanes.	S	U
	L. The occupant impact velocity in the longitudinal direction should not exceed 12 m/sec and the occupant ridedown acceleration in the longitudinal direction should not exceed 20 G's.	NA	S
	M. The exit angle from the test article preferably should be less than 60 percent of test impact angle, measured at time of vehicle loss of contact with test devise.	NA	U

S - (Satisfactory)
M - (Marginal)
U - (Unsatisfactory)
NA - Not Available

11 RECOMMENDATIONS

A long-span guardrail system designed for use over low-fill culverts, as described in this report, was not successfully crash tested according to the criteria found in NCHRP Report No. 350. Due to the failure of the end anchor assembly in Design No. 1, the results of this test indicate that this design was not a suitable design for use on Federal-aid highways. The results of the second test indicate that Design No. 2 was not a suitable design since the vehicle experienced rollover.

Analysis of test OLS-2 indicates that interaction of the impacting vehicle's front tire and suspension with the CRT posts immediately beyond the long-span section was a significant contributor to the vehicle's instability. Redesign efforts will include alternatives such as double blockouts adjacent to the free span to reduce this tire-post interaction. With appropriate modification, it is suggested that the long-span design described herein be retested.

It is also suggested that the research described herein could be further developed using the data collected from testing to modify future designs of different lengths. However, any design modifications made to the long-span guardrail system may require verification through the use of full-scale vehicle crash testing.

12 REFERENCES

1. Michie, J.D., *Recommended Procedures for the Safety Performance Evaluation of Highway ssAppurtenances*, National Cooperative Highway Research Program (NCHRP) Report No. 230, Transportation Research Board, Washington, D.C., March 1981.

2. Ross, H.E., Sicking, D.L., Zimmer, R.A. and Michie, J.D., *Recommended Procedures for the Safety Performance Evaluation of Highway Features*, National Cooperative Research Program (NCHRP) Report No. 350, Transportation Research Board, Washington, D.C., 1993.

3. *Standard Specifications for Highway Bridges*, Fifteenth Edition, American Association of State Highway and Transportation Officials, Washington, D.C., 1992.

4. Hirsch, T.J. and Beggs, D., *Use of Guardrails on Low Fill Bridge Length Culverts*, Transportation Research Record No. 1198, Transportation Research Board, National Research Council, Washington, D.C., 1988.

5. Pfeifer, B.G. and Luedke, J.K, *Safety Performance Evaluation of a Nested W-Beam with Half-Post Spacing Over a Low-Fill Culvert*, Final Report to the Kansas Department of Transportation, Transportation Report No. TRP-03-36-92, Midwest Roadside Safety Facility, University of Nebraska-Lincoln, March 1993.

6. *Memorandum on W-Beam Guardrail over Low-Fill Culverts*, September 9, 1991, File Designation HNG-14, Federal Highway Administration (FHWA), Washington, D.C., 1991.

7. Mak, K.K, Bligh, R.P., Gripne, D.J., and McDevitt, C.F., *Long-Span Nested W-Beam Guardrails over Low-Fill Culverts*, Transportation Research Record No. 1367, Transportation Research Board, National Research Council, Washington, D.C., 1992.

8. Buth, C.E., Campise, W.L., Griffin, III, L.I., Love, M.L., and Sicking, D.L., *Performance Limits of Longitudinal Barrier Systems - Volume I - Summary Report*, Report No. FHWA/RD-86/153, Submitted to the Office of Safety and Traffic Operations, Federal Highway Administration, Performed by Texas Transportation Institute, May 1986.

9. Ivey, D.L., Robertson, R., and Buth, C.E., *Test and Evaluation of W-Beam and Thrie-Beam Guardrails*, Report No. FHWA/RD-82/071, Submitted to the Office of Research, Federal Highway Administration, Performed by Texas Transportation Institute, March 1986.

10. Ross, H.E., Jr., Perera, H.S., Sicking, D.L., and Bligh, R.P., *Roadside Safety Design for Small Vehicles*, National Cooperative Highway Research Program (NCHRP) Report No. 318, Transportation Research Board, Washington, D.C., May 1989.

11. Hinch, J., Yang, T-L, and Owings, R., *Guidance Systems for Vehicle Testing*, ENSCO, Inc., Springfield, VA 1986.

12. *Center of Gravity Test Code - SAE J874 March 1981*, SAE Handbook Vol. 4, Society of Automotive Engineers, Inc., Warrendale, Pennsylvania, 1986.

13. Powell, G.H., *BARRIER VII: A Computer Program For Evaluation of Automobile Barrier Systems*, Prepared for: Federal Highway Administration, Report No. FHWA RD-73-51, April 1973.

14. *Vehicle Damage Scale for Traffic Investigators*, Second Edition, Technical Bulletin No. 1, Traffic Accident Data (TAD) Project, National Safety Council, Chicago, Illinois, 1971.

15. *Collision Deformation Classification - Recommended Practice J224 March 1980*, Handbook Volume 4, Society of Automotive Engineers (SAE), Warrendale, Pennsylvania, 1985.

13 APPENDICES

APPENDIX A

Relevant Correspondence

U.S. Department of Transportation
Federal Highway Administration

Memorandum

Subject: W-Beam Guardrail over Low-Fill Culverts

Date: SEP 9 1991

From: Chief, Federal-Aid and Design Division

Reply to Attn. of: HNG-14

To: Regional Federal Highway Administrators
Federal Lands Highway Program Administrator

Continuing a roadside guardrail across a low-fill culvert is a common situation on many highways throughout the country. In such cases, full embedment of the guardrail posts is not possible. Some designs specify shortened wood posts set in concrete; others use steel posts bolted to the culvert headwall. Both of these treatments increase installation costs and can be expensive to repair when hit. Several States construct a concrete safety shape across the culvert and attach the approach guardrail with an approved transition design, again significantly increasing project costs.

To reduce installation and repair costs, an alternate design was developed and tested. This design eliminated all posts over the culvert and reduced deflection by using nested w-beam throughout the clear span. The clear span length first tested was 3.8 meters (12.5-feet) long, using a 7.62 meter (25-foot) section of nested w-beam centered on the clear span. A second test demonstrated that a 5.72 meter (18-foot 9-inch) span, with the nested w-beam 11.4 meters (37-feet, 6 inches) long and centered on the clear span, also performed well. Summary sheets of these two designs and tests are attached for your review and transmittal to Federal Highway Administration Division Offices and appropriate State highway agencies. Either design may be used on Federal-aid projects if proposed by a State.

The full research report will be distributed normally when it is printed.

L. A. Staron

L. A. Staron

5 Attachments

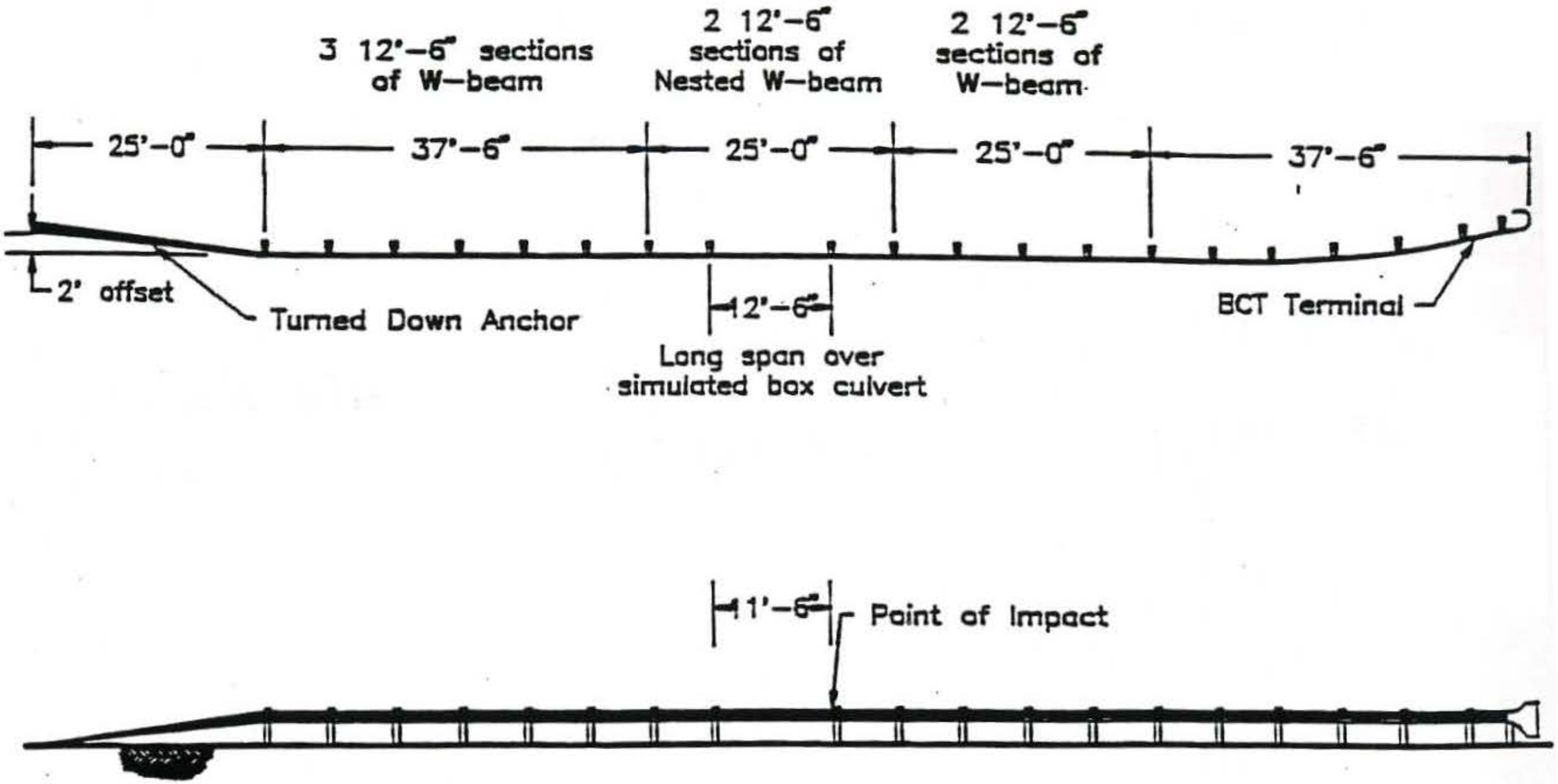

Figure 1. Schematics of installation for test 7147-2.

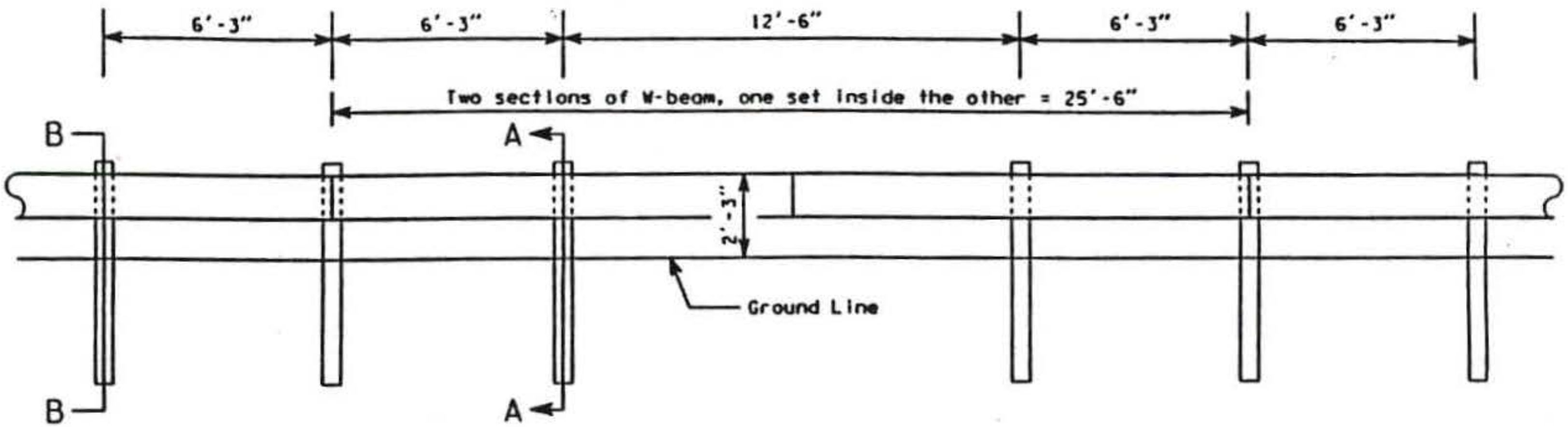

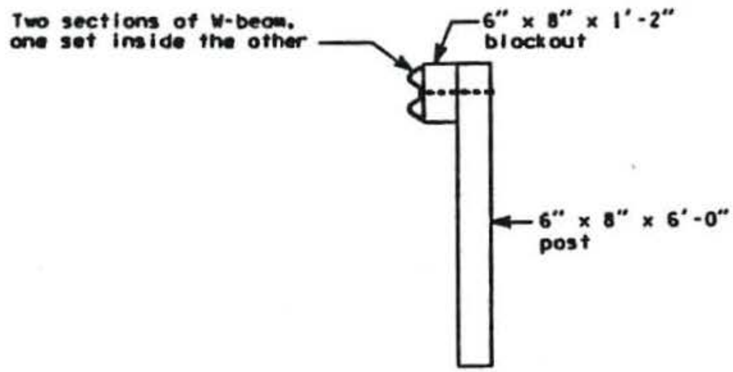

Section A-A

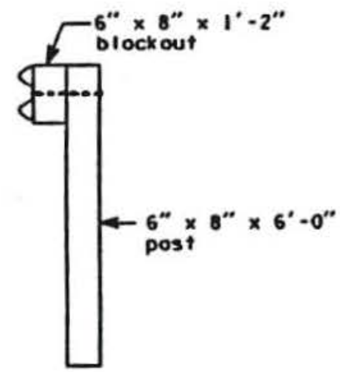

Section B-B

GUARDRAIL PLACEMENT

Case 19

(For splice in center of 12'-6" spacing)

STANDARD PLAN C-2k

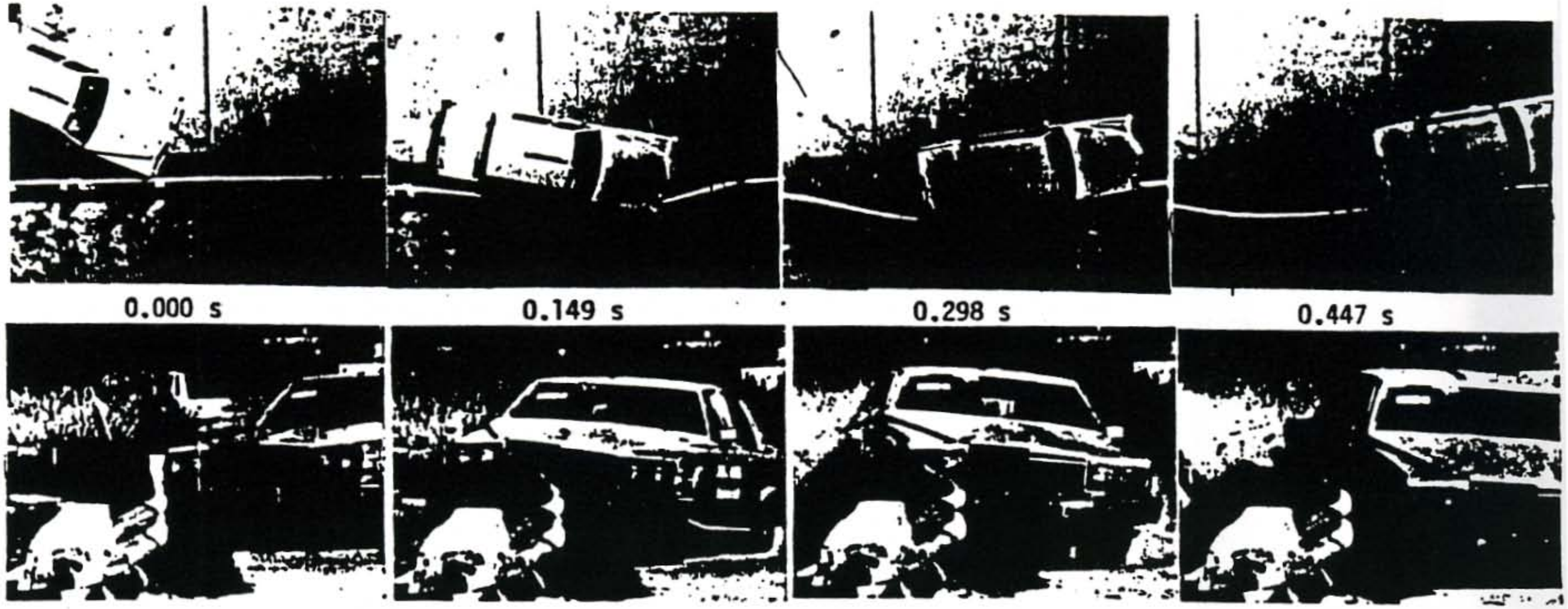

Test No. 7147-2
Date 09/25/90
Test Installation. . . . . Washington Nested W-beam with wood posts
Installation Length. . . 150 ft (46 m)
Max. Dynamic Deflection. 3.1 ft (0.9 m)
Max. Perm. Deformation . 2.4 ft (0.7 m)
Vehicle . . . . 1981 Cadillac Fleetwood
Vehicle Weight
Test Inertia . . . . . 4,500 lb (2,043 kg)
Gross Static . . . . . 4,669 lb (2,120 kg)
Vehicle Damage Classification
TAD . . . . 01FR5 & 01RD4
CDC . . . . 01FREK2 & 01RDEW3
Maximum Vehicle Crush . 13.0 in (33.0 cm)

Impact Speed . . . 62.7 mi/h (100.9 km/h)
Impact Angle . . . 24.5 degrees
Speed at Parallel . 49.4 mi/h (79.5 km/h)
Exit Speed . . . . 42.2 mi/h (67.9 km/h)
Exit Trajectory . . 11.0 degrees
Vehicle Accelerations
(Max. 0.050-sec Avg)
Longitudinal . . -4.5 g
Lateral . . . . . 7.1 g
Occupant Impact Velocity
Longitudinal . . 17.8 ft/s (5.4 m/s)
Lateral . . . . . 15.9 ft/s (4.8 m/s)
Occupant Ridedown Accelerations
Longitudinal . . -6.5 g
Lateral . . . . . 12.9 g

Figure 13. Summary of results for test 7147-2.

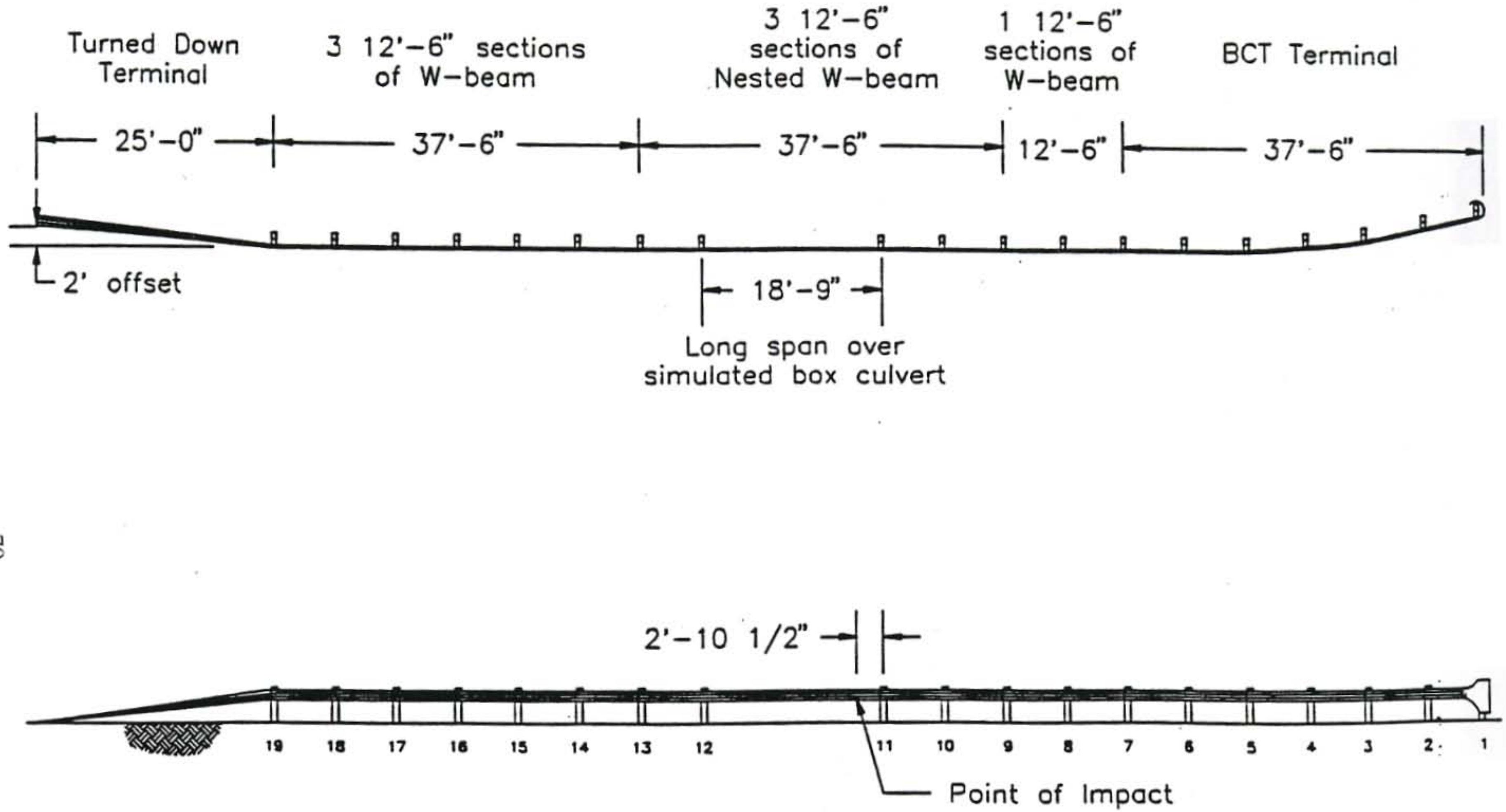

Figure 1. Details of Washington nested W-beam wood post guardrail with two posts over culvert for test 7147-5.

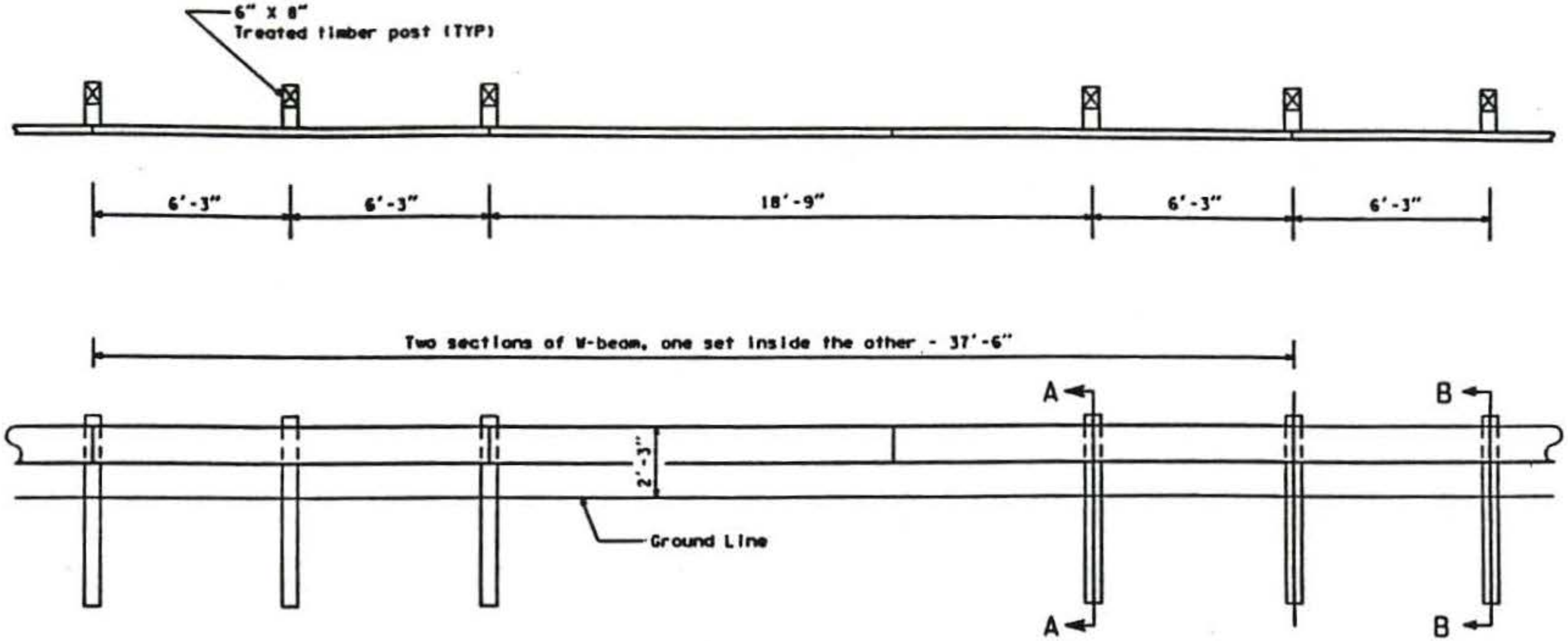

All rail elements are 12'-6".

For other details, see Standard Plan C-1.

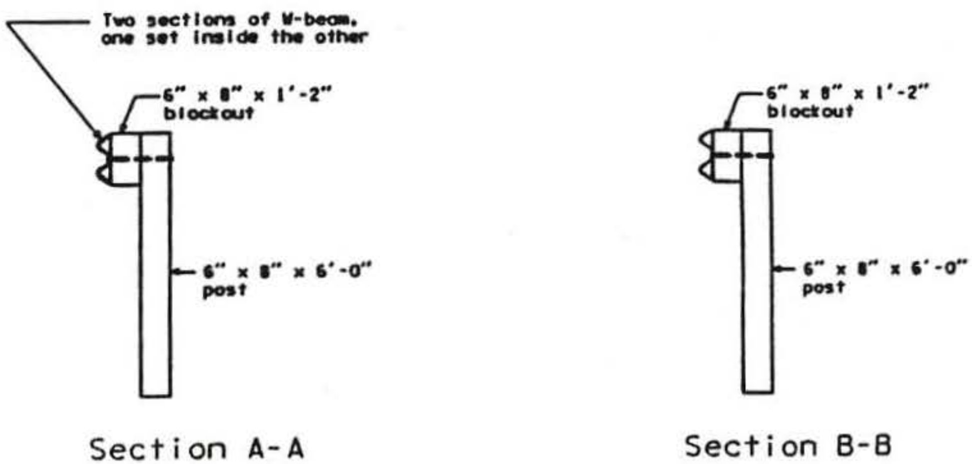

Case 2

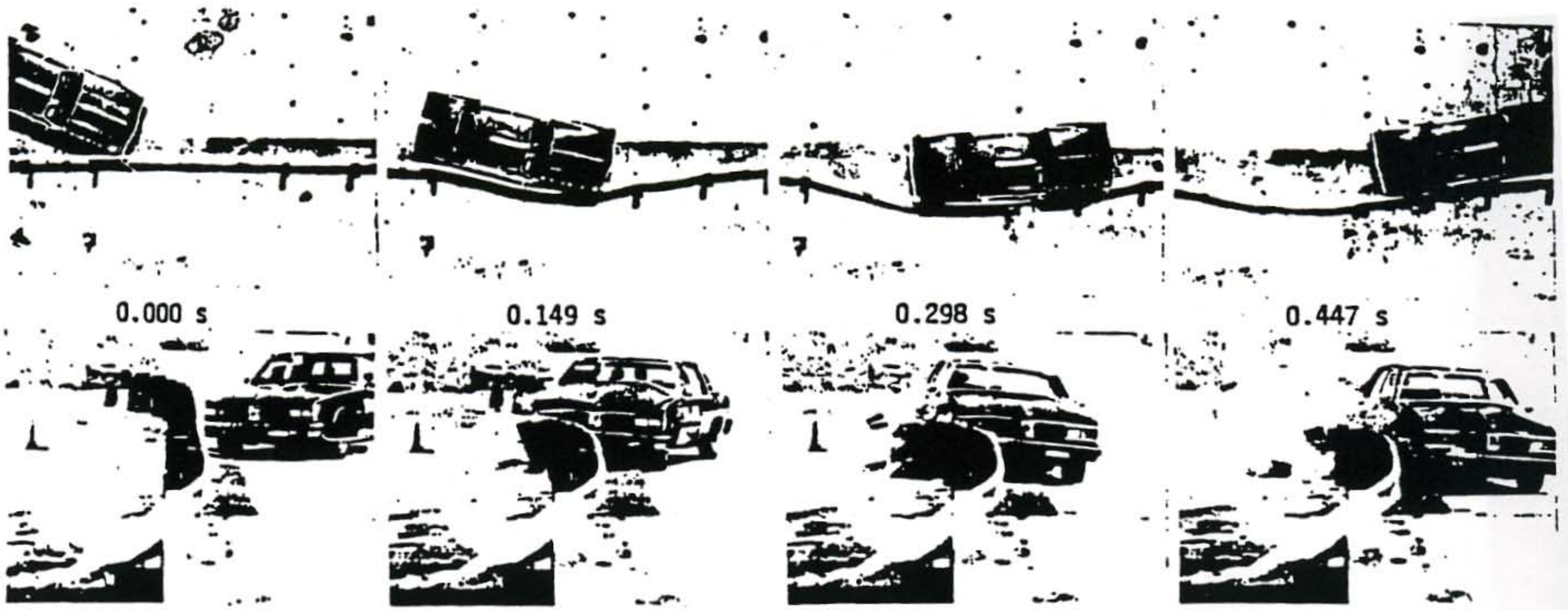

Test No.	7147-5
Date	05/30/91
Test Installation.	Washington Nested W-beam with wood posts
Installation Length. . .	150 ft (46 m)
Max. Dynamic Deflection.	3.2 ft (1.0 m)
Max. Perm. Deformation .	2.5 ft (0.8 m)
Vehicle	1982 Oldsmobile Regency 98
Vehicle Weight	
Test Inertia	4,500 lb (2,043 kg)
Gross Static	4,670 lb (2,120 kg)
Vehicle Damage Classification	
TAD	01FR4 & 01RD3
CDC	01FREK2 & 01RDEW2
Maximum Vehicle Crush .	8.0 in (20.3 cm)

Impact Speed . . .	60.9 mi/h (98.0 km/h)
Impact Angle . . .	25.1 degrees
Speed at Parallel .	48.6 mi/h (78.2 km/h)
Exit Speed	44.2 mi/h (71.1 km/h)
Exit Trajectory . .	10.4 degrees
Vehicle Accelerations (Max. 0.050-sec Avg)	
Longitudinal . .	-2.7 g
Lateral	6.8 g
Occupant Impact Velocity	
Longitudinal . .	14.7 ft/s (4.5 m/s)
Lateral	14.2 ft/s (4.3 m/s)
Occupant Ridedown Accelerations	
Longitudinal . .	-3.5 g
Lateral	9.7 g

Figure 1C. Summary of results for test 7147-5.

APPENDIX B

BARRIER VII Computer Models

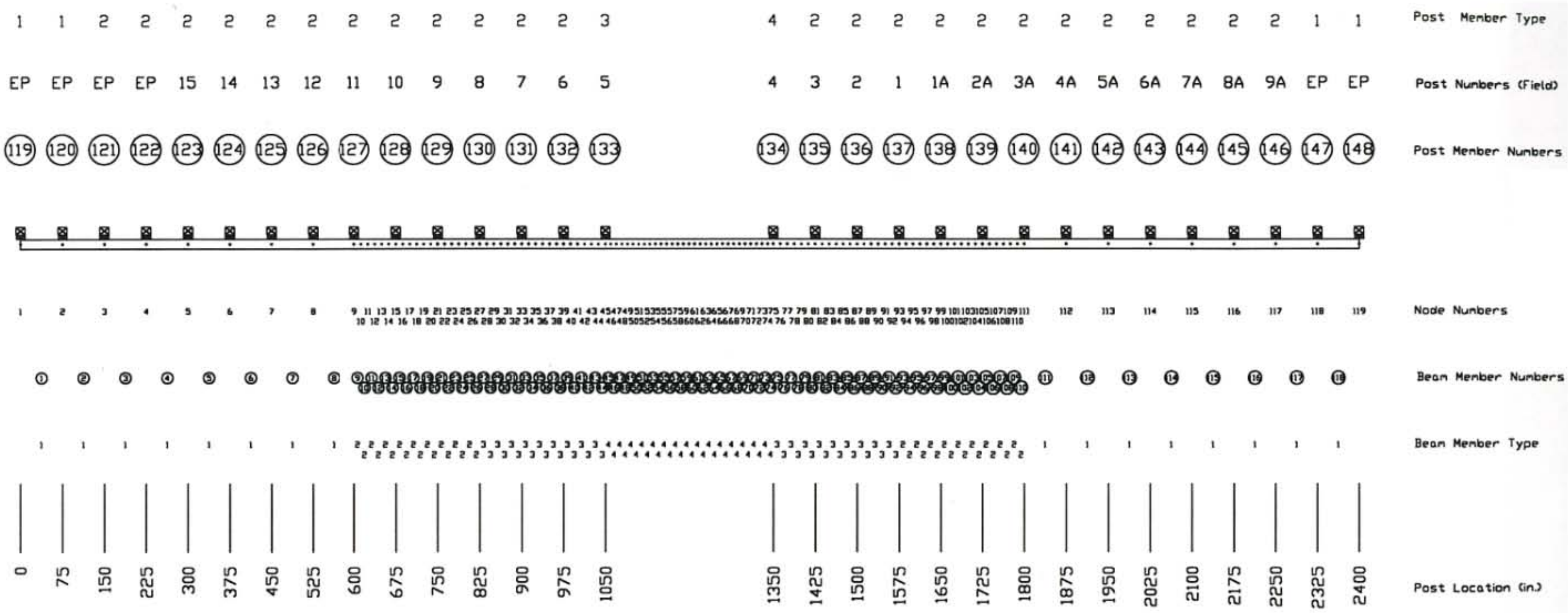

EP - Extra post that was used in Barrier VII computer simulation modeling but not included in actual tested installation.

Figure B-1. Model of the Long-Span Guardrail System, 19.05-m Nested Section

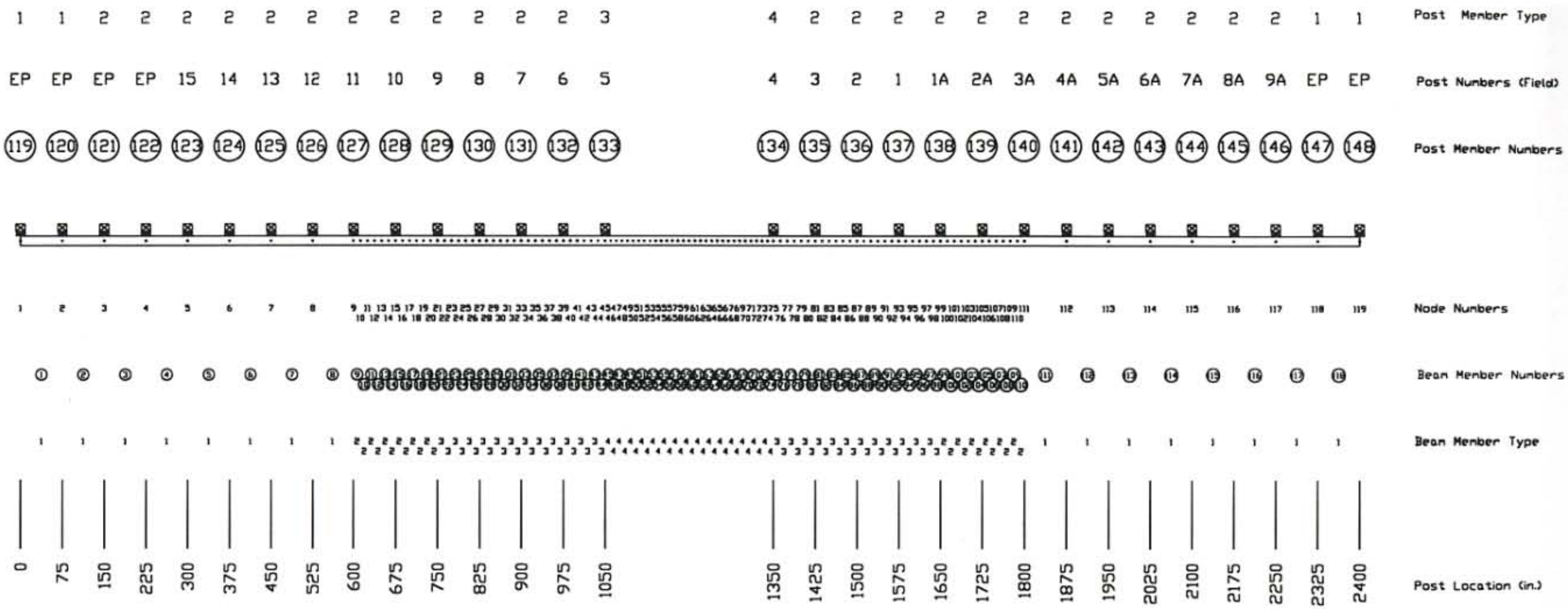

EP - Extra post that was used in Barrier VII computer simulation modeling but not included in actual tested installation.

Figure B-2. Model of the Long-Span Guardrail System, 22.86-m Nested Section

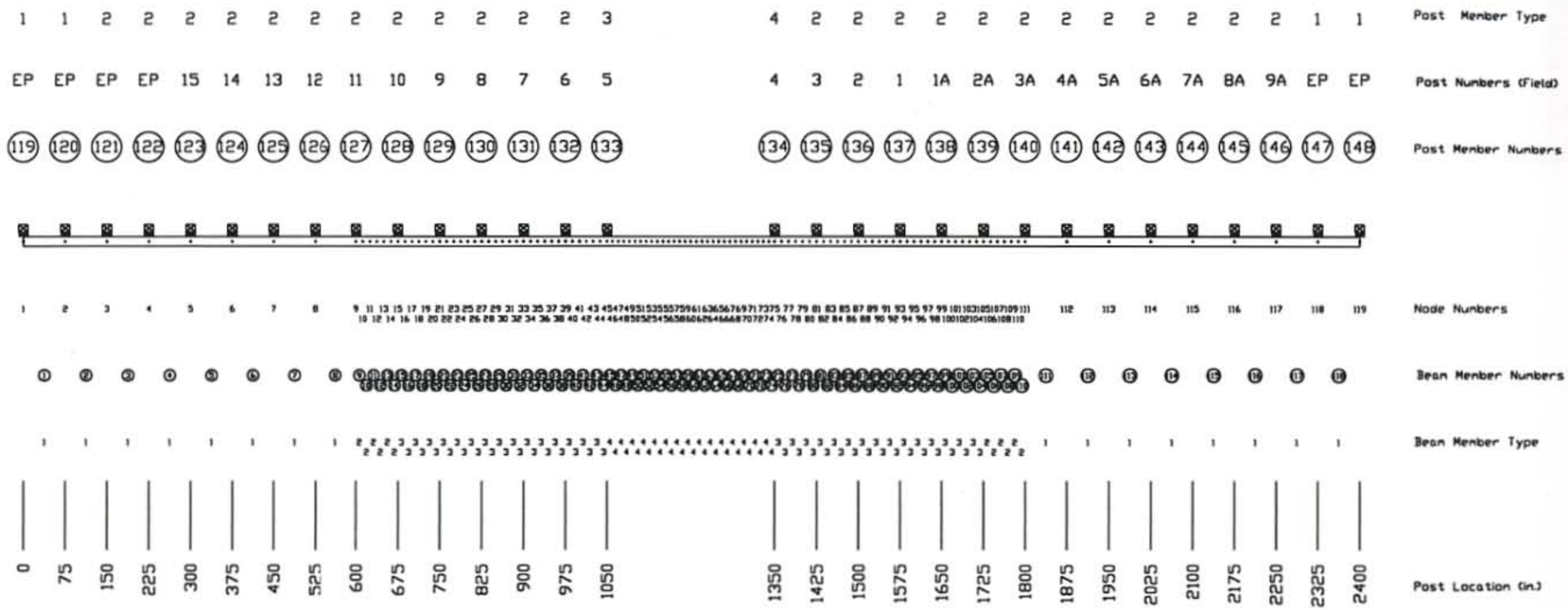

EP - Extra post that was used in Barrier VII computer simulation modeling but not included in actual tested installation.

Figure B-3. Model of the Long-Span Guardrail System, 26.67-m Nested Section

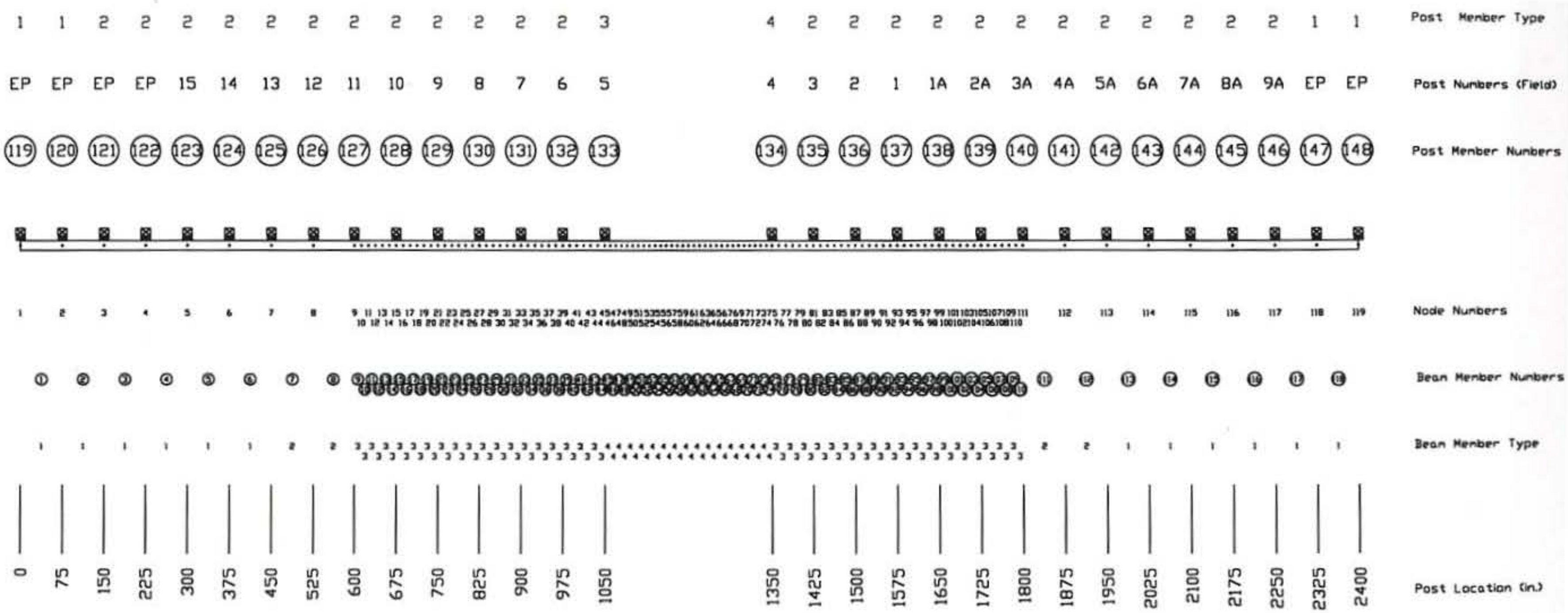

EP - Extra post that was used in Barrier VII computer simulation modeling but not included in actual tested installation.

Figure B-4. Model of the Long-Span Guardrail System, 30.48-m Nested Section

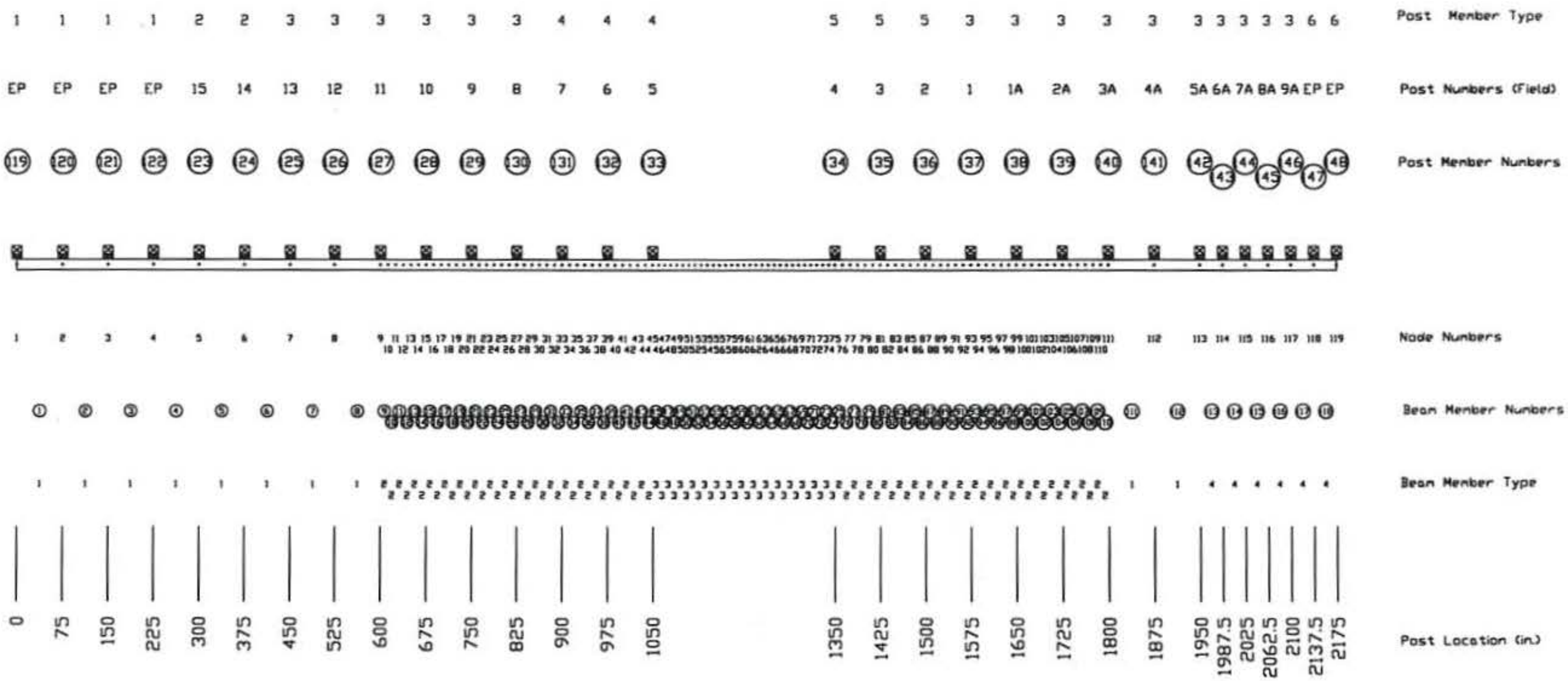

EP - Extra post that was used in Barrier VII computer simulation modeling but not included in actual tested installation.

Figure B-5. Model of the Long-Span Guardrail System, 30.48-m Nested Section (Design No. 1)

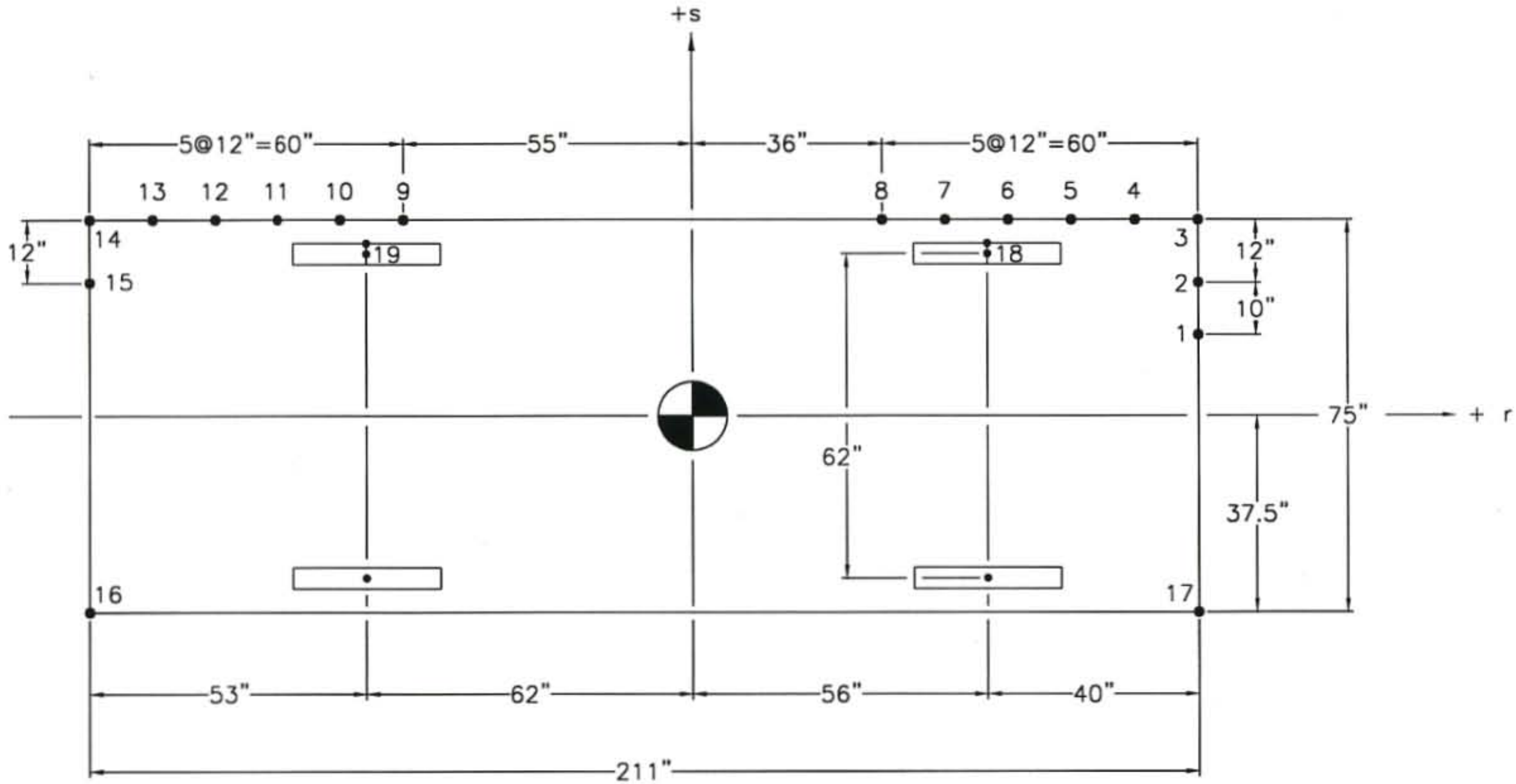

Figure B-6. Idealized Finite Element, 2 Dimensional Vehicle Model for the 2,041-kg Sedan

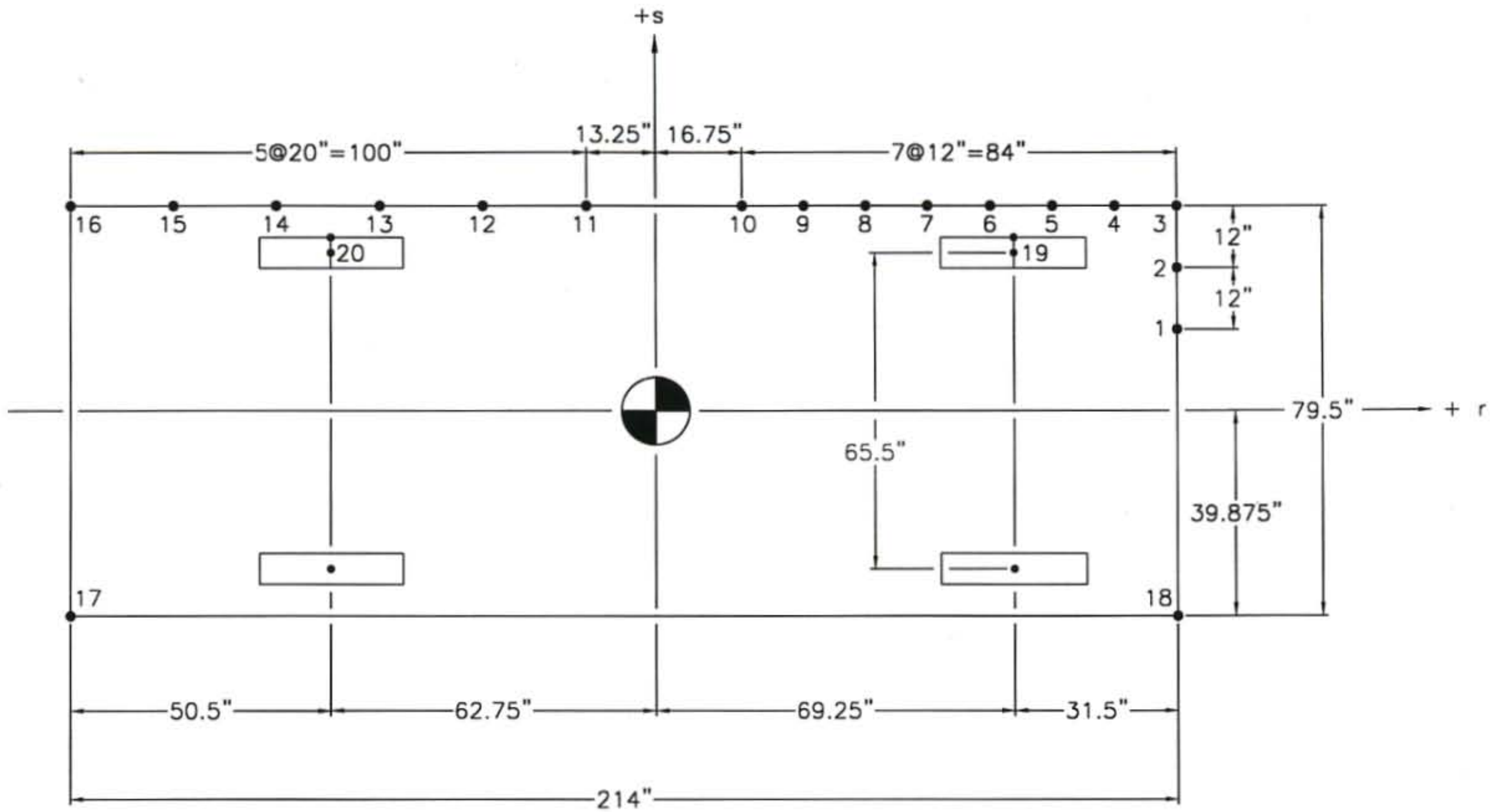

Figure B-7. Idealized Finite Element, 2 Dimensional Vehicle Model for the 1,996-kg Pickup Truck

APPENDIX C

Typical BARRIER VII Input File

Note that the example BARRIER VII input data file included in Appendix C corresponds with the critical impact point for test OLS-1.

```
OHIO LONG SPAN RAIL OVER BOX CULVERT - TRUCK100/W-BEAM (NESTED W-BEAM WITH 25'-0" LONG
SPAN)
  119    30    13     1   148    15     2     0
    0.00025     0.00025       0.70   300     0          1.0     1
    1    10    10    10    10
    1        0.0          0.0
    2      75.00          0.0
    3     150.00          0.0
    4     225.00          0.0
    5     300.00          0.0
    6     375.00          0.0
    7     450.00          0.0
    8     525.00          0.0
    9     600.00          0.0
   15     675.00          0.0
   21     750.00          0.0
   27     825.00          0.0
   33     900.00          0.0
   39     975.00          0.0
   45    1050.00          0.0
   75    1350.00          0.0
   81    1425.00          0.0
   87    1500.00          0.0
   93    1575.00          0.0
   99    1650.00          0.0
  105    1725.00          0.0
  111    1800.00          0.0
  112    1875.00          0.0
  113    1950.00          0.0
  114    2025.00          0.0
  115    2100.00          0.0
  116    2175.00          0.0
  117    2250.00          0.0
  118    2325.00          0.0
  119    2400.00          0.0
    9    15     5     1         0.0
   15    21     5     1         0.0
   21    27     5     1         0.0
   27    33     5     1         0.0
   33    39     5     1         0.0
   39    45     5     1         0.0
   45    75    29     1         0.0
   75    81     5     1         0.0
   81    87     5     1         0.0
   87    93     5     1         0.0
   93    99     5     1         0.0
   99   105     5     1         0.0
  105   111     5     1         0.0
    1   100        0.35
  112   111   110   109   108   107   106   105   104   103
  102   101   100    99    98    97    96    95    94    93
   92    91    90    89    88    87    86    85    84    83
   82    81    80    79    78    77    76    75    74    73
   72    71    70    69    68    67    66    65    64    63
   62    61    60    59    58    57    56    55    54    53
   52    51    50    49    48    47    46    45    44    43
   42    41    40    39    38    37    36    35    34    33
   32    31    30    29    28    27    26    25    24    23
   22    21    20    19    18    17    16    15    14    13
  100     4
    1       2.29        1.99       75.00   30000.0       6.92        99.5        68.5 0.05
    2       4.58        3.98       75.00   30000.0      13.84       199.0       137.0 0.05
    3       4.58        3.98       12.50   30000.0      13.84       199.0       137.0 0.05
    4       4.58        3.98       10.00   30000.0      13.84       199.0       137.0 0.05
```

```
300     4
  1        21.0         0.0        30.0         15.      64.50   10000.0       191.1 0.05
 10000.0          9.1        20.0        15.5
  2        21.0         0.0        1.95         2.0      64.50     214.2       231.0 0.05
    10.2        15.0         4.7         15.5
  3        21.0         0.0        1.95         2.0      64.50     214.2       231.0 0.05
    10.2        15.0         4.7         15.5
  4        21.0         0.0        1.95         2.0      64.50     214.2       231.0 0.05
    10.2        15.0         4.7         15.5
  1    1     2     6     1   101         0.0         0.0         0.0
  7    7     8     9     1   102         0.0         0.0         0.0
  9    9    10    44     1   103         0.0         0.0         0.0
 45   45    46    74     1   104         0.0         0.0         0.0
 75   75    76   110     1   103         0.0         0.0         0.0
111  111   112   112     1   102         0.0         0.0         0.0
113  113   114   118     1   101         0.0         0.0         0.0
119    1         120     1   301         0.0         0.0         0.0         0.0         0.0
121    3         127     1   302         0.0         0.0         0.0         0.0         0.0
128   15         132     6   302         0.0         0.0         0.0         0.0         0.0
133   45                     303         0.0         0.0         0.0         0.0         0.0
134   75                     304         0.0         0.0         0.0         0.0         0.0
135   81         140     6   302         0.0         0.0         0.0         0.0         0.0
141  112         146     1   302         0.0         0.0         0.0         0.0         0.0
147  118         148     1   301         0.0         0.0         0.0         0.0         0.0
  4400.0    40000.0   20     6      4      0      1
  1      0.055       0.12       6.00      17.0
  2      0.057       0.15       7.00      18.0
  3      0.062       0.18      10.00      12.0
  4      0.110       0.35      12.00       6.0
  5       0.35       0.45       6.00       5.0
  6       1.45       1.50      15.00       1.0
  1     100.75     15.875    1      12.0     1     0     0     0
  2     100.75     27.875    1      12.0     1     0     0     0
  3     100.75     39.875    2      12.0     1     0     0     0
  4      88.75     39.875    2      12.0     1     0     0     0
  5      76.75     39.875    2      12.0     1     0     0     0
  6      64.75     39.875    2      12.0     1     0     0     0
  7      52.75     39.875    2      12.0     1     0     0     0
  8      40.75     39.875    2      12.0     1     0     0     0
  9      28.75     39.875    2      12.0     1     0     0     0
 10      16.75     39.875    2      12.0     1     0     0     0
 11     -13.25     39.875    3      12.0     1     0     0     0
 12     -33.25     39.875    3      12.0     1     0     0     0
 13     -53.25     39.875    3      12.0     1     0     0     0
 14     -73.25     39.875    3      12.0     1     0     0     0
 15     -93.25     39.875    3      12.0     1     0     0     0
 16    -113.25     39.875    4      12.0     1     0     0     0
 17    -113.25    -39.875    4      12.0     0     0     0     0
 18     100.75    -39.875    1      12.0     0     0     0     0
 19      69.25      37.75    5       1.0     1     0     0     0
 20     -62.75      37.75    6       1.0     1     0     0     0
  1      69.25      32.75        0.0      608.
  2      69.25     -32.75        0.0      608.
  3     -62.75      32.75        0.0      492.
  4     -62.75     -32.75        0.0      492.
  1        0.0        0.0
  3     1146.0        0.0       25.0     60.00       0.0       0.0       1.0
```

APPENDIX D

Accelerometer Data Analysis, Test OLS-1

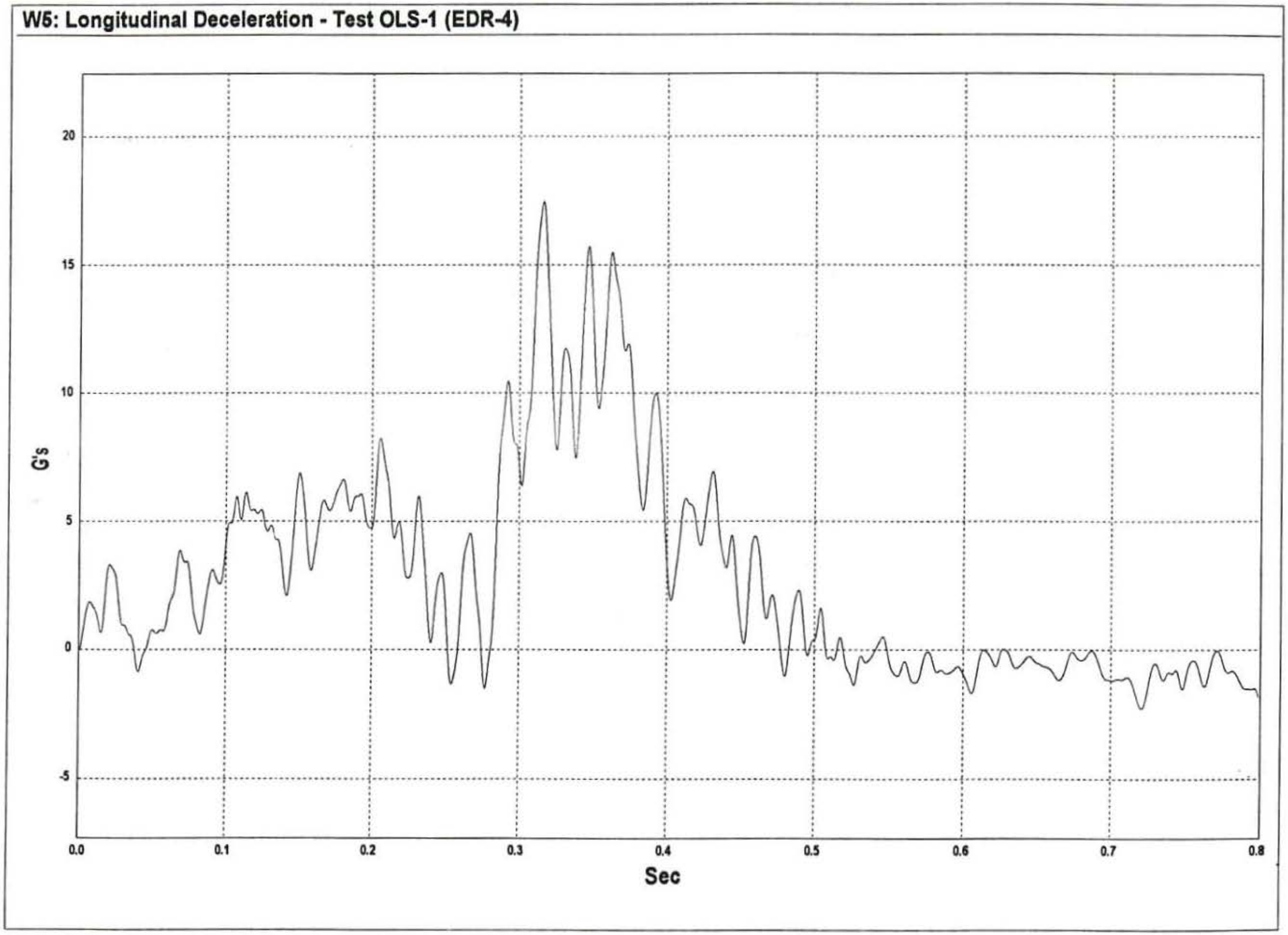

Figure D-1. Graph of Longitudinal Deceleration, Test OLS-1

Figure D-2. Graph of Longitudinal Occupant Impact Velocity, Test OLS-1

Figure D-3. Graph of Longitudinal Occupant Displacement, Test OLS-1

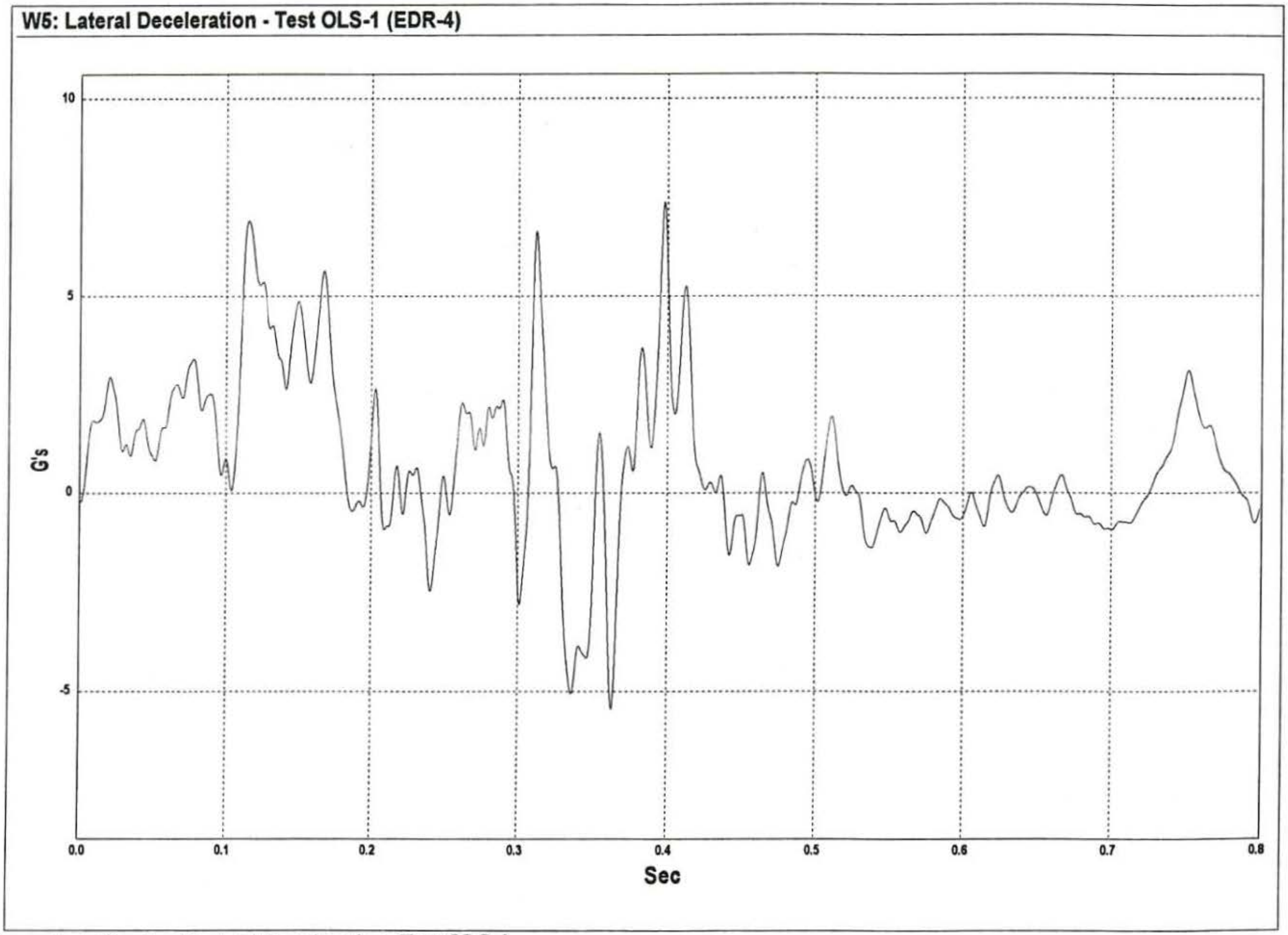

Figure D-4. Graph of Lateral Deceleration, Test OLS-1

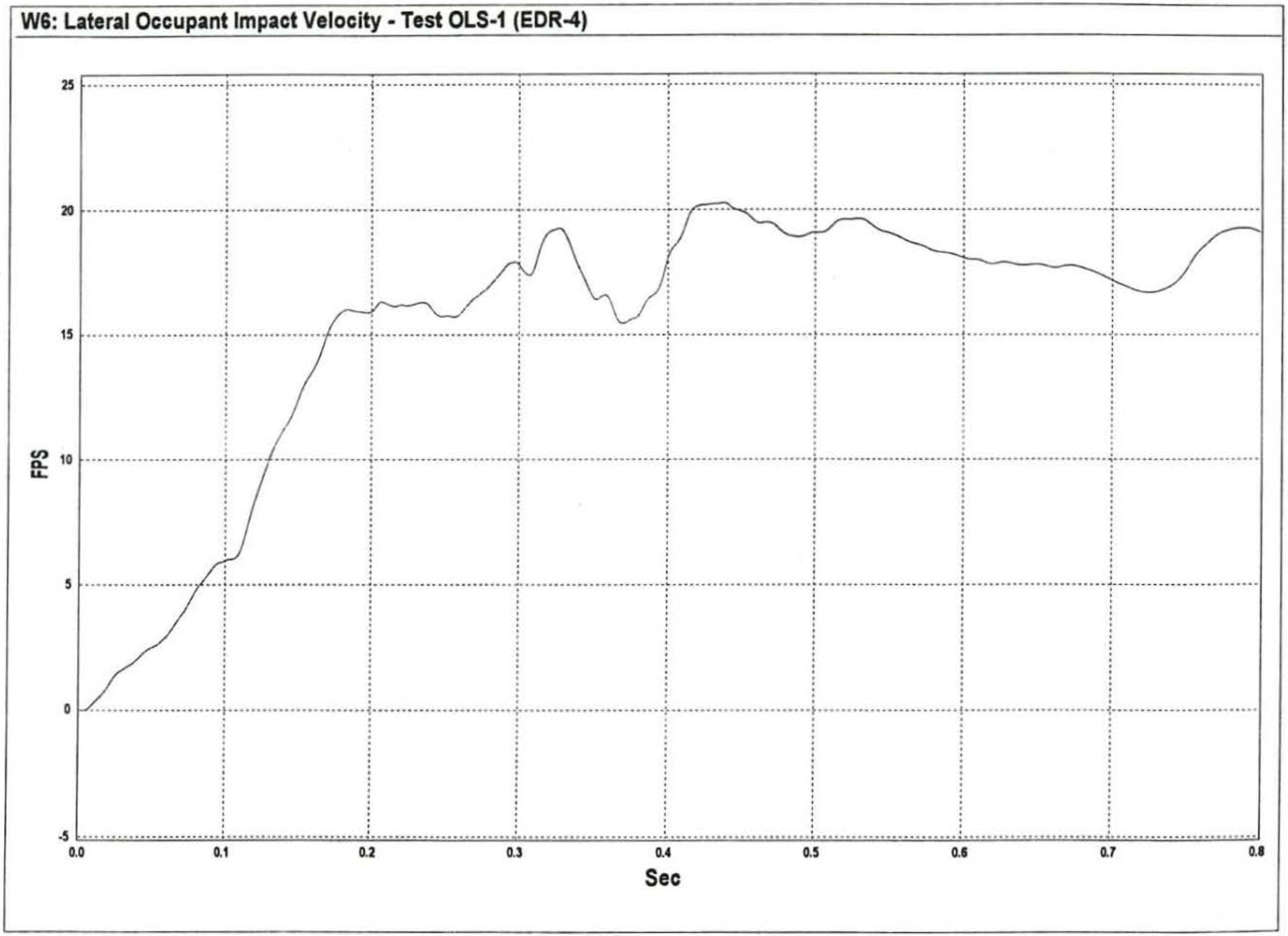

Figure D-5. Graph of Lateral Occupant Impact Velocity, Test OLS-1

Figure D-6. Graph of Lateral Occupant Displacement, Test OLS-1

APPENDIX E

Accelerometer Data Analysis, Test OLS-2

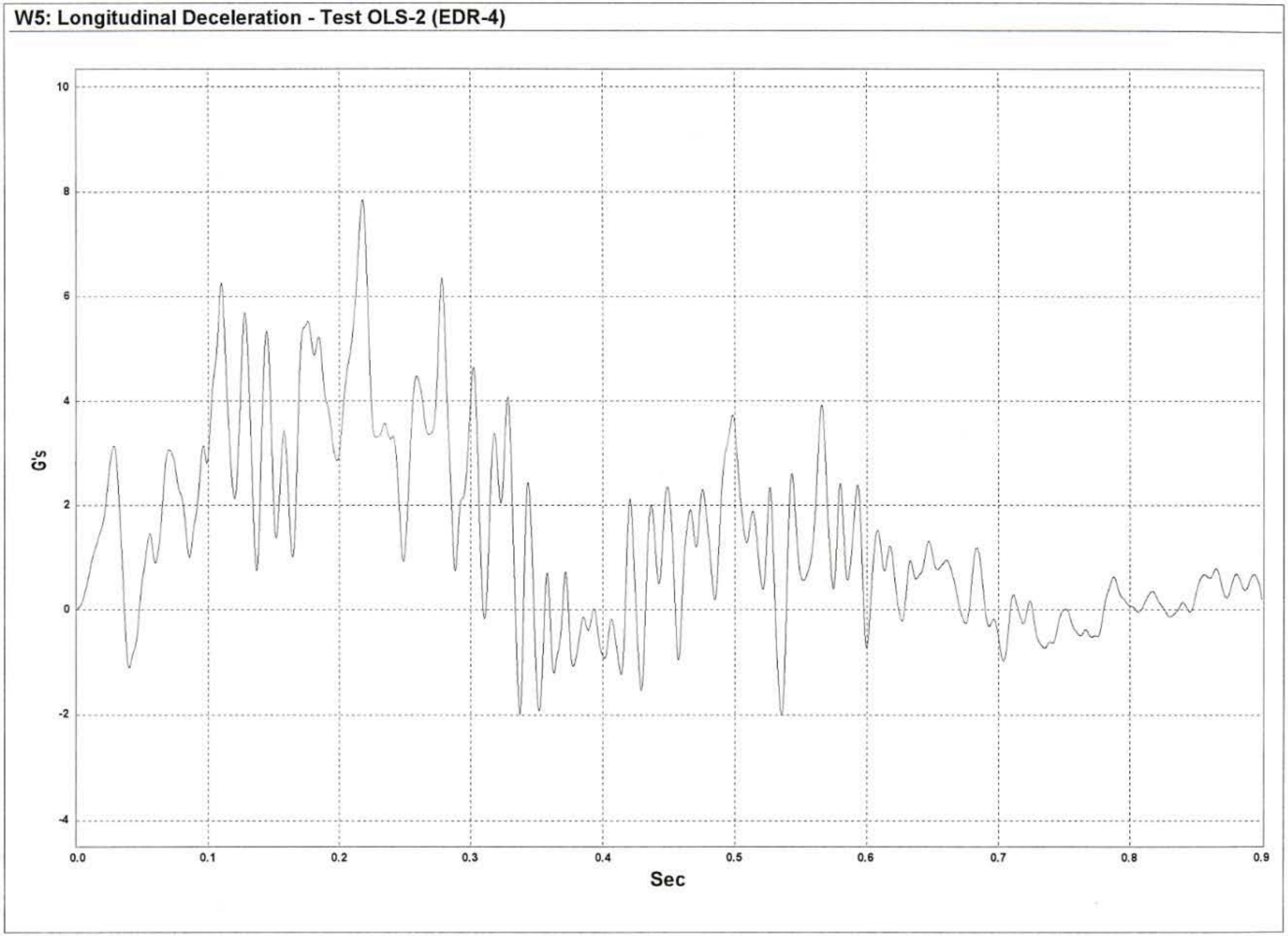

Figure E-1. Graph of Longitudinal Deceleration, Test OLS-2

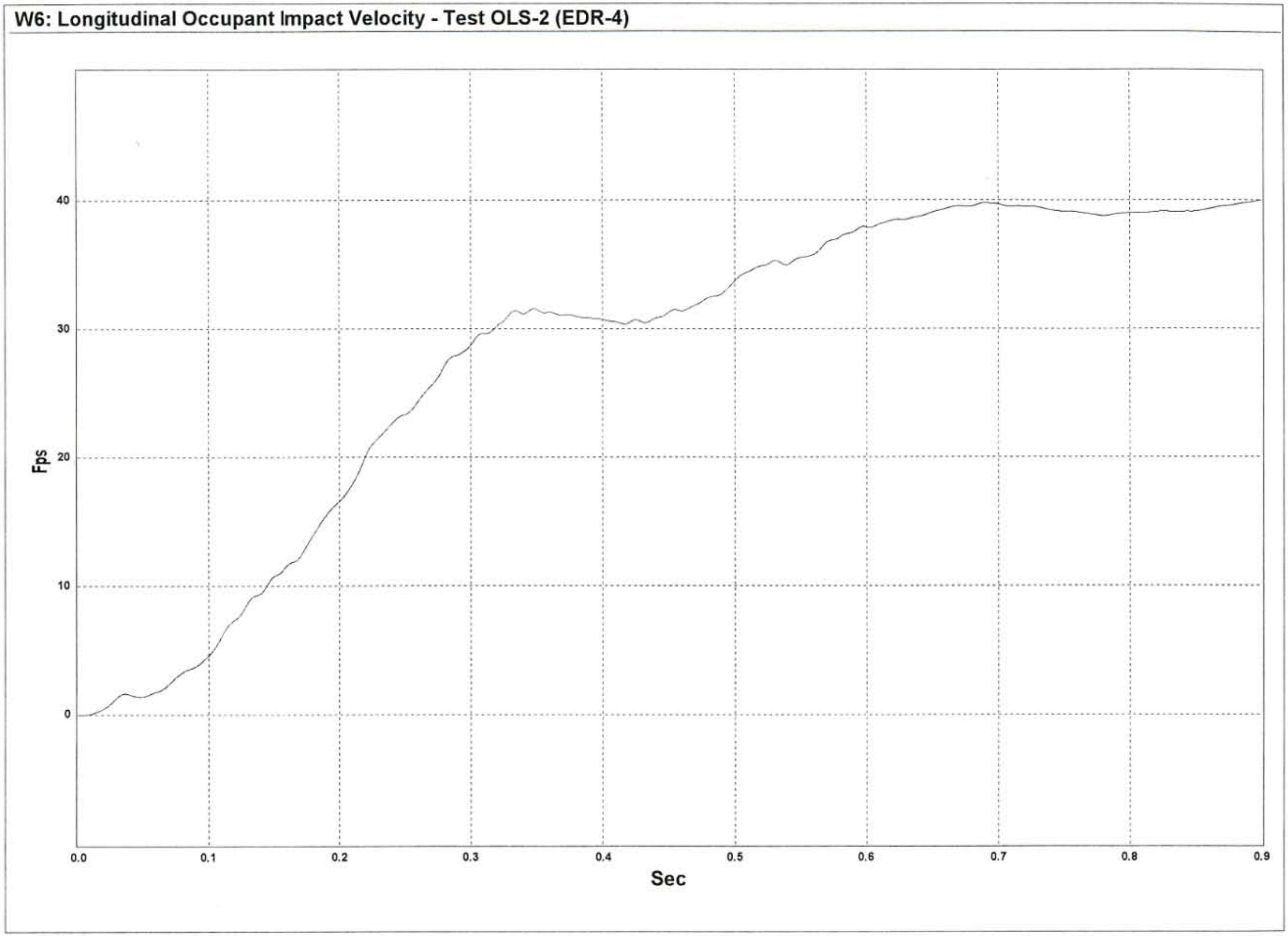

Figure E-2. Graph of Longitudinal Occupant Impact Velocity, Test OLS-2

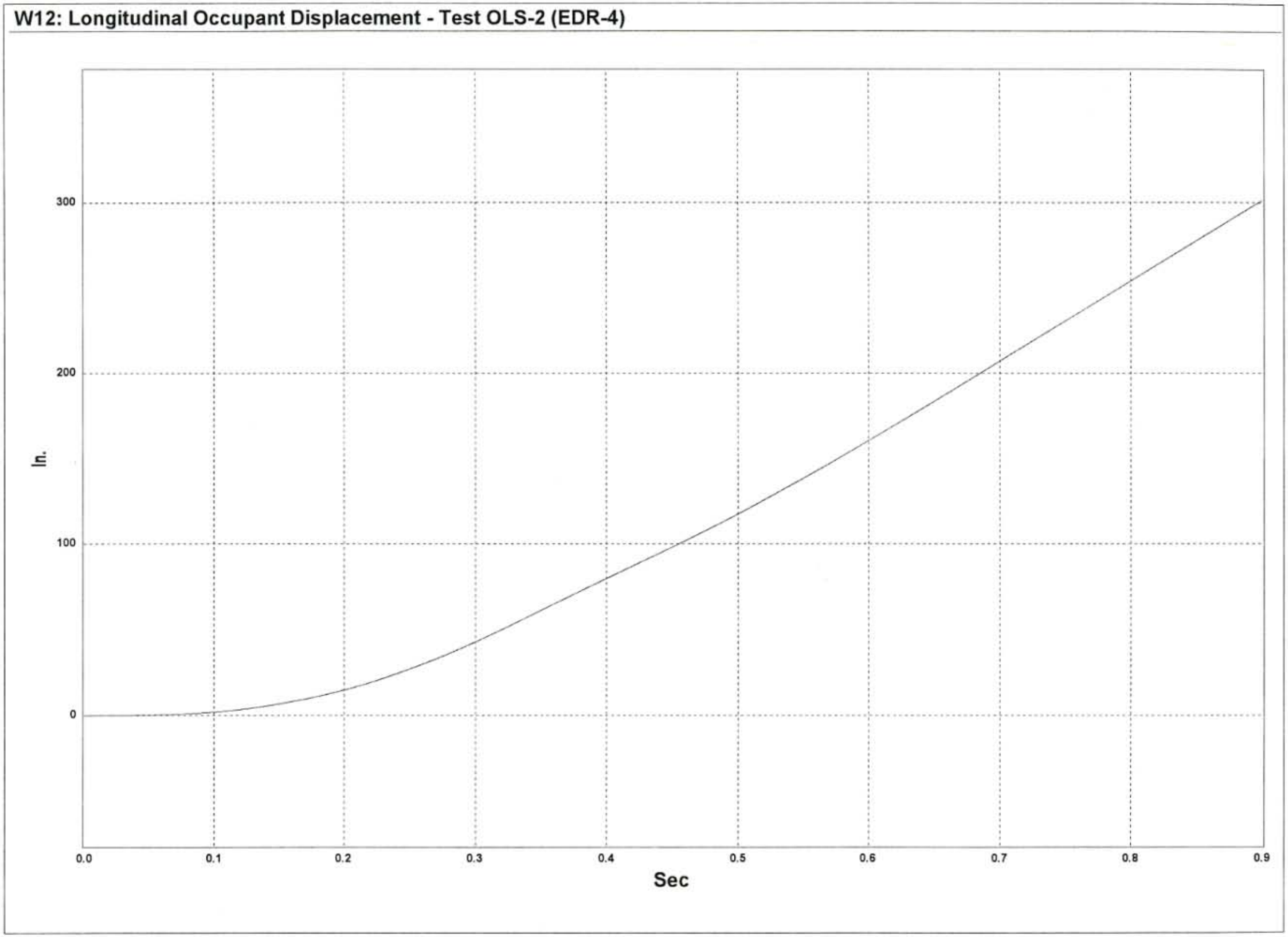

Figure E-3. Graph of Longitudinal Occupant Displacement, Test OLS-2

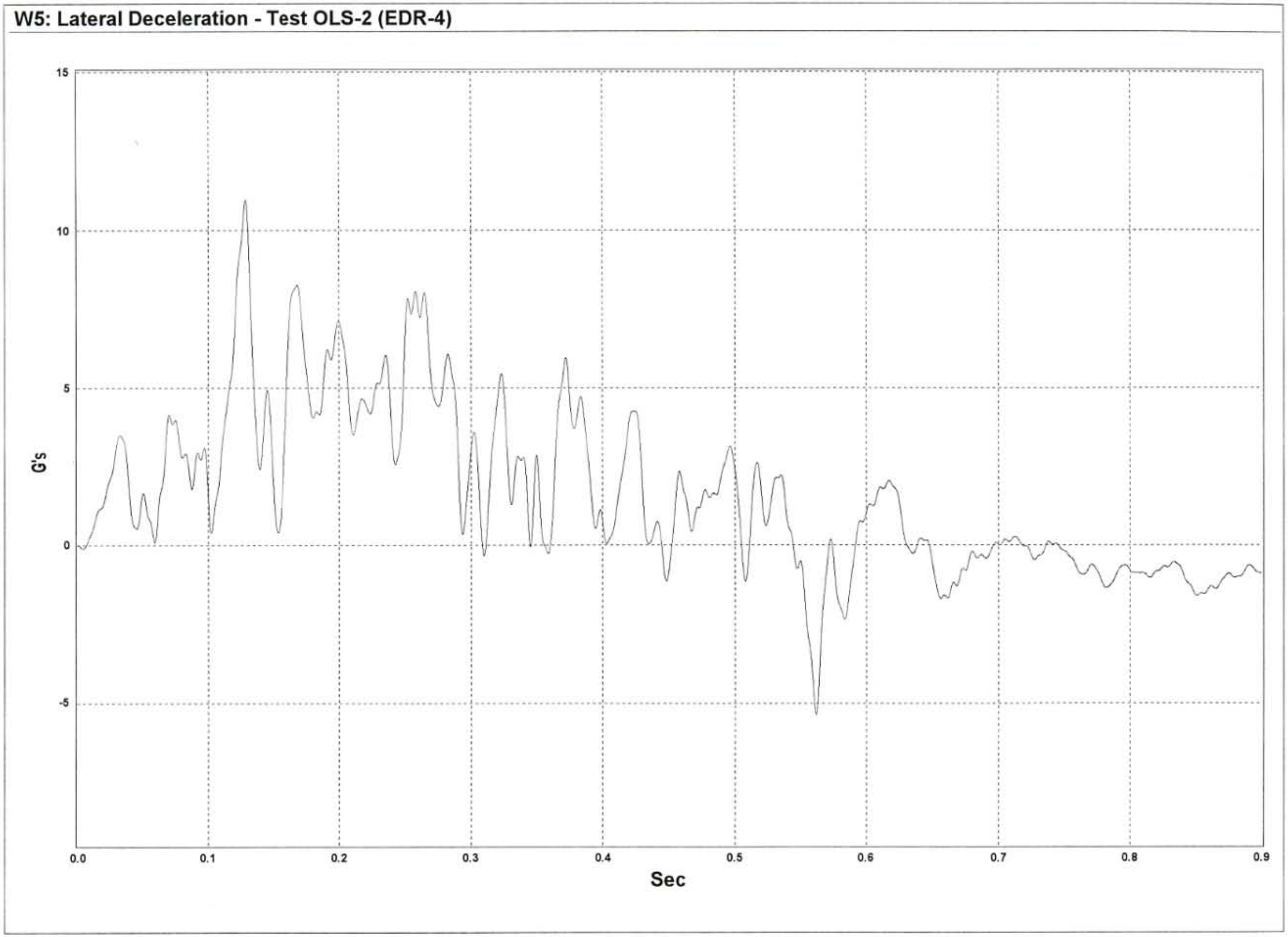

Figure E-4. Graph of Lateral Deceleration, Test OLS-2

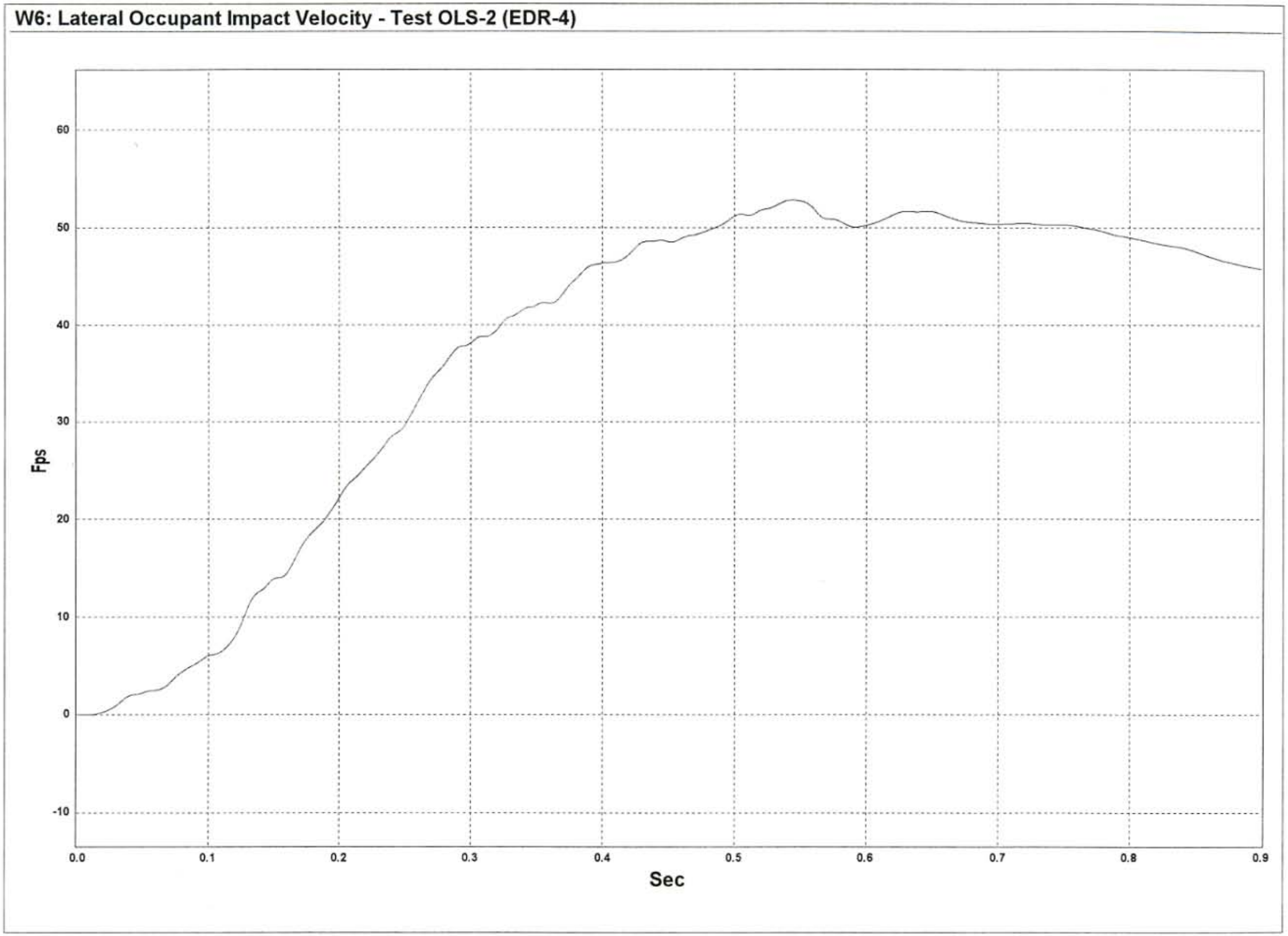

Figure E-5. Graph of Lateral Occupant Impact Velocity, Test OLS-2

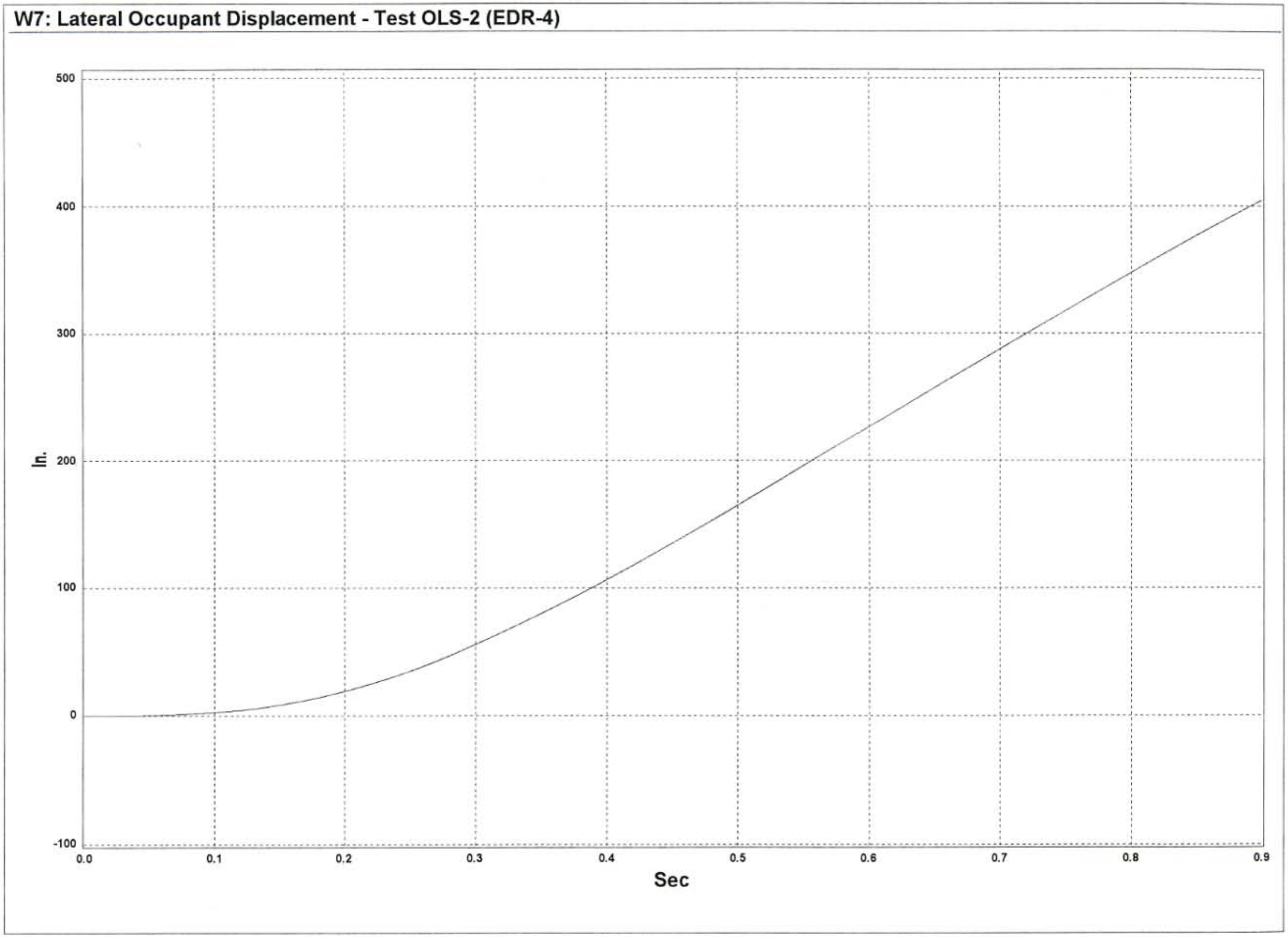

Figure E-6. Graph of Lateral Occupant Displacement, Test OLS-2

APPENDIX F

Rate Transducer Data Analysis, Test OLS-2

Figure F-1. Graph of Roll, Pitch, and Yaw Angular Displacements, Test OLS-2

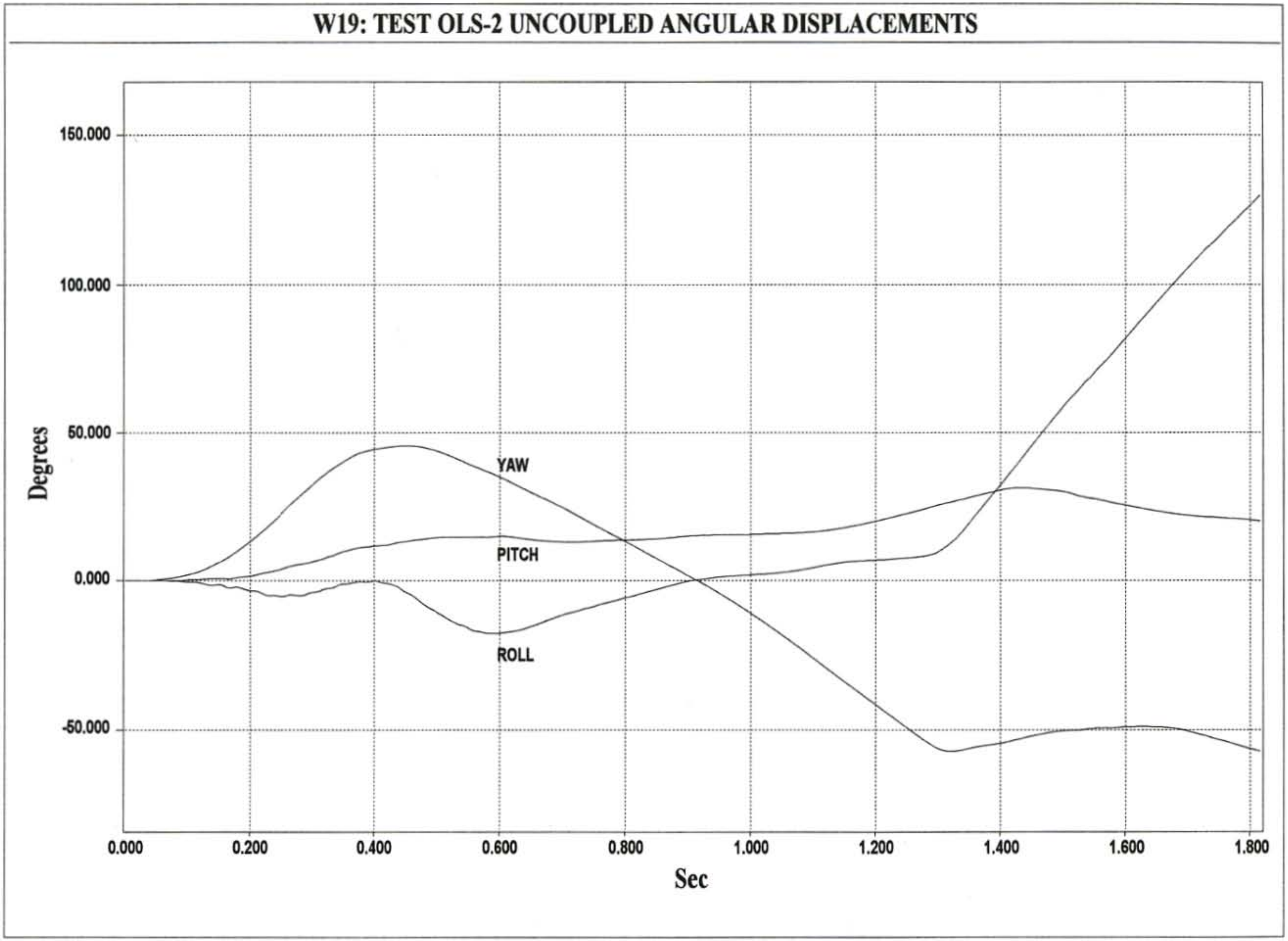

Figure F-1. Graph of Roll, Pitch, and Yaw Angular Displacements, Test OLS-2

APPENDIX G

Strain Gauge Data Analysis, Test OLS-2

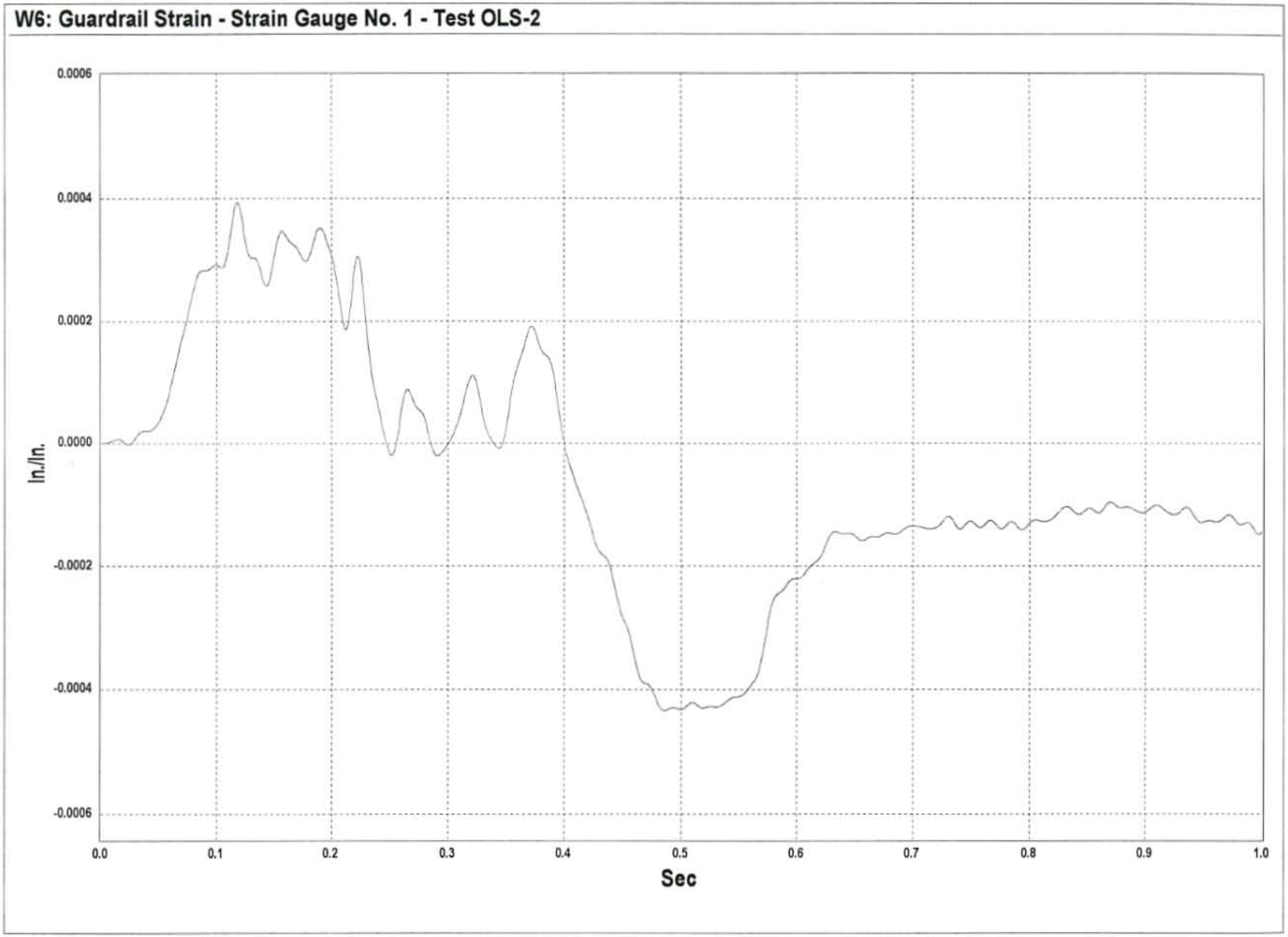

Figure G-1. Graph of Traffic-Side (near post no. 25) Top Peak Strain, Test OLS-2

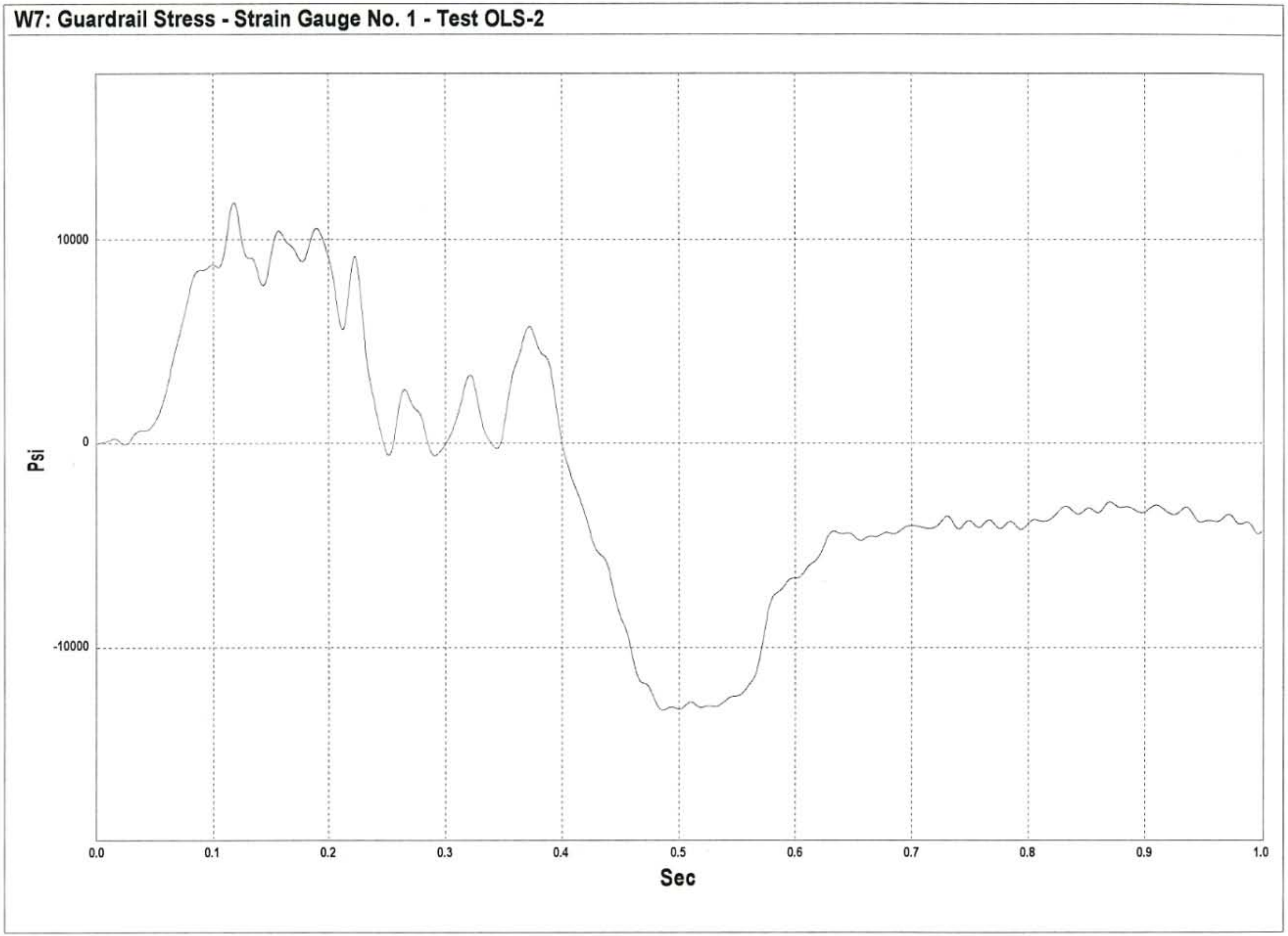

Figure G-2. Graph of Traffic-Side (near post no. 25) Top Peak Stress, Test OLS-2

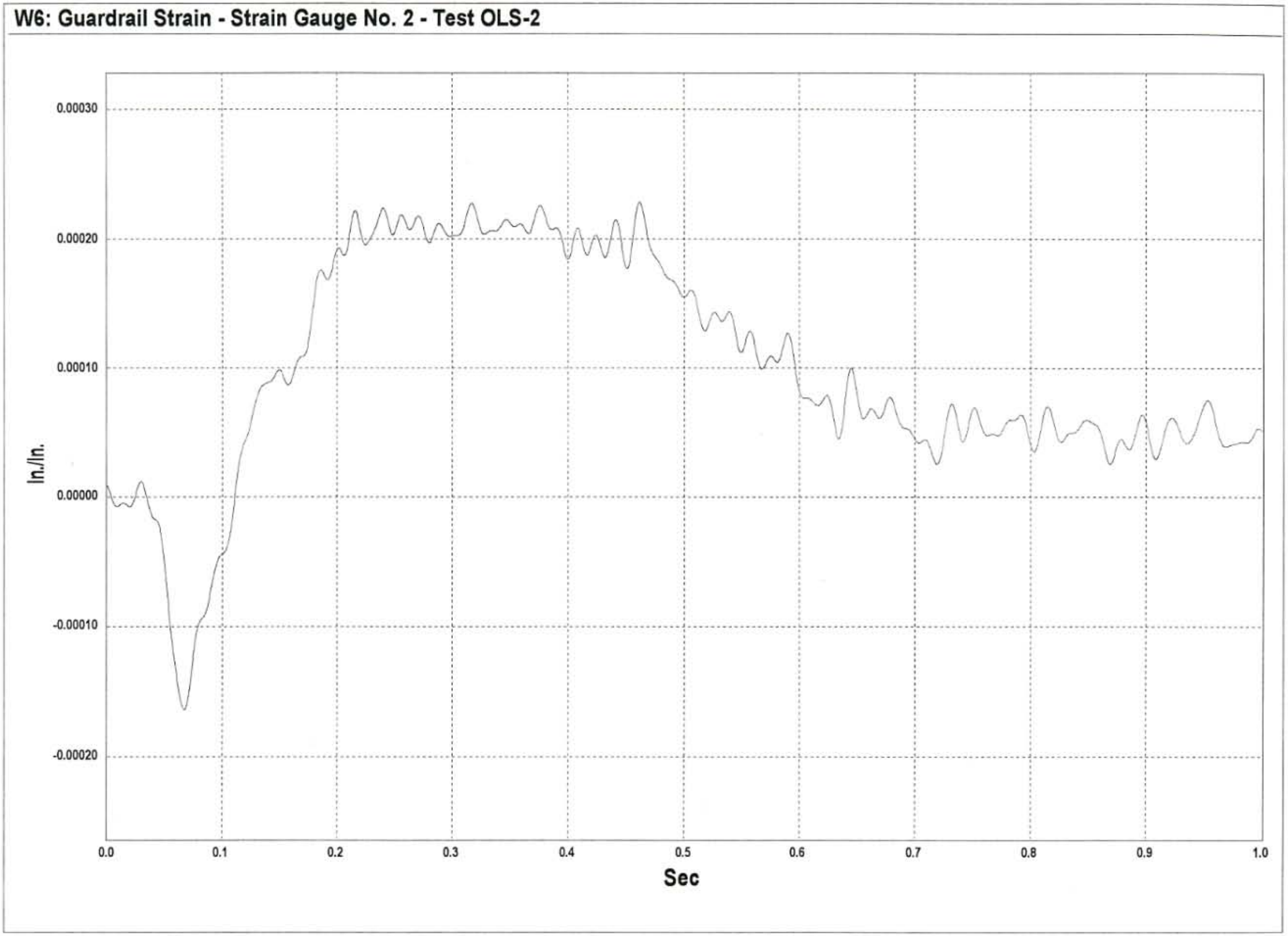

Figure G-3. Graph of Traffic-Side (near post no. 25) Bottom Peak Strain, Test OLS-2

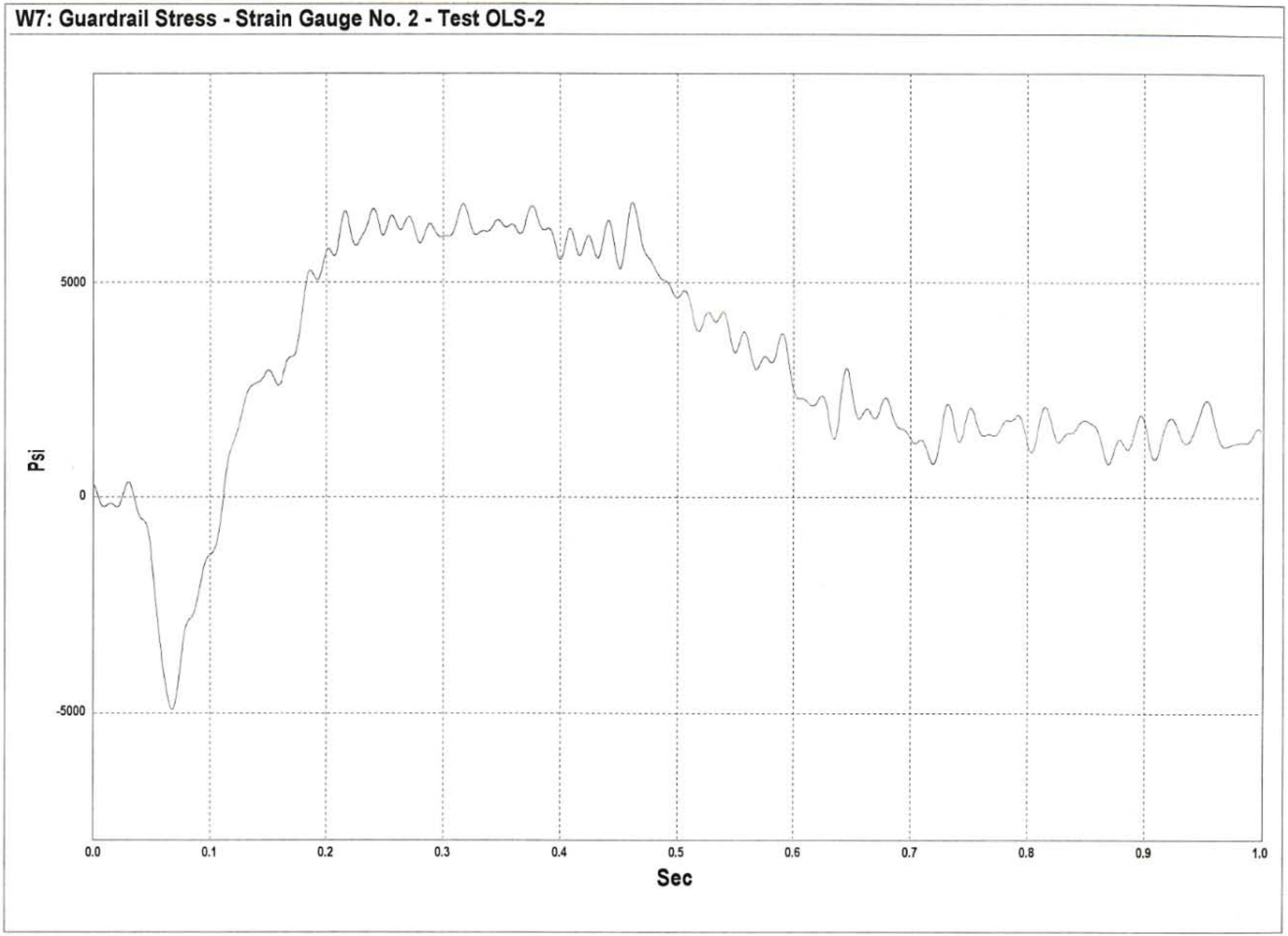

Figure G-4. Graph of Traffic-Side (near post no. 25) Bottom Peak Stress, Test OLS-2

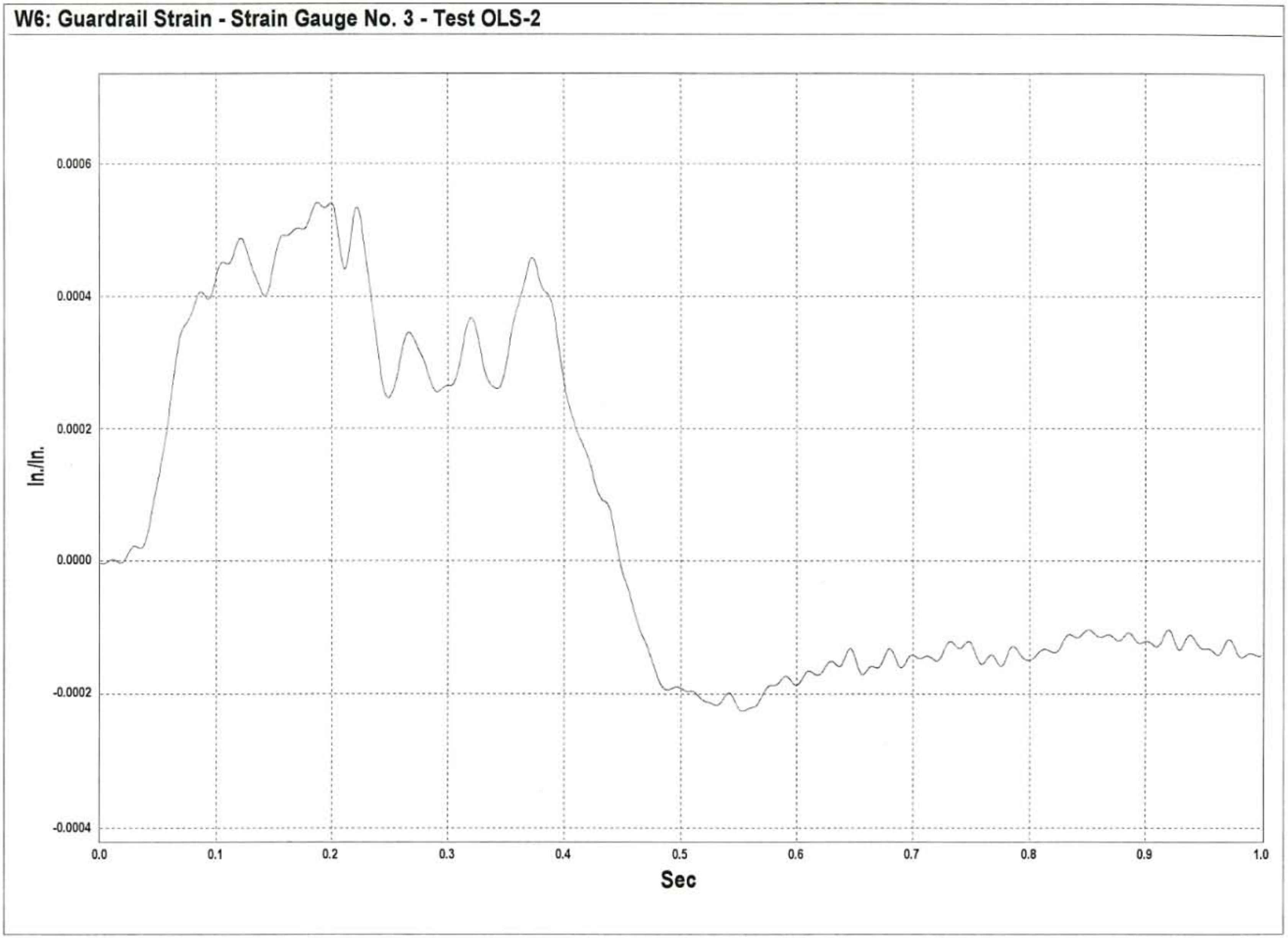

Figure G-5. Graph of Back-Side (near post no. 25) Neutral Axis Upper Middle Region Strain, Test OLS-2

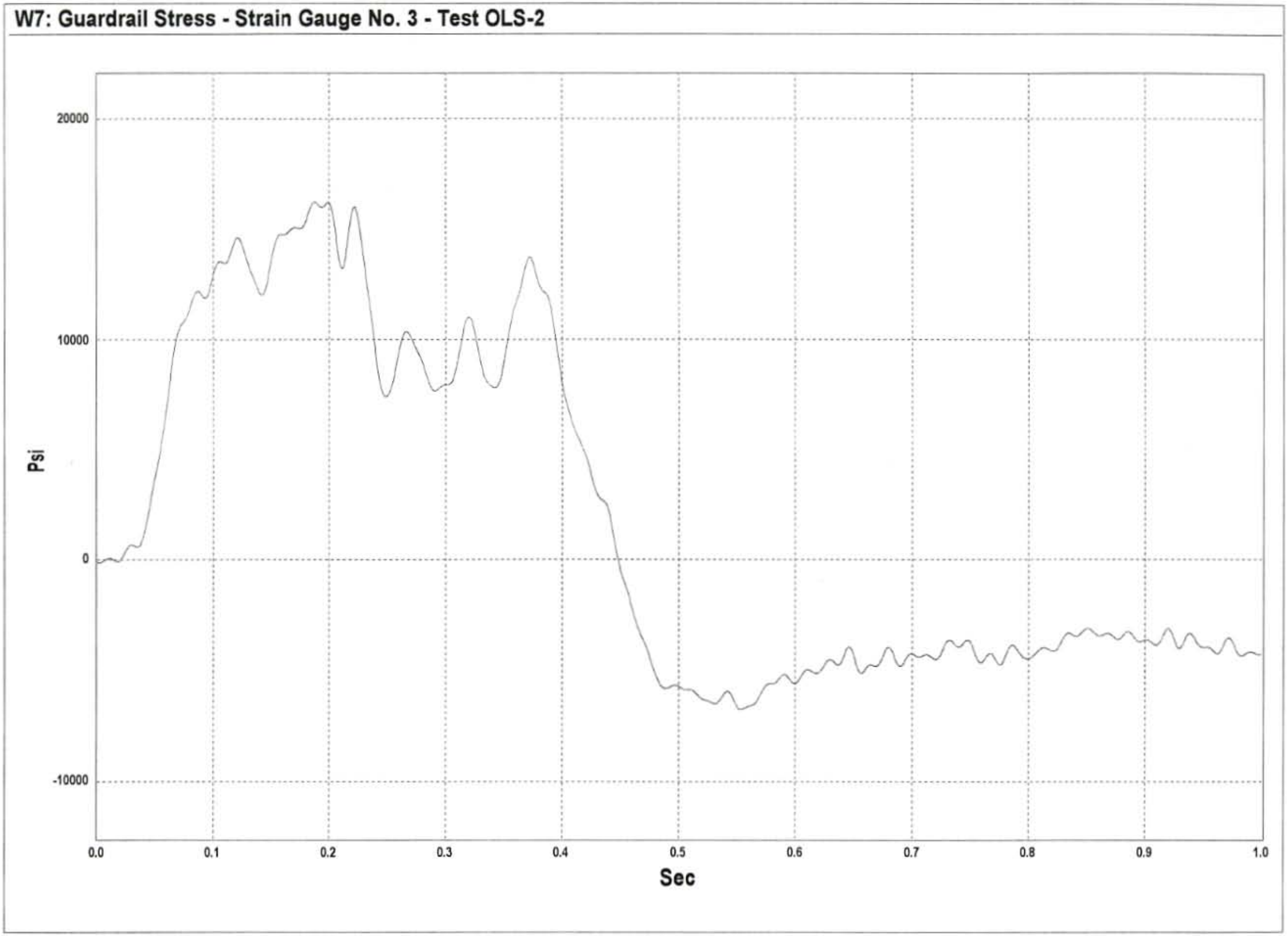

Figure G-6. Graph of Back-Side (near post no. 25) Neutral Axis Upper Middle Region Stress, Test OLS-2

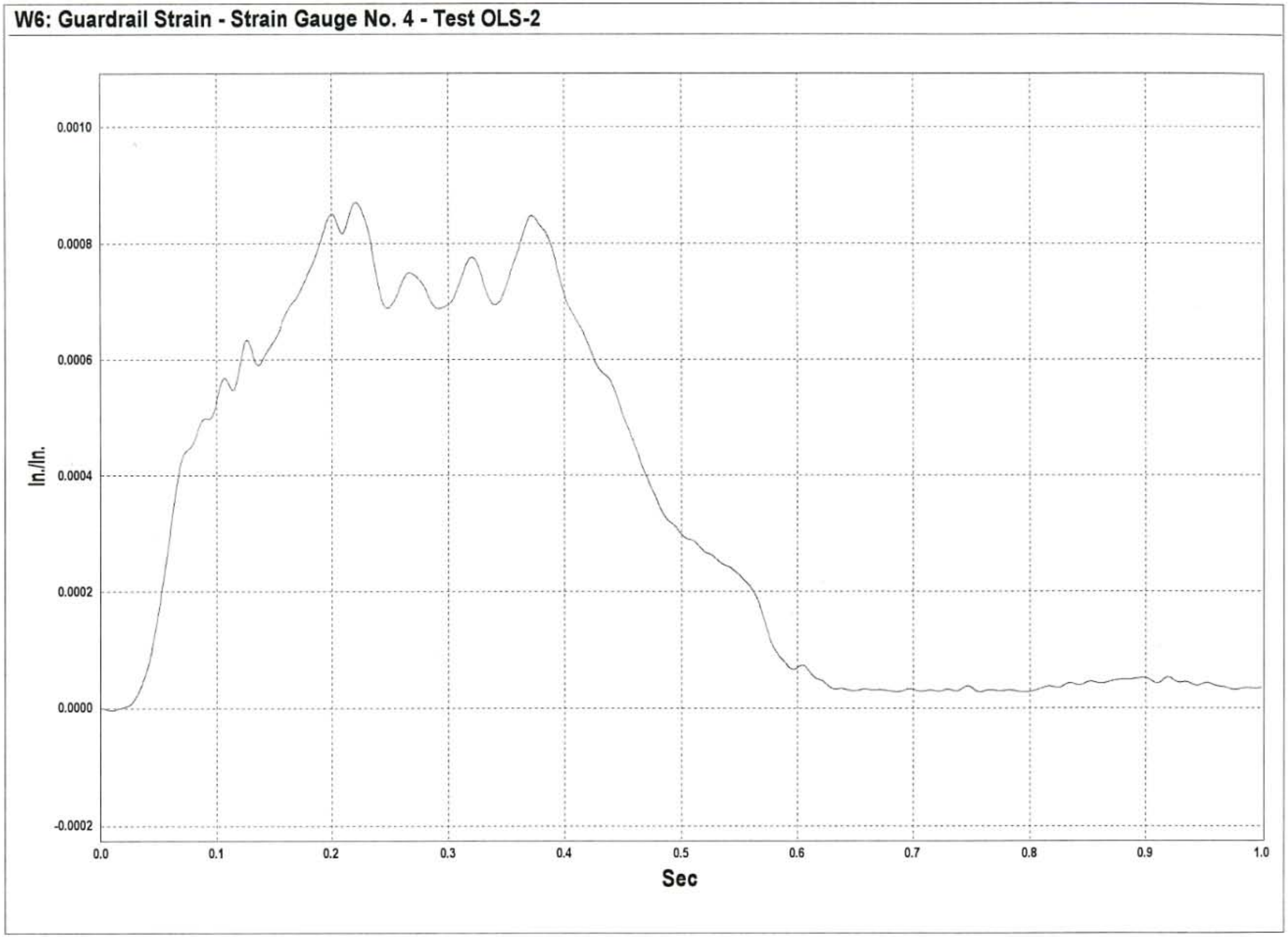

Figure G-7. Graph of Back-Side (near post no. 25) Flat Region Strain, Test OLS-2

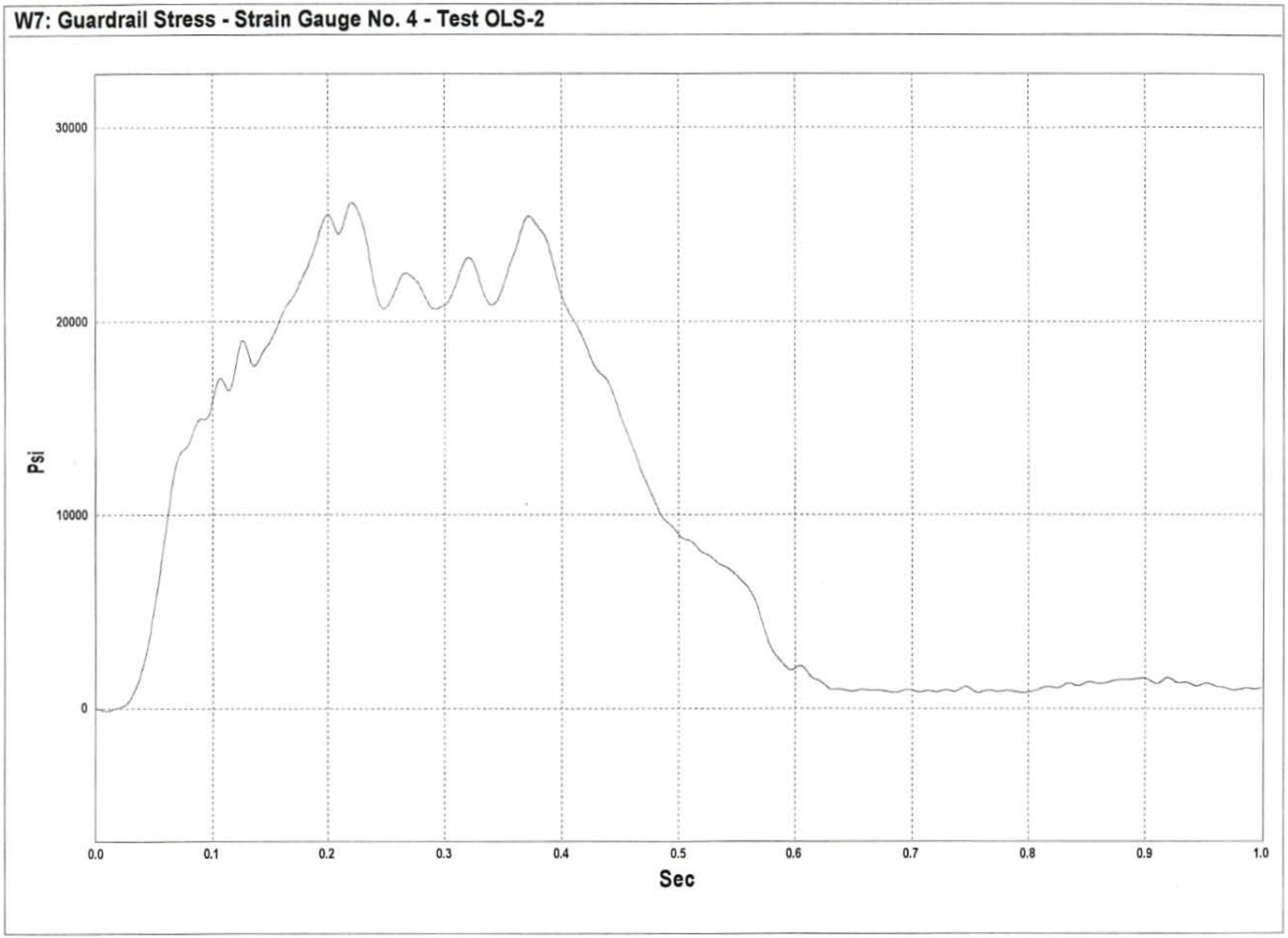

Figure G-8. Graph of Back-Side (near post no. 25) Flat Region Stress, Test OLS-2

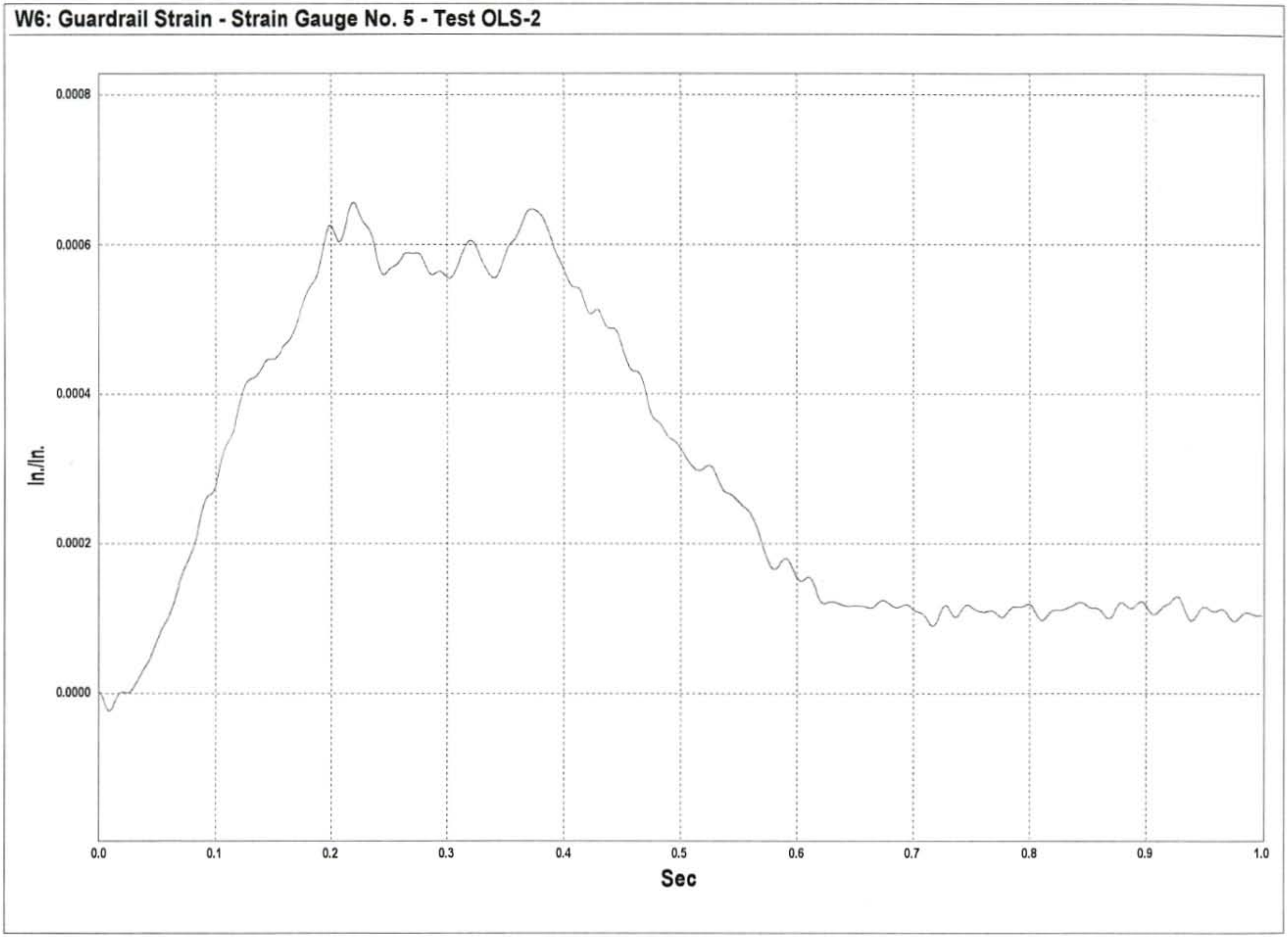

Figure G-9. Graph of Back-Side (near post no. 25) Neutral Axis Lower Middle Region Strain, Test OLS-2

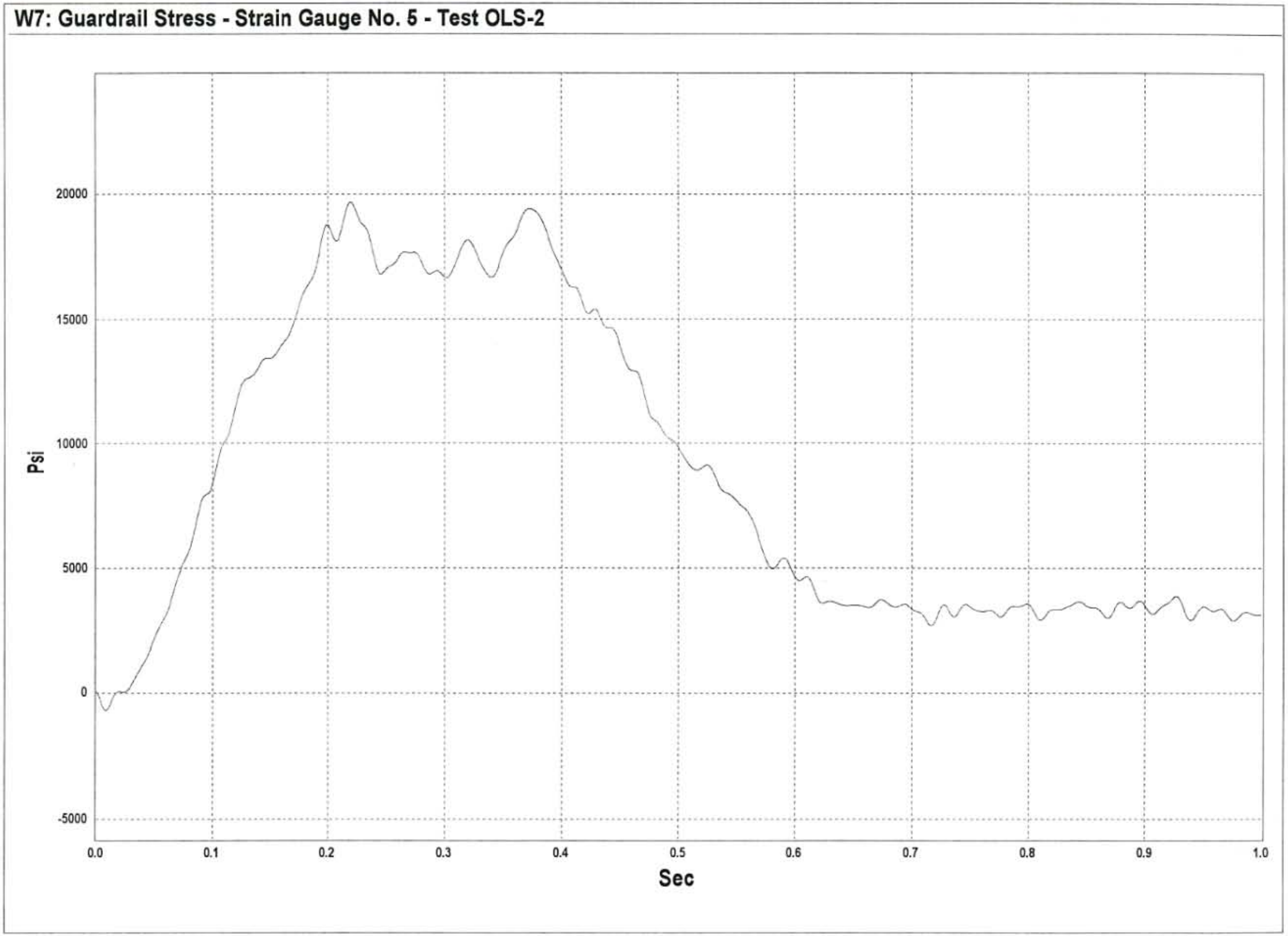

Figure G-10. Graph of Back-Side (near post no. 25) Neutral Axis Lower Middle Region Stress, Test OLS-2

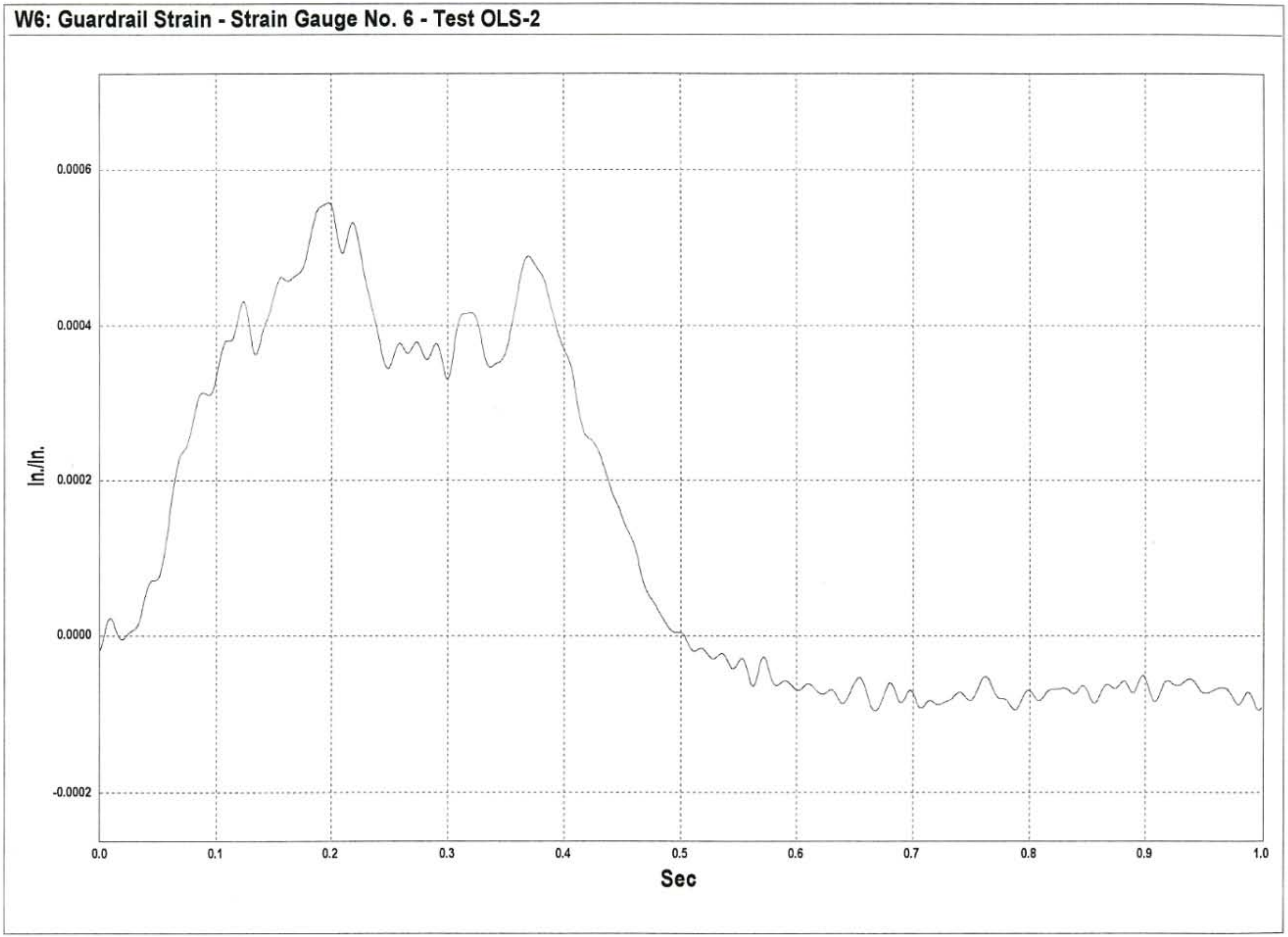

Figure G-11. Graph of Traffic-Side (near post no. 22) Top Peak Strain, Test OLS-2

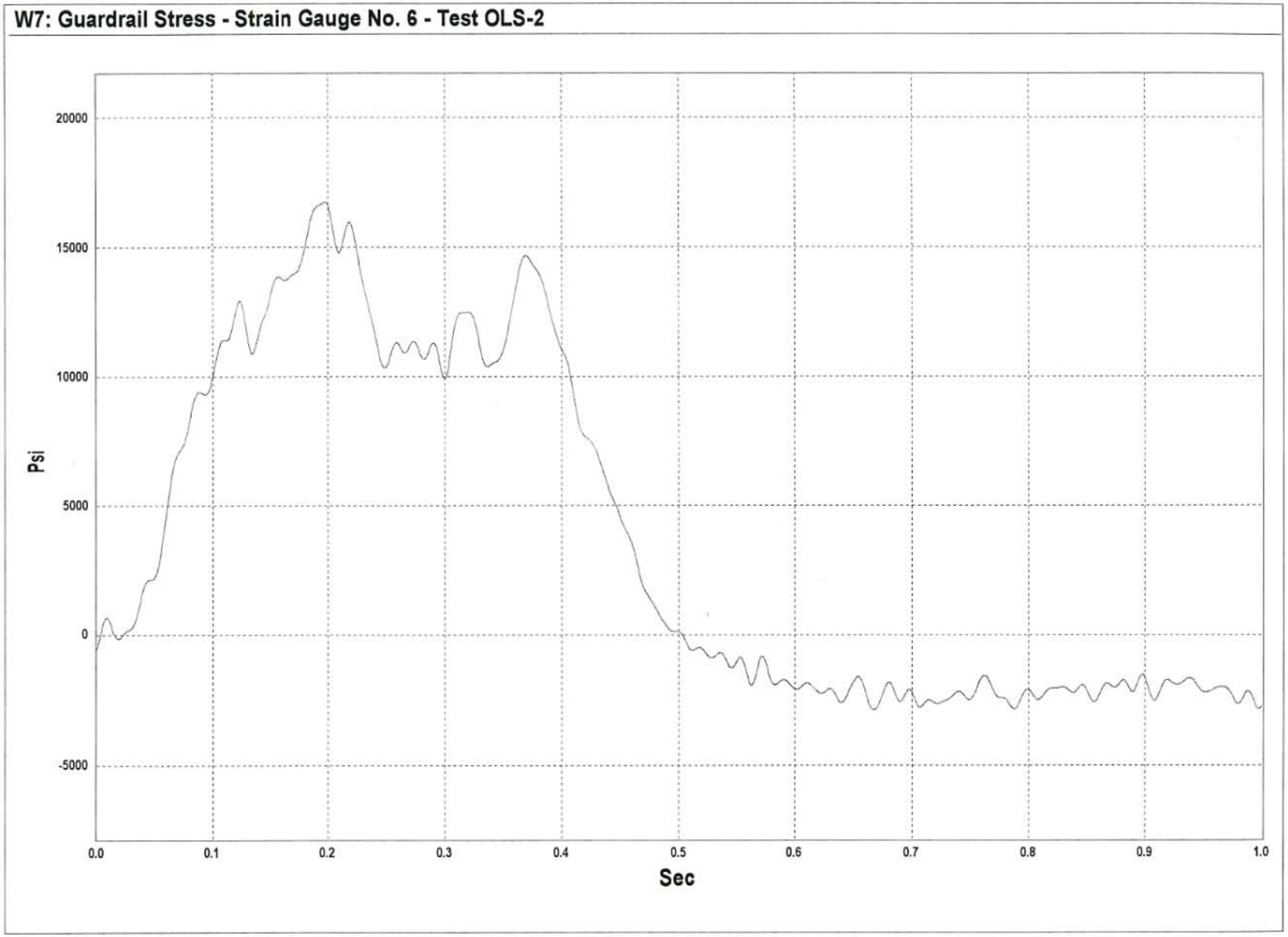

Figure G-12. Graph of Traffic-Side (near post no. 22) Top Peak Stress, Test OLS-2

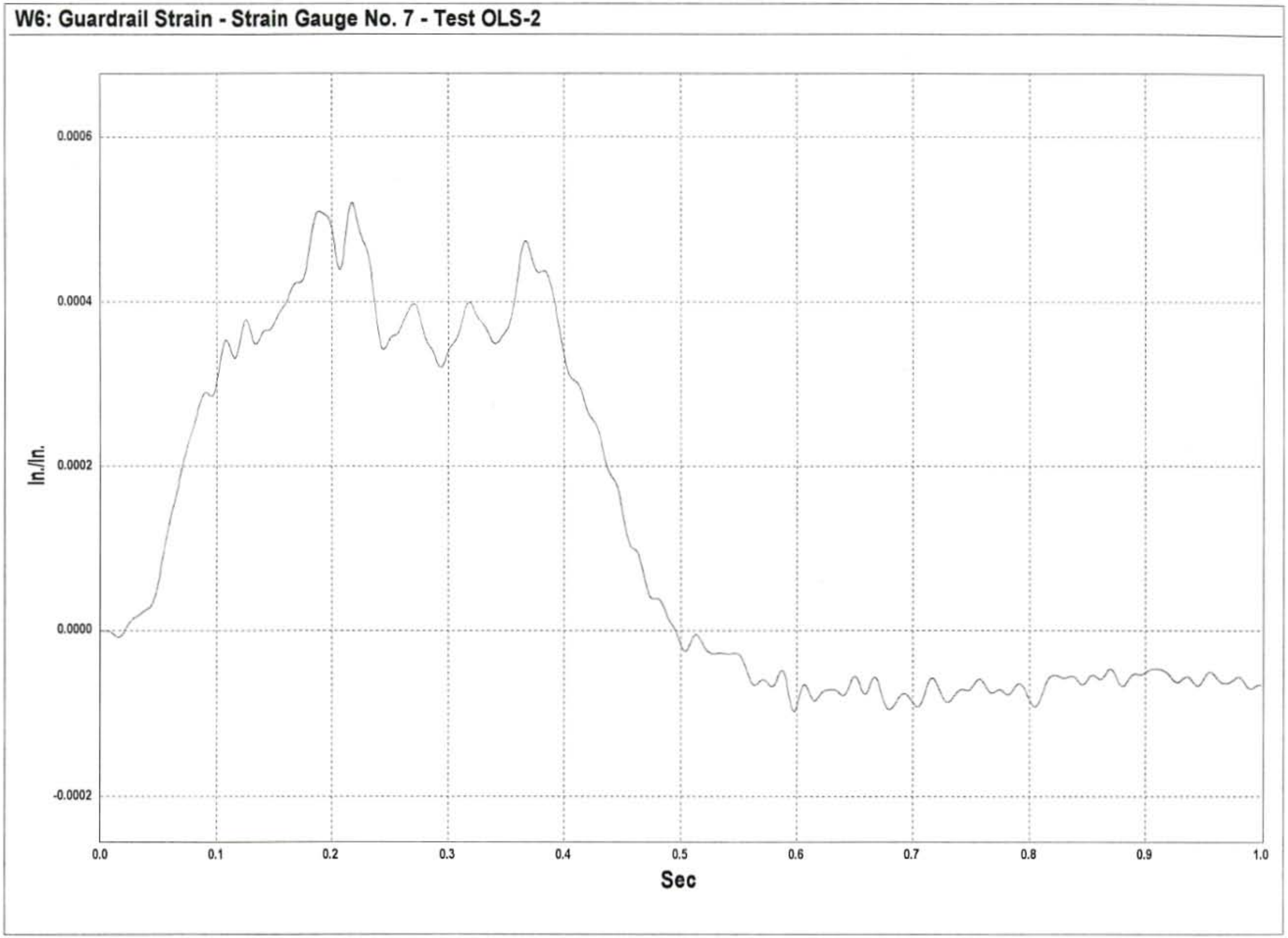

Figure G-13. Graph of Traffic-Side (near post no. 22) Bottom Peak Strain, Test OLS-2

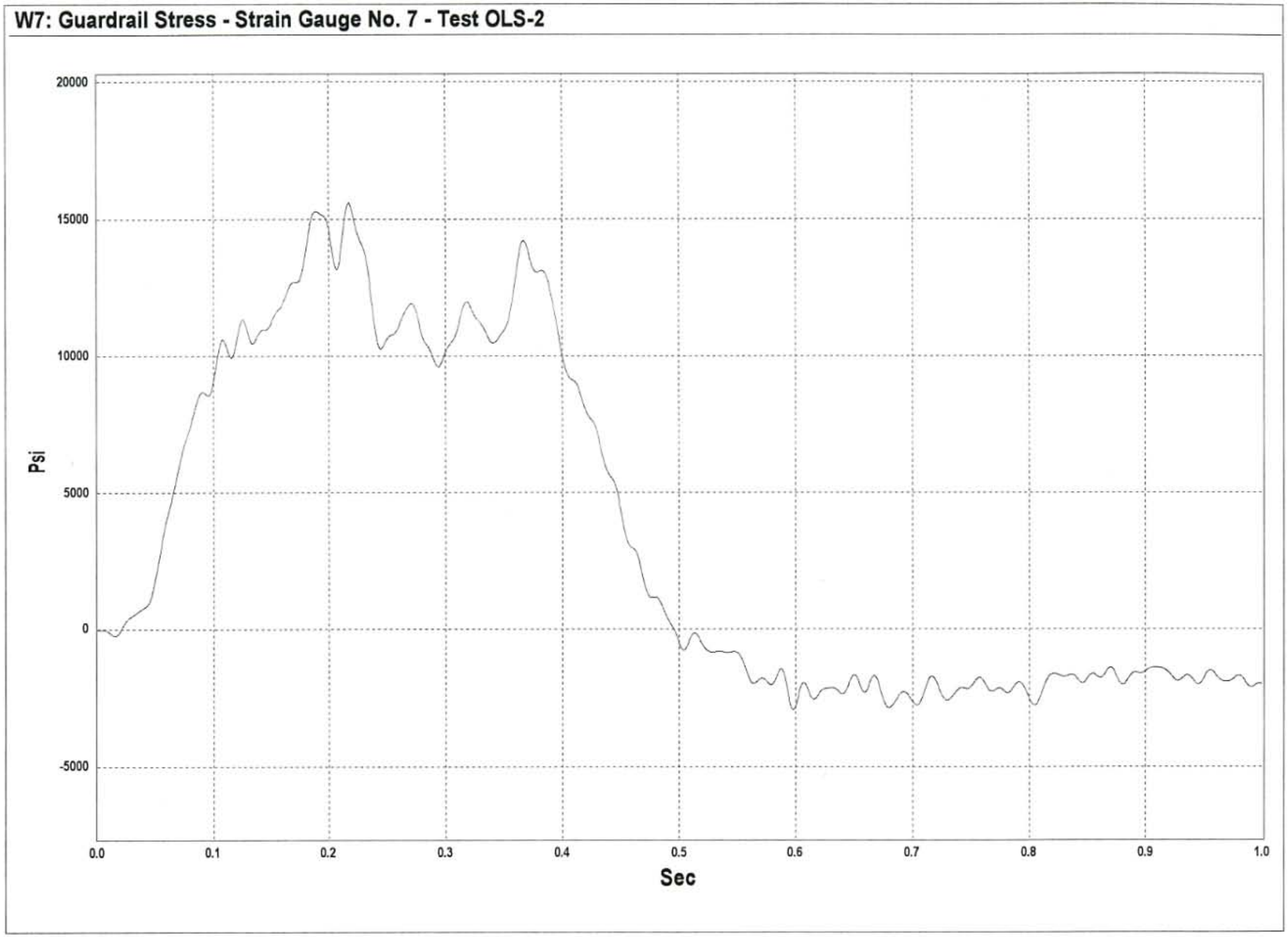

Figure G-14. Graph of Traffic-Side (near post no. 22) Bottom Peak Stress, Test OLS-2

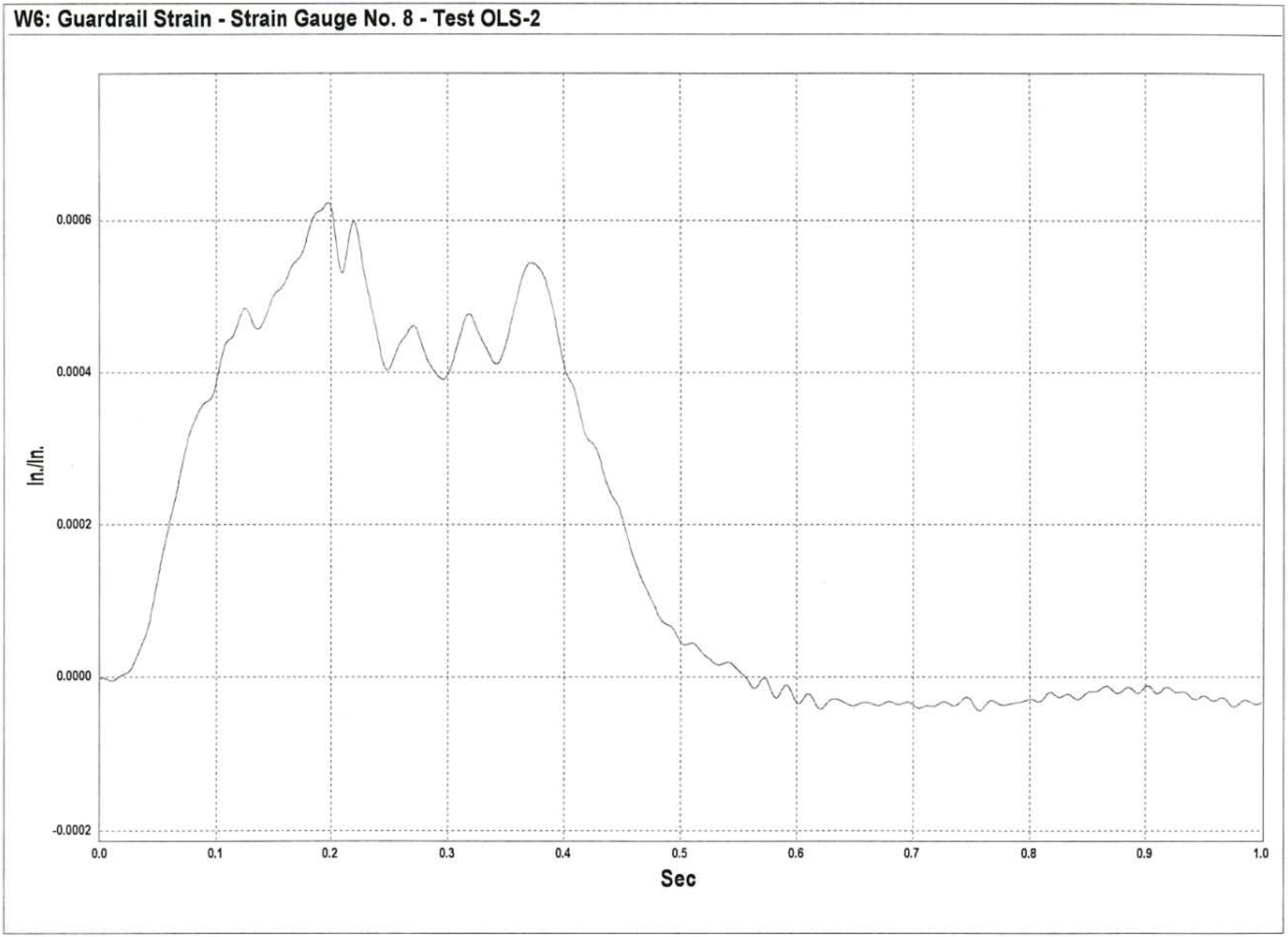

Figure G-15. Graph of Back-Side (near post no. 22) Neutral Axis Upper Middle Region Strain, Test OLS-2

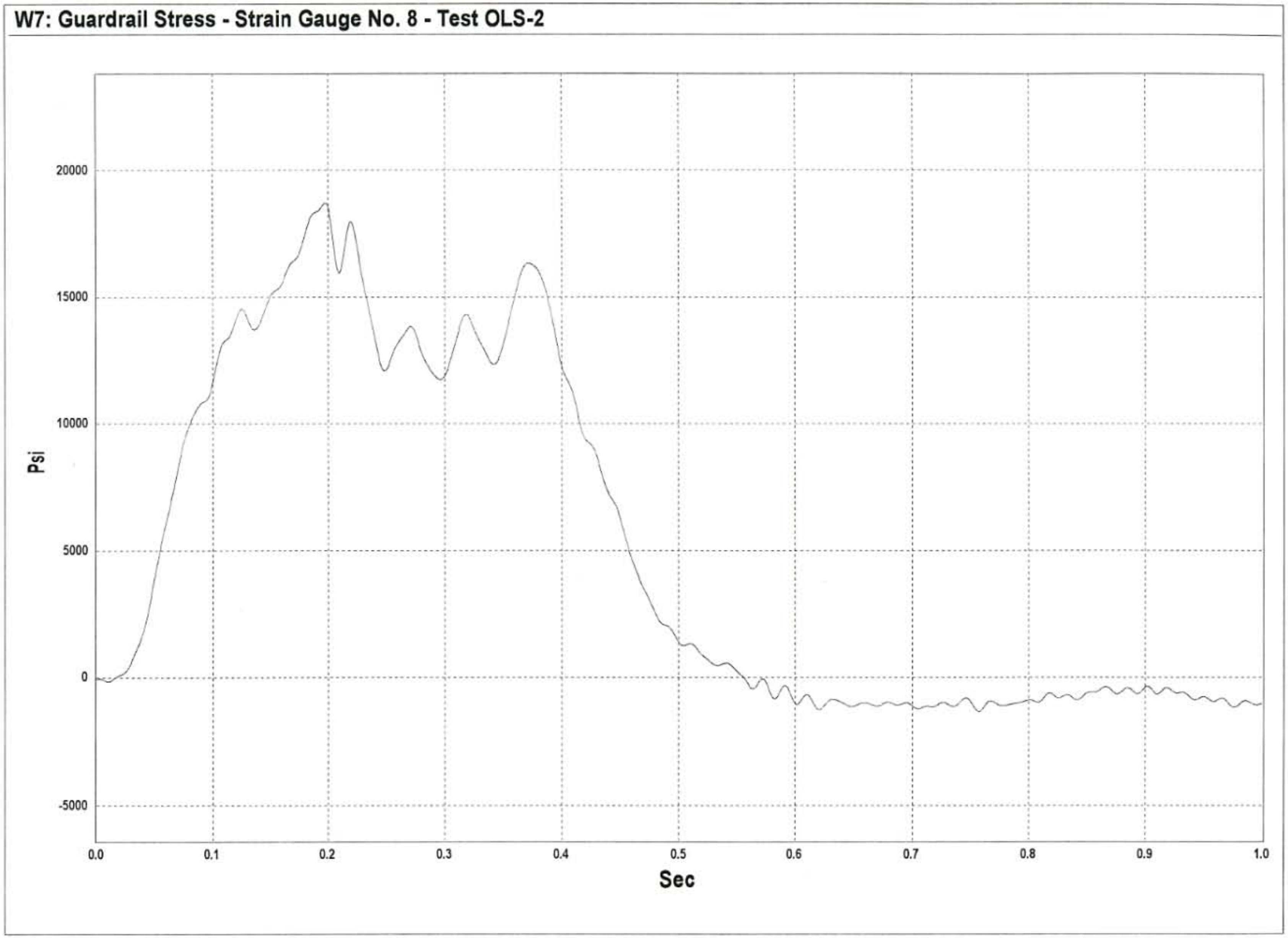

Figure G-16. Graph of Back-Side (near post no. 22) Neutral Axis Upper Middle Region Stress, Test OLS-2

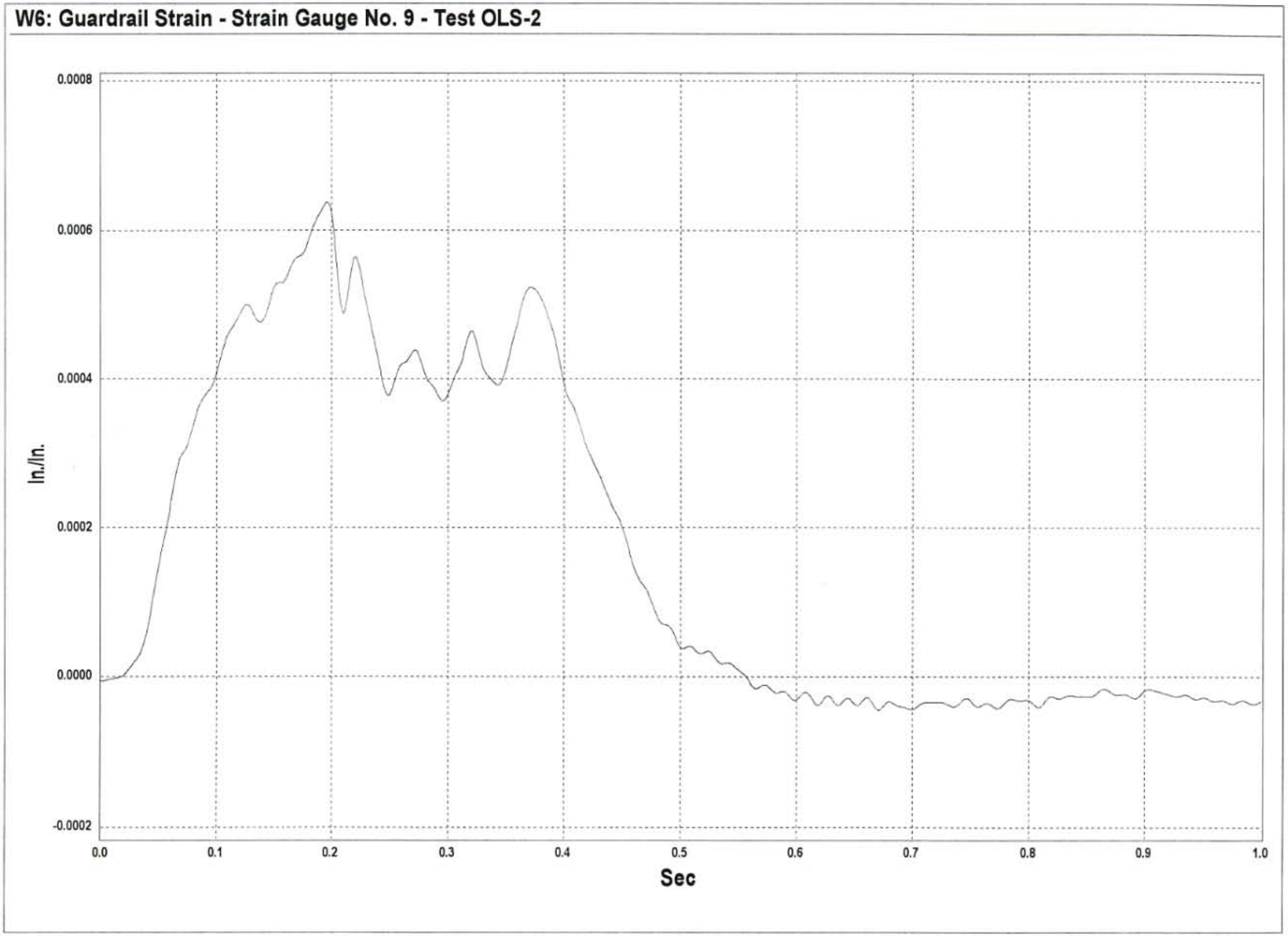

Figure G-17. Graph of Back-Side (near post no. 22) Flat Region Strain, Test OLS-2

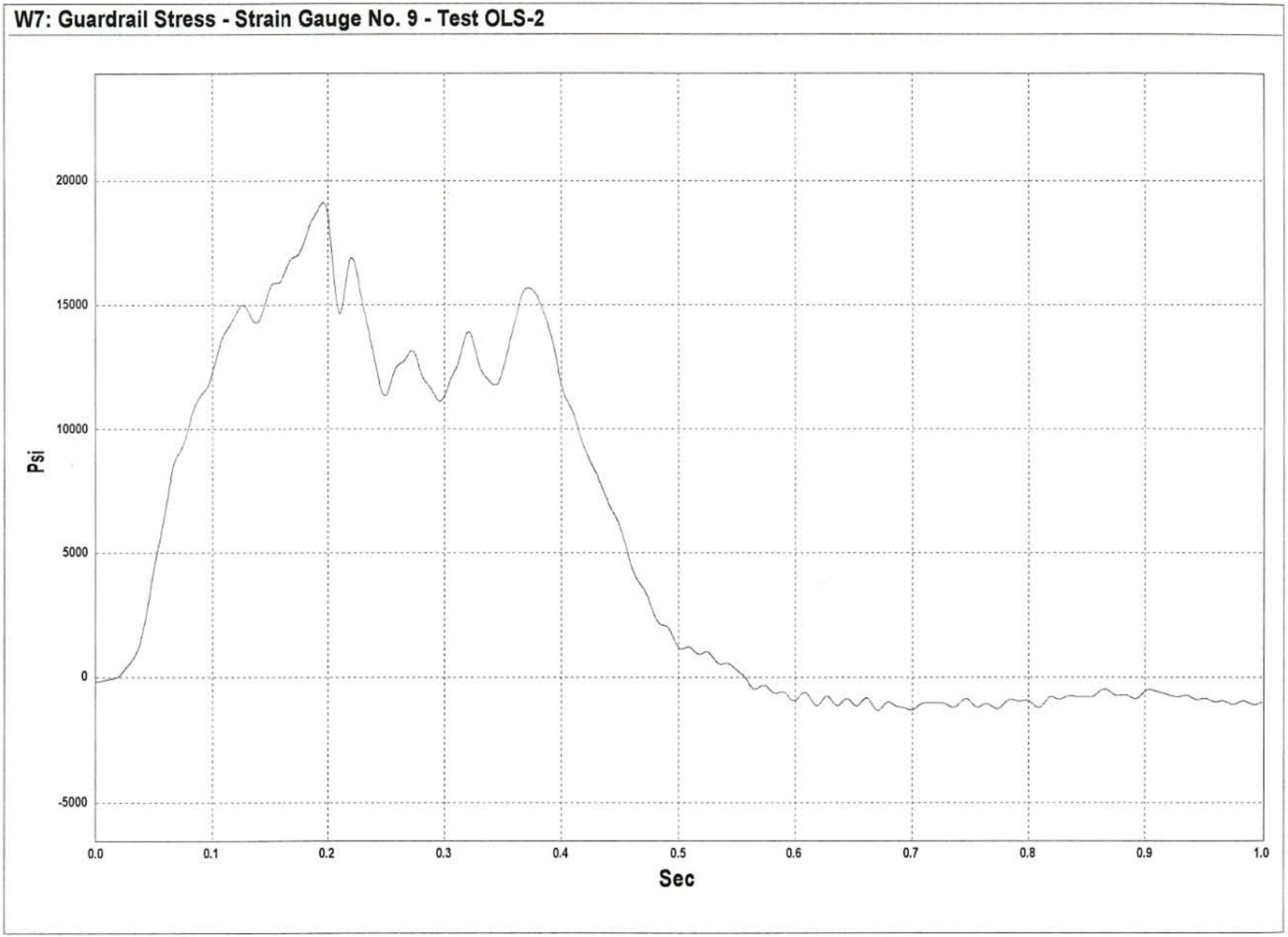

Figure G-18. Graph of Back-Side (near post no. 22) Flat Region Stress, Test OLS-2

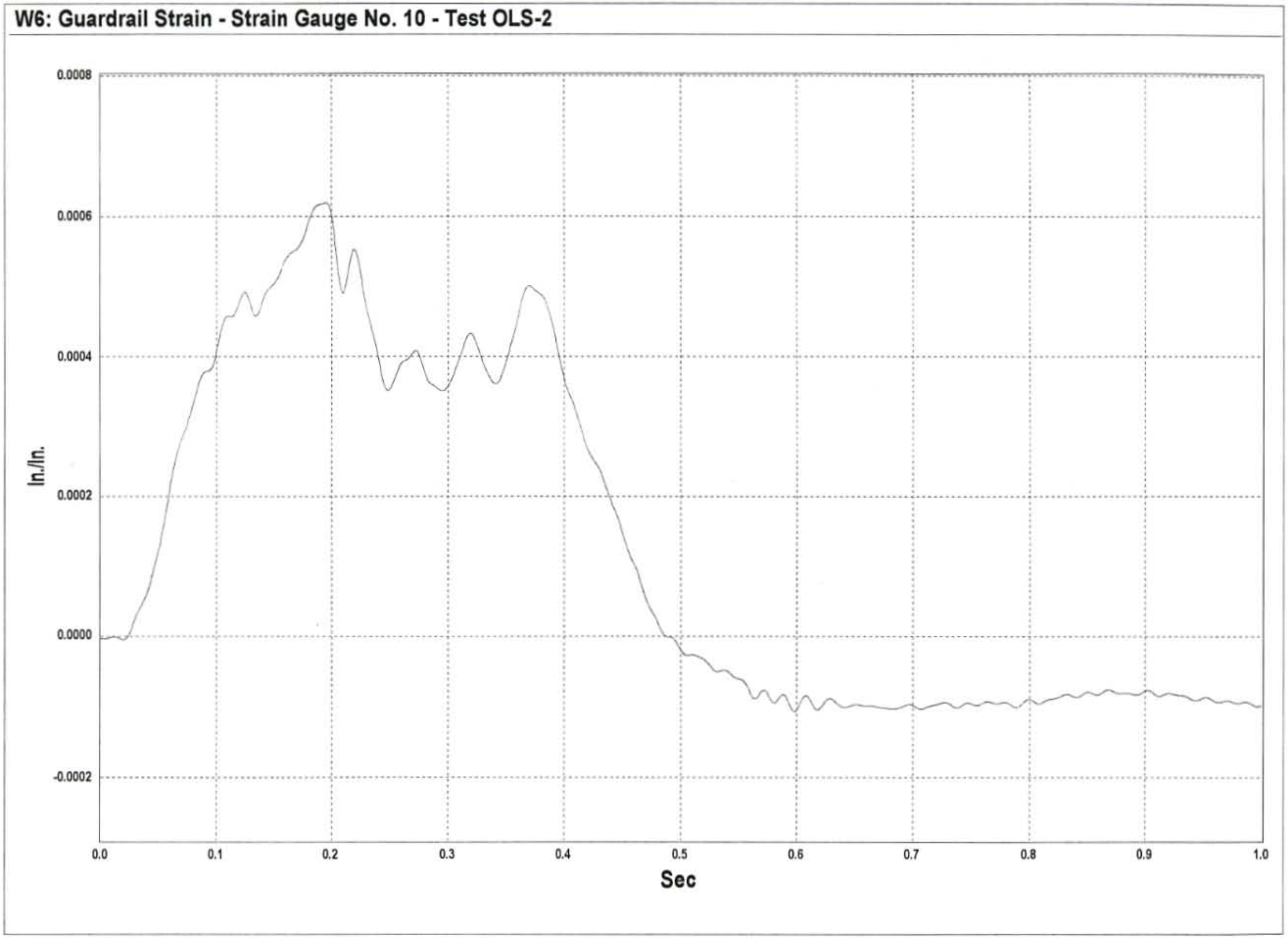

Figure G-19. Graph of Back-Side (near post no. 22) Neutral Axis Lower Middle Region Strain, Test OLS-2

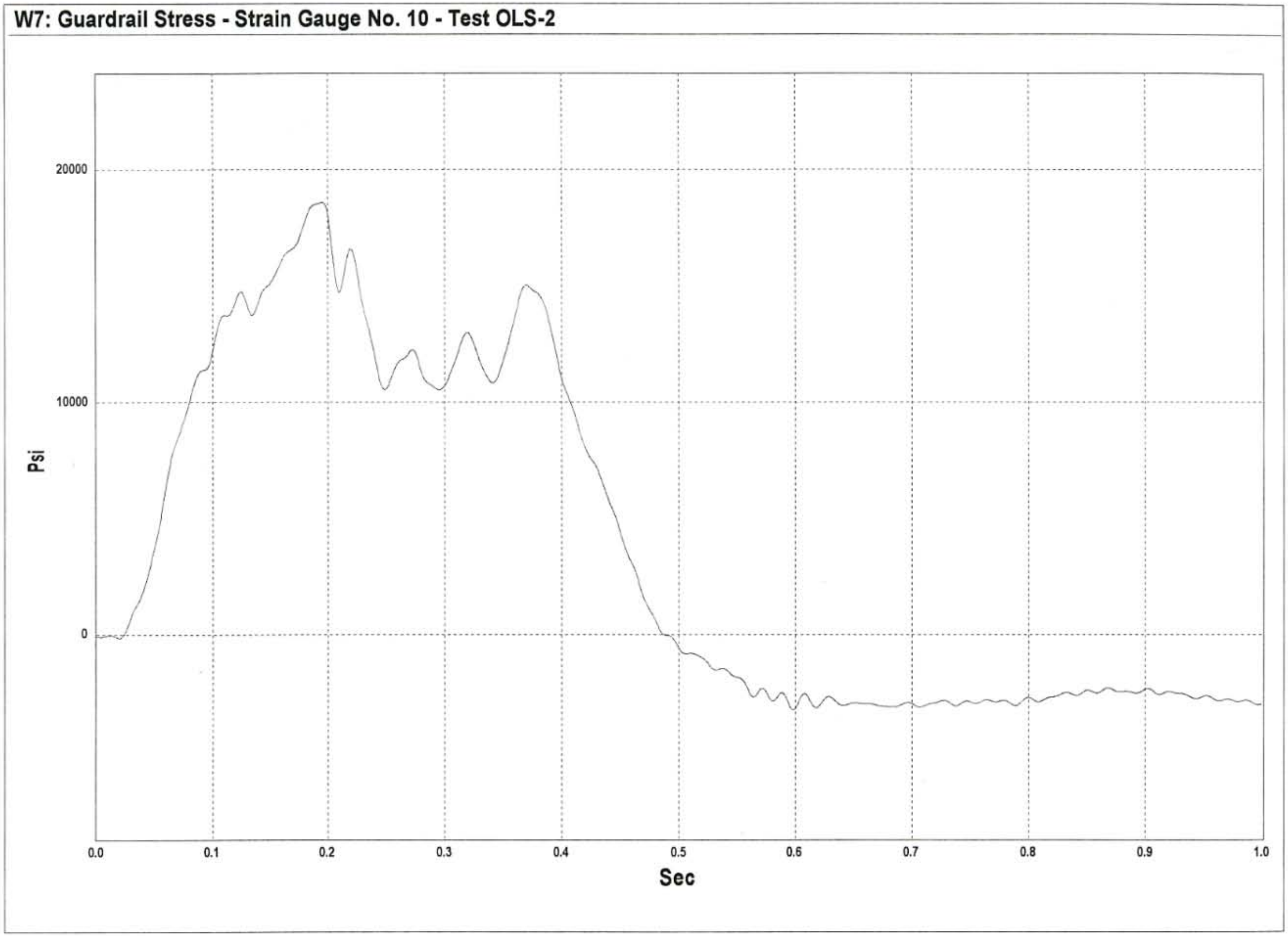

Figure G-20. Graph of Back-Side (near post no. 22) Neutral Axis Lower Middle Region Stress, Test OLS-2

APPENDIX H

String Potentiometer Data Analysis, Test OLS-2

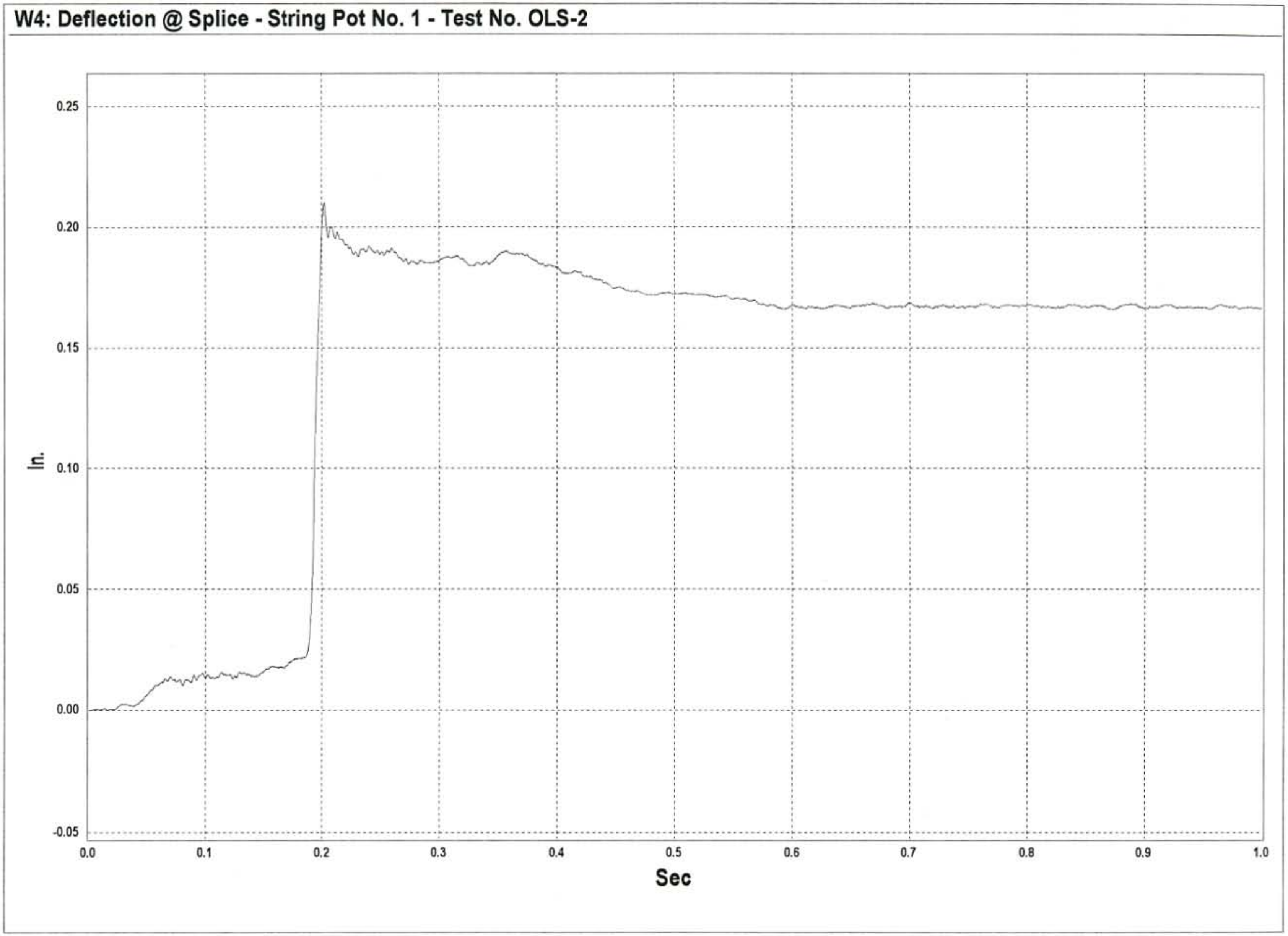

Figure H-1. Graph of Deflection at Splice near Post No. 22, Test OLS-2

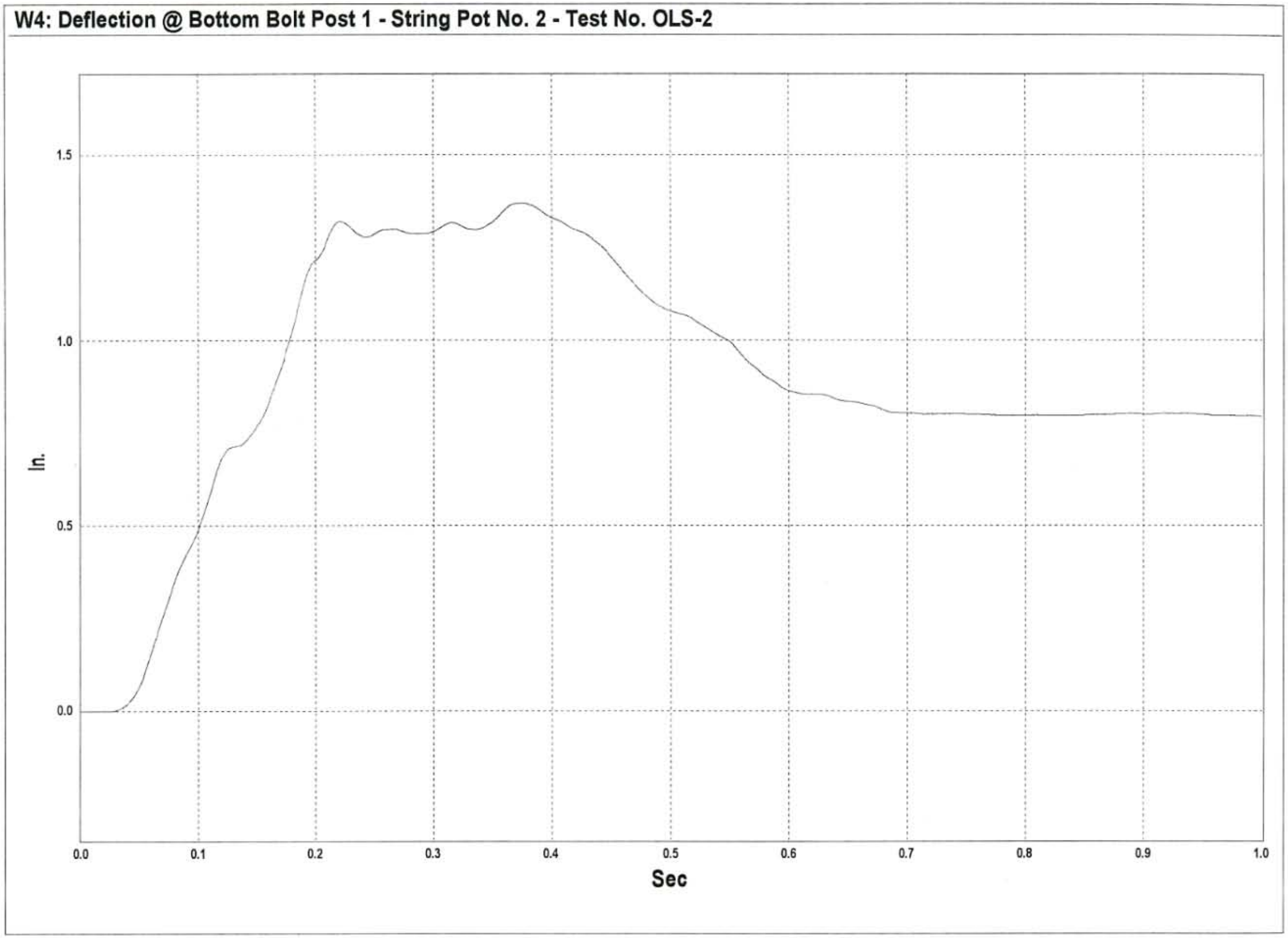

Figure H-2. Graph of Deflection at Bottom Bolt of Post No. 26, Test OLS-2

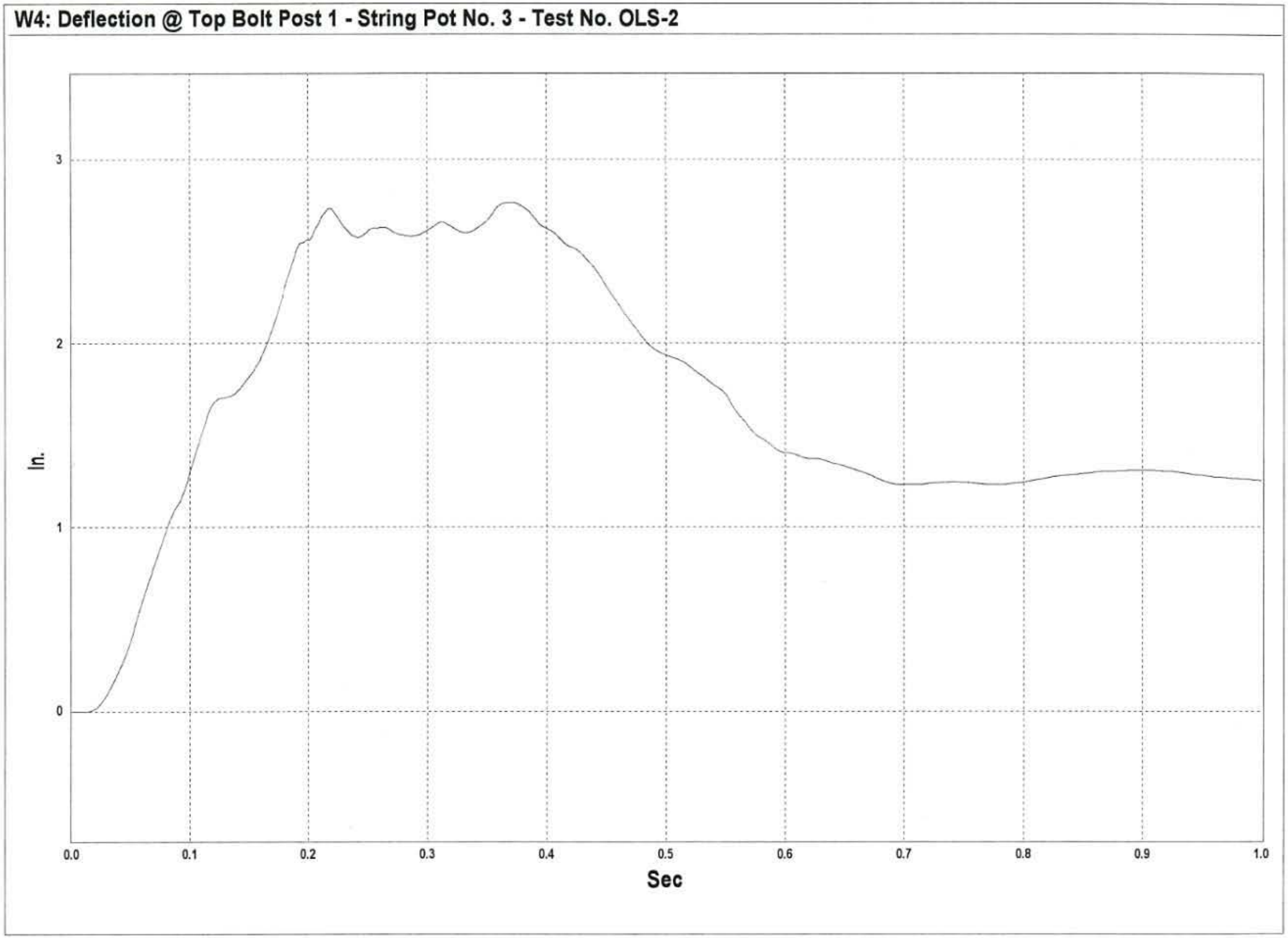

Figure H-3. Graph of Deflection at Top Bolt of Post No. 26, Test OLS-2